Adsorption of Hexavalent Chromium from Aqueous Solution using Various Adsorbents

Thesis submitted to

NATIONAL INSTITUTE OF TECHNOLOGY
ROURKELA 769 008, INDIA

FOR THE DEGREE OF

DOCTOR OF PHILOSOPHY
IN CHEMICAL ENGINEERING

By

SAROJ SUNDAR BARAL

INSTITUTE OF MINERALS AND MATERIALS TECHNOLOGY
(*Council of Scientific & Industrial Research*)
BHUBANESWAR 751 013, INDIA
OCTOBER 2007

DEDICATED

TO

MY PARENTS

DECLARATION BY THE CANDIDATE

This is hereby declared that the work presented in the thesis entitled 'Adsorption of Hexavalent Chromium from Aqueous Solution using Various Adsorbents' has been carried out at the Department of Chemical Engineering, NIT, Rourkela and Department of Environment and Sustainability, Institute of Minerals and Materials Technology (CSIR), Bhubaneswar.

It is also declared that the work is original in nature and to the best of my knowledge, it has not been submitted earlier in part or full to any other university or institute for award of any other degree or diploma.

Saroj Sundar Baral

CERTIFICATE

Certified that the work presented in the thesis entitled 'Adsorption of Hexavalent Chromium from Aqueous Solution using Various Adsorbents' has been carried out in Chemical Engineering Department of the National Institute of Technology, Rourkela and Environment and Sustainability Department of the Institute of Minerals and Materials Technology (CSIR), Bhubaneswar under our joint supervision. It is the bonafide work of Mr. Saroj Sundar Baral, Senior Research Fellow (CSIR). The work presented here is within the area of his registration.

Further, it is certified that the work is original in nature and to the best of our knowledge, has not been submitted earlier in part or full to any other university or institution for the award of any other degree or diploma

Prof. Pradip Rath
Department of Chemical Engineering
National Institute of Technology
Rourkela-769008
Tel: +91-661-2462256
Email: pradip_rath@indiatimes.com
prath@nitrkl.ac.in

Dr. S. N. Das
Department of Environment and
Sustainability
Institute of Minerals and
Materials Technology
Bhubaneswar-751013
Tel: +91-674-2581636 (ext. 540)
Email: sn_das@yahoo.com

ACKNOWLEDGEMENTS

I express my deep sense of gratitude and reverence to the supervisors, Prof. P. Rath, Department of Chemical Engineering, National Institute of Technology (NIT), Rourkela and Dr. S. N. Das, Institute of Minerals and Materials Technology (IMMT), Bhubaneswar for their invaluable encouragement, helpful suggestions and supervision throughout the course of this work.

It is indeed, a great pleasure for me to express my heartfelt gratitude to Dr. G. Roy Chaudhury, Scientist, E&S Department of IMMT, Bhubaneswar for his valuable suggestions and help throughout the work. I am also grateful to Dr. Y. V. Swamy, Scientist, IICT, Hyderabad for his encouragement during the experimental work.

I am thankful to Prof. B. K. Mishra, Director IMMT, Bhubaneswar for providing the laboratory facilities to carry out work in this premiere institute of the country with excellent facilities. I am also thankful to the Director, NIT, Rourkela for his kind permission to register and submit the thesis. The financial support provided to me as JRF/SRF by the Human Resource Development unit wing of CSIR, New Delhi during the period of my research is gratefully acknowledged.

I would like to thank all the staff members of Chemical Engineering Department, NIT, Rourkela for their kind cooperation during the course work. I am also thankful to all the scientists of E&S Department, IMMT, Bhubaneswar for their constant inspiration and encouragement.

I acknowledge with thanks the help rendered by my colleagues Dr, Ruby Das, Subhalakxmi Rout, Susmita Sen, Sujata Sengupta, Namrata Das, T. S. Ramulu and Soumendra Sahoo while carrying out laboratory experiments and analysis.

Lastly, I would like to thank my family members and friends who provided me with physical and mental support all through.

Saroj Sundar Baral

ABSTRACT

The removal of Cr(VI) from aqueous solution by batch adsorption technique using different low-cost adsorbents was investigated. The objective of the study was to find out a suitable low cost, environmental friendly and highly effective adsorbent. In the present study different low cost adsorbents such as bauxite, sawdust and sweet water weed were used to determine the adsorption efficiency. All these adsorbents were used as such or after pretreatment. Among all, the pretreated materials were found to be better adsorbents as compared to untreated materials. The influence of agitation speed, pH, temperature, adsorbent dose, initial adsorbate concentration and contact time on the selectivity and sensitivity of the removal process were investigated. The physico-chemical properties of all the adsorbents were studied using different characterization techniques such as FTIR, SEM, XRD, BET surface area and porosity.

Effect of agitation speeds on the Cr(VI) adsorption capacity of the adsorbents were studied. In general, uptake capacity of the adsorbents increase with the increase of agitation speed upto certain level and thereafter, further increase in agitation speed hardly improved the kinetics. The increase of agitation speed overcomes the resistance of mass transfer from the bulk solution to adsorbent surface and hence increased the adsorption capacity of the adsorbents

Adsorption studies were carried out upto 12 h to evaluate the effect of time on adsorption efficiency. From the contact time variation experiments, it was found that the kinetics followed dual rate, i.e., an initial faster rate followed by a slower one. For calcined Bauxite, the faster kinetics was limited to an initial 10 minutes period and the equilibrium was achieved within 60 minutes. For all other adsorbents such as formaldehyde treated sawdust, weed as such, acid treated weed and carbonized weed the faster rate and equilibrium time varied between 30-60 minutes and 2-12 h respectively.

The pH of the Cr(VI) solution was varied between 1.7-6.0. Adsorption process was found to be highly pH dependent. The optimum pH for adsorption on calcined

bauxite and formaldehyde treated sawdust were observed to be 3.5 and 6.0 respectively. The optimum adsorption capacity of the three forms of weed were observed to be at pH 1.7. The adsorption studies were also carried out by varying the temperature from 30-70 ^{0}C. In all the cases except calcined bauxite, the efficiency increased with the increase of temperature. Further, in all the cases the uptake capacity also increased with the increase of adsorbate concentration but it showed a reverse trend with increase of adsorbent concentration.

The basic data obtained were interpreted kinetically by using first order reversible, pseudo first order, Ritchie second order and pseudo second order rate kinetics. In all the cases the kinetics followed pseudo second order rate equation. Using the results from the temperature variation experiments, the activation energies along with other thermodynamic parameters such as ΔH, ΔG^0 and ΔS^0 were calculated. Experimental data for all the adsorbents were fitted to different isotherm models such as Freundlich, Langmuir and Temkin adsorption isotherms. The theoretical maximum uptake capacity of each of the adsorbents was found out by using Langmuir adsorption isotherm equation. Acid treated weed and carbonized weed were observed to be the most effective among all the selected adsorbents for the removal of Cr(VI) from aqueous solution. Therefore, all further studies were carried out using these two adsorbents only. Since all adsorbents were porous in nature, it was concluded that the adsorption process might follow surface or intraparticle diffusion or both. In both the cases, the mass transfer coefficients were evaluated from the experimental data. From the values of mass transfer coefficient it was concluded that the initial faster rate was due to surface diffusion and the latter slower part was due to intraparticle diffusion.

Adsorption studies were also carried out to evaluate the optimum parameters of the process for two most suitable adsorbents such as acid treated and carbonized weed. Scale-up experiments were performed after optimization of the adsorption parameters using the batch data of stirred tank reactors. For this purpose, adsorption studies were carried out in a fixed-bed up-flow reactor to evaluate the performance of thermally activated weed for the removal of Cr(VI) ion from the aqueous solutions. The Cr(VI) uptake capacity of the thermally activated weed was investigated as a function of

different operating conditions such as flow rate, initial Cr(VI) concentration and retention time, which was supposed to be a function of bed height. In this study, breakthrough point and numbers of bed volume (BV) were used to compare and evaluate the adsorption performance of the activated weed. After saturation with Cr(VI) ions, the spent adsorbent in the column was regenerated using 0.1M NaOH solution. From the regeneration studies, it was observed that the adsorbent could be regenerated and reused over ~ 5 times for the treatment of Cr(VI) contaminated waste water. Thus, the study concluded that the fresh water weed after carbonization could serve as an inexpensive and easy to operate adsorbent to remove Cr(VI) from industrial and mine water discharges.

CONTENTS

LIST OF FIGURES

LIST OF TABLES

CHAPTER-1

EXECUTIVE SUMMARY

Executive summary

Pollution load of the environment is increasing due to global rise in population and our quest to lead comfortable life resulting in explosive growth of industrial and agricultural activities. The pollutants are of three kinds: gaseous, liquid and solid. Pollutants may consist of heavy metal ions or toxic chemicals in soluble form and green house gases, acid precursors, ozone depletions substances etc. In order to maintain the ecological balance, scientists are making all out efforts either to decrease the emission of pollutants at the source or undertake measures for removal of pollutants after discharge. So it is a herculean task and technologists are joining hands to save our environment from complete deterioration and maintain quality of life.

Environment embraces a vast and varied field of observation and research. The current study is a benign effort to deal with hexavalent chromium generated as industrial and mining effluents discharged into the environment. Chromium compounds are widely used in industries such as electroplating, metal finishing, leather tanning, pigments etc and therefore the effluents of these industries contain chromium in soluble form. Chromium is also found in mine water of chromite mines. Hexavalent chromium containing effluents are environmental hazard since it is recognized as harmful to human health. The chromium containing wastewater can be treated by various techniques such as reverse osmosis, electro-dialysis, ultra-filtration, membrane separation, ion exchange and adsorption. All the processes are quite efficient in treating chromium containing wastewater but considering the economy and ease of operation, adsorption outscores all the other processes. The adsorption process is especially suitable for countries like India as it involves simple process control steps.

Keeping in view the importance of the adsorption technique for the removal of Cr(VI) from wastewater, various low cost and easily available adsorbents were used and reported in this work. The main objective was not only to develop a low cost and efficient adsorbent but also to reduce the cost of operation so that villagers can use the same. For this purpose, both naturally occurring minerals and biomaterials have been used as

adsorbents. The mineral used is bauxite. Bauxite is widely found in Orissa and available at an affordable price. The biomaterials used were sawdust of salwood (*Shorea robusta)* and a fresh water weed *Salvinia cucullata*. The salwood sawdust is available in plenty. The weed used in the present studies grows profusely in ponds and fresh water lakes and is disposed off regularly to maintain the quality of water bodies.

The materials were used either untreated or after pre-treatment. Bauxite, an ore of aluminum, was used as such or in calcined or acid treated form. Sawdust was also used as such or after processing with formaldehyde. The weed was used as such or acid treated or after activation by heating in an inert atmosphere. All the adsorbents were characterized by different physio-chemical methods.

In all the cases, the adsorption studies were carried out in batch scale to evaluate the different adsorption parameters vis-à-vis the efficiency of Cr(VI) removal from solution. By comparing the efficiency of Cr(VI) removal using three different forms of bauxite, the calcined bauxite was found to be the best. During calcination, gibbsite and goethite were converted to bohemite and hematite respectively. In the process of calcination, the change of crystal structure resulted in the increase of surface area for a better adsorption efficiency. The formaldehyde treated sawdust was observed to be a better adsorbent compared to the untreated one. The increase of adsorption efficiency in formaldehyde treated sawdust might be due to the protonation of different functional groups. Among the three forms of weed, carbonized and acid treated weed showed better results.

Adsorption studies were carried out, by varying parameters like agitation speed, contact time, pH, temperature and concentration of adsorbate and adsorbent. In all the cases, it was found that agitation speed was an important parameter in determining the adsorption kinetics. In general, adsorption kinetics increased with increase of agitation speed up to a certain level and thereafter, further increase in agitation speed hardly improved the kinetics. The increase in agitation speed overcame the resistance of Cr(VI) mass transfer from bulk solution to adsorbent surface. The attainment of stationery phase

after threshold agitation speed indicated the insignificant role played by the bulk mass transfer coefficient. In all the cases, the attainment of stationery phase was achieved at the agitation speed of ~ 600 rpm.

Contact time was also an important factor in determining the reaction kinetics. In general, it was observed that the kinetics followed dual rate, i.e., initial faster rate followed by the slower one. For calcined bauxite, the faster kinetics was limited to initial 10 minutes and the equilibrium was achieved within 60 minutes. For all other adsorbents, the faster rates continued up to 30-60 minutes and equilibrium was achieved in 2-12 h. The faster kinetics in all cases accounted for 60-80% of the total adsorption efficiency. The results are summarized in Table 1.1.

The pH of the solution was varied between 1.7 to 6.0. For calcinated bauxite, the optimum pH of adsorption was observed to be 4.0. Between pH 4.0-7.4 there was decrease in adsorption efficiency and beyond that it attained a steady state. The acid treated sawdust attained the maximum adsorption at pH 6.0. For three different forms of *Salvinia cucullata*, i.e., the weed as such, acid treated and carbonized forms, the adsorption efficiency increased with decrease in pH. The variation of adsorption efficiency with pH was due to the transformation of adsorbent particles as well as dissociation of Cr(VI) in aqueous solution. In the experimental pH range, Cr(VI) may occur as $Cr_2O_7^{-2}$, CrO_4^{-2} or $HCrO_4^-$ or a combination of all the three forms in different proportions. The change in charge of the adsorbent was due to the protonation and de-protonation and it depended mainly on the pH of the solution. The adsorption phenomenon might be either due to electrostatic force of attraction (physical adsorption) or ligand exchange or both. The optimum pH for adsorption of different adsorbents is due to predominance of the adsorption mechanism it followed. In all cases, FTIR studies were carried out before and after adsorption to assess the different group contribution the adsorption process. The peaks either shifted or minimized the intensity after adsorption indicating the coordination of the active functional groups with Cr(VI). So, in general, adsorption followed both physical as well as ligand coordinated steps. The Scanning Electron Microscope (SEM) studies also showed the change in morphology. The

elemental analysis through EDAX showed considerable increase in Cr(VI) count which indicated the adsorption of the same over the adsorbent material.

Temperature was varied within 30-70 ^{0}C for all the adsorbents. In all cases, adsorption efficiency increased with the increase of temperature. For each process, the activation energy as calculated and the values indicated the ease of reaction. Other important thermodynamic properties like 'ΔH', 'ΔG^0' and 'ΔS^0' were also calculated.

Adsorption experiments were also carried out by varying the absorbent and adsorbate concentrations. The uptake capacity decreased with increase of adsorbent concentration in all cases whereas a reverse trend was observed when the adsorbate concentration was varied.

Adsorption kinetics data were used to interpret the order of reaction. Four different rate equations were used, such as first order, pseudo first order, pseudo second order and Ritchie second order. In all cases, the kinetic data were well explained by pseudo second order rate equation. Based on pseudo second order rate equation, a unified rate equation was developed considering all the adsorption parameters.

Various adsorption isotherm equations such as Freundlich, Langmuir and Temkin were tested. The 'R^2' values obtained in most of the cases indicated that the adsorption process followed Langmuir adsorption isotherm. Using Langmuir adsorption isotherm, the maximum uptake capacity was also calculated. The calculated values were compared with the values reported in literature. The results are shown in Table 1.1.

The rate-determining step was also evaluated by using appropriate equations. The coefficients of intra-particle diffusion, 'k_{id}' were determined along with 'D_1' and 'D_2' values. From these values, it could be concluded that intra-particle diffusion was the rate-determining step.

After evaluating the adsorption kinetics by varing different adsorption parameters, the next step was to optimize the adsorption parameters for the most suitable adsorbent. The criteria followed in determining the best adsorbent were uptake capacity and kinetics. Based on the above two criteria, carbonized and acid treated weed were found to be the best adsorbents. For acid treated weed, four process parameters like pH, contact time, temperature and adsorbate concentration were varied whereas for carbonized weed, three adsorption parameters i.e. pH, contact time and temperature were varied. In both the cases, the insignificant terms were rejected by student 't' test and the adequacy of the model equations were tested using Fisher adequacy test. The findings are shown in Table 1.1, which indicate the extent of influence of different parameters vis-à-vis adsorption efficiency.

After optimization of the adsorption parameter using the batch data of stirred tank reactor, the next step was to scale up. For this, adsorption studies were carried out in an up-flow reactor where adsorption parameters like adsorbate concentration, flow rate and bed height were varied. Different column adsorption kinetic models such as Bohart-Adams, Yoon-Nelson, BDST and Thomas models were applied to the experimental data. From the column studies it was observed that the experimental data were well fitted to the Bohart-Adams model. After carrying out the adsorption studies, desorption studies were also carried out to find out the stability of the adsorbents for reuse. 0.1M NaOH was used for desorption studies followed by water washing. The efficiency of desorption was found to be more than 80%. The adsorption-desorption process was carried out for five cycles and in the entire process there was hardly any decrease in the adsorption or desorption efficiency, which indicate the suitability of the adsorbent in treating Cr(VI) contaminated water.

As per scientific practice, a part of the work has been published/accepted for publication in different peer reviewed international journals as listed below

1. Baral, S. S., Das, S. N., Rath, P., Hexavalent chromium removal from aqueous solution by adsorption on treated sawdust, Biochemical Engineering J 31 (2006) 216–222 (Elsevier)

2. Baral, S. S., Das, S. N., Rath, P., Roy Chaudhury, G., Chromium(VI) removal by calcined bauxite, Biochemical Engineering J 34 (2007) 69–75 (Elsevier)

3. Baral, S. S., Das, S. N., Rath, P., Roy Chaudhury, G., Swamy, Y. V., Removal of Cr (VI) from aqueous solution using waste weed, *Salvinia cucullata*, Chemistry and Ecology, 23(2007), 1-13 (Taylor and Francis).

4. Baral, S. S., Das, S. N., Rath, P., Roy Chaudhury, G., Swamy, Y. V., Biosorption of Cr(VI) using Thermally Activated Weed *Salvinia Cucullata*, Chemical Engineering J, (in Press) (Elsevier)

5. Baral, S. S., Das, S. N., Rath, P., Roy Chaudhury, G., Adsorption of Cr (VI) by treated weed *Salvinia cucullata*: Kinetics, thermodynamics and mechanism, Adsorption, (Revised manuscript submitted) (Springer)

Table 1.1. Summary of results

	Adsorbent				
Parameter	Calcined bauxite	Treated sawdust	Weed as such	Acid treated weed	Carbonized weed
Optimum pH	3.5	4.5	1.7	1.7	1.7
Equilibrium time (min)	60	300	720	720	720
Faster rate time (min)	10	30	30	30	30
%(of total) adsorbed during the faster rate	90	85	50	60	60
Temperature (^{0}C)	30-46	30-45	30-70	30-70	30-70
Max. uptake (mg/g)	2.021	9.55	232	196.5	254
Rate equation followed	Pseudo second order	Pseudo second order	Pseudo second order	Pseudo second order	Pseudo second order
Isotherm followed	Freundlich & Langmuir	Langmuir	Langmuir	Freundlich & Langmuir	Temkin
Rate determining step	Intra-particle	Intra-particle	Film and pore	Film	Film
Optimization studies	-	-	-	$Y=37.1+3.2x_1-3.7x_2-2.4x_3+2.8x_4-0.5x_1x_2-0.6x_2x_3+3.2x_1x_2x_3x_4$	$Y=38.9+2.8x_1-4.6x_2+4.1x_3+0.9x_2x_3$
Column studies	-	-	-		

CHAPTER-2
INTRODUCTION AND
LITERATURE REVIEW

Introduction and Literature Survey

2.1. Importance of chromium

Due to increase in population coupled with mining, extraction and use of various metals as different industrial and household materials, the load of toxic metal pollution in the environment is increasing. The waste from metallurgical/mining sectors, in general, creates destabilization in the ecosystem, as most of the heavy metal ions are toxic to the living organisms. But some of these heavy metals, in traces, play significant role in the human metabolism. The demand of chromium has been increasing globally due to its extensive use in various metallurgical, chemical and leather tanning industries due to its various physico-chemical properties. Some of its important applications are enumerated below:

- Corrosion resistance property of chromium expanded its application in hardened steel, stainless steel and alloys.
- Use in electro-plating to produce a hard, shining surface and prevent corrosion.
- Use to impart a greenish tint to glass.
- Wide use in catalysts preparation.
- Use of $K_2Cr_2O_7$ as an oxidizing agent.
- Use as yellow pigments (e.g. lead chromate).
- Use in the textile as a mordant.
- Use in the aircraft and other industries for anodizing and corrosion resistance.
- Use (as chromate) in refractory for aluminum forming bricks to give a defined shape as it has a high melting point, moderate thermal expansion and stable crystalline structure.
- Use in open-hearth steel melting furnaces as a major component due to its high melting point (1700-1900 ^{0}C) and neutrality, being ideal for separating acidic and basic refractory in wall linings.
- Use in leather tanning.
- Use in industrial chemical synthesis.

Apart from industrial uses, Cr(III) plays an important role in our body (Wang, T., 2004). Without Cr(III) in our diet, the body loses its ability to use sugar, protein and fat properly, which may result in weight loss or impaired growth, improper function of nervous system and imbibe diabetic conditions. The best-known nutritional effect of chromium is to assist insulin in regulating blood sugar (glucose) levels in human body as established through radio tracing. Insulin is a protein hormone that is released into the blood when blood glucose level gets high. Insulin then binds to the receptor cells outside, causing them to absorb more glucose from blood, returning blood glucose levels to normal.

Due to its strategic importance in different metallurgical processing, chromite is traded in world market either as high-grade ore or intermediate like ferrochrome/charge chrome. The finished products of modern technology use ferrochrome of various grades worldwide. There have been attempts to replace chromium by other metals like cobalt, nickel, vanadium, molybdenum and columbium in the manufacture of alloy steels. But these are not universally accepted due to their higher cost and marginal advantages over chromium. Therefore, chromium is still the most sought after metal in alloy steel production in addition to its traditional outlets like stainless steel or refractory bricks. A brief list of important uses of chromium for different purposes are given in Table 2.1 (TERI, 2001).

Table 2.1. Application of chromium and chromium chemicals in different sectors

Sl. No.	Use	Percentage of total consumption
1	Metal finishing and corrosion control	37
2	Pigment and allied products	26
3	Leather tanning and textiles	20
4	Wood preservatives	5
5	Drilling mud	4
6	Catalyst/batteries/magnetic tapes etc.	8

Consumption of chromite in India is increasing simultaneously with its global demand. India earns important foreign exchange by exporting high-grade chromite and ferrochrome. In 2001, India's consumption was 0.5 million tons out of which 86% accounted for metallurgical use, 8% for refractories and the balance (6%) for chemical synthesis. The total supply of chromite that year was 1.05 million tons and so more than 50% of it was exported. (TERI, 2001)

2.2. Harmful effects of Cr(VI)

For quite some time, the chromite matrix was considered to be the most stable and hexavalent chromium pollution due to chromite mining or handling was thought to be impossible. Later, studies revealed that the Cr(III) lodged in chromite gets oxidized by various physico-chemical (Sahoo, R. K., 1974) and biological processes to produce Cr(VI).

The waste and effluent stream of chromite mines and processing units contain chromium in two oxidation states, i.e., Cr(VI) and Cr(III) in aqueous solution. Out of these, Cr(VI) is highly toxic in nature (Agarwal, G. S., 2006). The first report on harmful effects of Cr(VI) appeared in 1930s because of the incidence of lung-cancer cases among workers in chromate handling industries. Machale (Machale, M., 1948) and Mancuso (Mancuso, T., 1951) catalogued further evidence in support of the harmful effects of chromate after detailed epidemiological studies. The relationship between trivalent and a hexavalent form of chromium is given by:

$$Cr_2O_7^{2-} + 14H^+ + 6e \Leftrightarrow 2Cr^{3+} + 7H_2O + 1.33\ V \qquad (2.1)$$

The difference in oxidizing potential of these two oxidation states show strong oxidizing power of the Cr(VI) species. On the other hand, high energy required to oxidize the trivalent form is not available with the biological systems and so almost all the Cr(VI) found in nature are derived from human activities. Cr(III), which generally

occurs in the form of Cr^{3+}, $Cr(OH)^{2+}$ or $Cr(OH)_2^{+}$, are adsorbed on the negatively charged soil particles and thus are less mobile (Deng, S., 2004). On the contrary, Cr(VI) is present in the aqueous solution in the form of dichromate ($Cr_2O_7^{-}$), hydro chromate ($HCrO_4^{-}$) or chromate (CrO_4^{2-}). These anionic species are generally poorly adsorbed by the negatively charged soil particles due to their repulsive electrostatic interaction. So Cr(VI) is mobile and present in aqueous solution only. In experiments using cell culture, investigators found that Cr(VI) penetrates the cell membrane and gets into the cells much more easily than Cr(III). The later doesn't normally enter into cells because of its slightly bigger size as compared to Cr(VI) ions. The Cr(VI) inside the cell is reduced rapidly to Cr(III). The process of Cr(VI) reduction can create reactive oxygen (O^{-}) and other free radicals inside the cell. This combination of reactive intermediates has been postulated to be able to attack DNA leading to its damage. Since they are unstable, these intermediates are reduced to stable Cr(III), found on the DNA at the end of the process. DNA damage can lead to mutations, which in certain cancer-associated genes of the cell are believed to be the basis for initiating cancer.

Breathing in high levels of Cr(VI) (>2 $\mu g/m^3$) containing dust particles in the form of compounds like chromic acid or chromium tri-oxide, can cause irritation to the respiratory system. The symptoms include running nose, sneezing, itching, nose bleeding, ulcers and damage to the nasal septum. These ailments are found in mining and industrial workers who handle Cr(VI) for a long period. A prolonged exposure of Cr(VI) is likely to cause allergic reaction consisting of severe redness and swelling of the skin leading to skin ulcer. In the animals that breathe high levels of Cr(VI), harmful effects on the respiratory system and a lower ability to fight diseases are noticed.

2.3. World chromite scenario

The largest proven deposits of chromite are found in South Africa, Zimbabwe and former Soviet Russia. Country-wise data (IBM, 2005) on reserves and production are shown in Table 2.2 and 2.3:

Table 2.2. Country wise proven reserve of chromite

Country	Chromite (tons)
Albania	20,000
Brazil	9,000
Finland	29,000
India	88,350
Philippines	29,000
South Africa	5,700,000
Turkey	70,000
United State of America	10,000
U. S. S. R.	102,000
Zimbabwe	750,000
All World	6,800,000

Table 2.3. Worldwide production of chromite for different years

Country	1981 (in tons)	1991 (in tons)	2001(in tons)
Albania	720	1,101	800
Finland	147	574	475
India	287	1,003	900
Iran	180	60	80
Philippines	580	379	200
Rhodesia (Zimbabwe)	400	627	600
South Africa	1,650	4,951	5,078
Turkey	560	850	800
U. S. S. R.	1,900	3,800	3,800

The chromites are widely distributed in India. Details of their occurrence (TERI, 2001) are shown in Table 2.4. Considering the chemical composition and field association, most of these deposits fall under stratiform type, except the ones occurring in the Himalayan region like Ladakh and Nagaland, which are associated with the

ophiolite belt. However, Orissa holds a prime place in chromite reserves of India and its production account for >98% of the country's chromite wealth. Details of chromite reserves of different grades in India are shown in Table 2.5.

Table 2.4. Chromite reserves in India (-000)

Grade/State	Proved	Probable	Possible	Total
All India	27,404	31,210	29,737	88,351
Metallurgical	10,927	12,292	7,315	30,534
Refractory	1,607	409	2,204	4,220
Charge chrome	8,635	6,936	10,062	25,633
Low grade	-	21	31	52
Beneficial	5,747	9,939	8,944	24,630
Others	-	15	-	15
Unclassified	471	1,598	1.042	3,111
Not known	17	-	139	156
Andhra Pradesh	-	15	52	67
Bihar	13	21	300	334
Karnataka	272	491	82	845
Maharashtra	44	21	300	334
Manipur	-	-	2	2
Orissa	27,069	30,662	28,660	86,391
Tamilnadu	6	-	234	240

Table 2.5. Production of Chromite in India.

State		Production in tons	Value Rs. (-000)
All India		9,26,148	12,24,248
Andhra Pradesh		460	211
Karnataka		48,145	22,173
Maharashtra		86	21
Manipur		92	48
Orissa	Jajpur	6,96,652	10,48,967
	Dhenkanal	26,241	24,152
	Bhadrak	1,54,472	1,28,676
	Total	8,77,365	12,01,795

Indian chromite deposits can be classified into three types (Srinivasachari, K. N., 1976):

- Those associated with the Eastern Ghat group of rocks such as chromites from Andhra Pradesh and Tamilnadu.
- Those associated with the iron ore (Dharwad) group such as chromite from Bihar, Orissa, Karnataka and Maharastra.
- Those associated with tertiary formations such as the chromite from Manipur, Nagaland and Assam.

Orissa accounts for ~98% of the country's deposit of chromite located in Sukinda valley of Jajpur district and Baula-Nuasahi belt of Bhadrak district. The Sukinda valley is flanked by the Mahagiri and Daitary ranges extending over an area of 50 km^2 from Kansa ($21^0$3' N, $85^0$52'E) in the east to Moruabil (21^0' N, $85^0$43'E) in the west. There are six chromite horizons accounting for an aggregate reserve of 130 million tones. Chromite veins occur down to a depth of 50-250 meters. Regular chromite veins are associated with thick lim onite nickel enriched zone formed by vertical weathering and consequent leaching process controlled predominantly by gravity percolation of the meteoric lava.

The Boula-Nuasahi belt covers an area of about 50 km^2 extending from 21 ^{0}N, $86^0$18'E to $21^0$18'N, $86^0$20'E coordinates. The area consists of a cluster of low hills, the highest peak being Phuljhara Hulli, about 1340 ft. high. These hillocks constitute the NE spurs of the Boula range dissected by the river Salandi running in SE direction. The details of texture and mineralogy of these chromite deposits have been studied by workers like Prasad Rao (Prasd Rao, GHSV., 1964), Das (Das, S. N., 1999), Sahoo (Sahoo, R. K., 1974) and Mohanty (Mohanty, J. K., 1993) amongst many others.

2.4. Present pollution scenario due to chromium in Orissa

The recoverable reserve of chromite in India is about 88.35 million tons, out of which refractory and metallurgical grades are hardly 35 million tons. Reserves

amounting to 78.4 million tons, which can find end use, cannot be mined profitably under the present mining technology. Since the country's high-grade chromite resources are limited, mining of the ore is being done judiciously. Chrome chemical industry uses low-grade ores while some portions of low-grade ores are beneficiated mostly for exports and internal consumption. There are two beneficiation plants located in Sukinda chromite belt.

Export of high-grade chromite from the region has steeply declined due to a change in policy that the raw material should be processed to get value-added product like charge chrome/ferrochrome or other chrome alloys. There has also been a short supply of chromite, especially the high-grade ores preferred for charge-chrome production in domestic market and consequently rise in the cost of the raw material. Proven reserves in hitherto untapped areas of the region are being doled out to mostly private parties who have alloy plants or are interested in exports. Thus, there have been many new players in the chromium mining and manufacturing trades.

The discharge of Cr(VI) contaminated effluents from mines/industries contaminates the environment either in the form of dust in air or solubilized ions in aqueous solution. The details of the pollutants discharged by different industries are summarized below.

A. Mining industries

- Dust: A huge amount of dust is released into the atmosphere during blasting, mining, stacking loading and transport. The dust consists mainly of chromite. The dusts deposit on various surfaces including forest canopy and are leached by the rainwater. Water sprinkling method adopted in the mines is not sufficient to control the dust hazard. It also affects the respiratory channel of workers and residents.
- Water: Mine water is a major pollutant in the mining operation. Even-though chromium in chromite is in trivalent state, some Cr(VI) is always formed due to biochemical conversions. The contaminated mine water is released into the adjacent

water sources without adequate treatment. Very few mining establishments follow chemical treatment before discharge due to higher cost involved and slack measures from Govt. regulatory bodies.

B) Metallurgical industries

- Dust: Large quantities of dust from ore handling, arc reduction, power generation facilities etc. are released into atmosphere. Some units adopt dust control measures and in most cases, these are not adequate.
- Slag: Slag is dumped over ground. It contains chromium compounds in different valence states. Cr(VI) is formed due to chemical conversion, which percolates into subsoil/terrestrial water sources during rainy season. The ferrochrome slags are manually broken and washed to retrieve the adhering ferrochrome and the waste dumped in low lying lands or pits. In this process, some contaminated water and slime are generated.
- Water: Bichromate is added to water used in cooling water towers to prevent fungal growth. This water, unless treated, may cause pollution. However, this is not applicable where bichromate is not mixed with cooling water.

C) Chemical industries (mainly bichromate manufactures)

- Slag/Residue: The residue after extraction of chromate consists of calcium chromate and other sparingly soluble chromates. The soluble chromate leached into water bodies during rainy season from these slag dumps is the worst cause of health hazard.
- Dust: Dust released from the roasting operation affects workers since it contains high concentrations of Cr(VI). Small quantities of Cr(VI) laden dust are also released into the surrounding areas.
- Water: Wash water containing very high Cr(VI) is a major cause for contamination of nearby water resources.

D) Refractory industries

- Dust: Chromium content in the dust depends on the product.
- Solid wastes: Some of the solid waste contains chromium.

E) Others

i) Leather tanning: In recent years, chrome tanners have started using basic chromium sulphate for tanning. In chromates, chromium is mostly in trivalent state and not considered as a major cause of concern. However, if the tanner uses bichromate/chromic acid, the wastewater is to be treated for removal of Cr(VI).

ii) Electroplating: Since many electroplating units are in the unorganized/cottage or small-scale sectors, it is difficult to get proper information. Workers are exposed to airborne Cr(VI) and the effluent water invariably contains high levels of Cr(VI). Enforcement of control measures is difficult.

From a preliminary study (Das, S. N., 1999) it was found that the sediments of river Brahmani and Dhamra at their confluence point with the Bay of Bengal, contain higher levels of Cr(VI) due to mine water discharges. Further investigation showed that the effluents of metallurgical, chemical and refractory industries contain much higher amounts of Cr(VI) than the recommended limit for safe discharge. RRL Bhubaneswar carried out a comprehensive study of the scenario in the year 2000 and the findings can be summarized as follows:

- The huge volume of water pumped out of various open-cast or underground mines contains high levels (0.252 to 2.8 mg/L) of chromium in hexavalent form and are mostly discharged into adjacent water bodies without treatment. This water is being used by the nearby villagers in the valley and located down-stream for social, domestic and irrigation purposes.
- Plants and crops grown locally using mine discharge water, accumulate dangerously high levels of Cr(VI), mostly in their roots, stems and fruits. Some of the staple crops like rice grown under this condition accumulate as much as 60 mg/g Cr(VI) in

roots and 14.5 mg/g in shoots, while the seeds contain ~2 mg/g. Other edible plants and vegetables accumulate similarly high amounts of the heavy metal ion.

- The over-burden minerals and rocks, mostly unsystematically stacked, are bereft of vegetation, generating airborne dust. These heaps also crumble due to poor slope stability and soluble minerals or salts like Cr(VI) leach out of them during the rain.
- The dust and particulate matter concentration in the active zone was beyond the prescribed limit. The SPM and RSPM generated in mining and transport operations were found to contain Cr(VI) beyond prescribed limits.
- The processing industries are of two categories. While the ferrochrome or charge chrome producers are least polluting, some chromium chemical industries manufacturing basic chromium sulfate and dichromate, are most polluting. Their residual wastes are the main source of Cr(VI) in effluents.
- Social changes were found to be profound although there was slight rise in the wages of manual labors. Health impact of chromite mining in a limited survey, showed a rise in chromium related toxic manifestations, in some cases leading to malignancy.
- The pollution load analysis showed that the ecosystem was under severe strain and in absence of corrective measures, might lead to permanent and irreparable damages.

2.5. Different methods of treatment

According to the Indian standards (Baral, S. S., 2006), the permissible limit of Cr(VI) is 0.05 and 0.1 mg/L for potable and industrial discharge water respectively. Most of the chromite mine discharge water in Orissa contain 2 to 5 mg/L and the effluent from electroplating, ferrochrome and leather tanning industries contain 50 to 100 mg/L of Cr(VI), which is much higher than the permissible limit. So Cr(VI) removal or reduction in mining and industrial effluents is important before discharge into the aquatic environment.

There are various physical and chemical methods used to treat Cr(VI) contaminated mining and industrial effluents. Those methods can be broadly divided into the following categories:

- Chemical methods
- Electrolytic methods
- Biological or microbial methods
- Adsorption methods.

2.5.1. Chemical methods

Amongst the chemical methods, the use of $FeSO_4$ for reduction of Cr(VI) is by far the easiest and efficient process(Biedermann, W., 1996). Apart from the ease of process, the chemical is cheap and available in plenty. Water treatment plants in industrial belts use $FeSO_4$ extensively (Linche, J. J., 1995). Some industrial effluents like those from leather tanning plants contain very high levels of Cr(VI) as well as Cr(III). These are usually precipitated after reducing Cr(VI) to Cr(III) as hydroxides (at pH ~9.0) by the application of alkali and slight heating (60-80 ^{0}C) to coagulate the precipitate (Fujiwara, M., 1995). Iron scraps are most devoured as reducing agent followed by neutralization and precipitation of Cr(VI) from electroplating wastes (Shen, Z., 1995). At times, iron scraps are deliberately put into effluent treatment ponds to facilitate reduction. Polymeric ferrous sulphate is also used along with polyacrylamide as a coagulant for tannery wastewater treatment (He, Y., 1995). Ferric hydroxides have been found to catalyze the reduction of Cr(VI) to Cr(III) (Akter, H., 1994). Some of the exogenous heavy metal ions including Cr(VI) have been found to be retained by the iron oxide present in soil fraction (Xing, G. X., 1995).

In Sukinda valley pickle liquor is used to treat Cr(VI) contaminated water (Das, S. N., 1999). The process is effective provided the process parameters are maintained properly. Apart from the difficulty in maintaining stringent process parameters, it introduces other pollutants like hydrogen ions, iron, sulphate and toxic trace metals into the effluents. Some of the mines in Sukinda area are using ferrous sulphate reduction to

a limited extent. Therefore, Cr(VI) continues to contaminate the nearby water bodies.

Strongly acidic cation and basic anion resins packed in ion exchange columns were used to remove heavy metal ions and from electroplating effluents with an efficiency of >95% (Sapari, N., 1996). Emulsion free liquid membranes, hollow fiber containing liquid membranes (Guha, A., 1994), organic solvent soluble membrane filters (Goa, P., 1996), multiple emulsion liquid membranes (Chakravarty, A. K., 1995) etc. were also reported to be effective in separating Cr(VI) from various industrial effluents. Kendeewicz et al (Kendiweecz, T., 2000) studied the reaction of Cr(VI) on the surface of Fe_3O_4. According to them the tetrahedral by coordinated Cr(VI), which reacted with magnetite contaning Fe(III), was reduced by the heterogeneous reduction process to octahedral coordinated Cr(VI). Mukhopadhyay et al (Mukhopadhyay, B, 2007) reported removal of Cr(VI) by electrochemical addition of Fe(II). The Fe(II) ion released during the process was responsible for the reduction of Cr(VI). But these are mostly of academic interest and none have been tried on very dilute solutions like mine water discharges.

2.5.2. Electrolytic methods

An innovative technique (Das, S.N., 1999) of Cr(VI) reduction is the in-situ electrolytic generation of ferrous ion from consumable anodes immersed in feed water so that instantaneous reaction takes place. It is the most suitable method since the current applied and potential difference is very low. Consumable electrode is inexpensive. It does not add any undesirable ion into the downstream water.

Oren et al (Oren, Y., 1995) described the acidification of the waste in an anode compartment followed by reduction in the cathode compartment. The cathode used was porous carbon in which instantaneous reduction took place. Simultaneously, the reduced chromium was precipitated as insoluble chromium compound within the pores. Chaffot et al (Chaffot, C., 1995) reported an electro-coagulation process of separating chromium from electroplating wastewater. After separating the sludge, the water was recycled.

Mcintosh et al. (Mcintosh, K. R., 1995) reported the removal of Cr(VI) from partially saturated kaolinite clay soil using an electro-kinetic process. An electroplating wastewater containing Cr(VI) in the concentration range of 0.2 to 3.8 g/L and pH ~1.5 was subjected to electrochemical precipitation at 75 V, 4.8 A with 50 minutes retention time. The resultant concentration could be brought down to < 0.2 mg/L. (Kongsricharosn, N., 1995). The process economy showed good comparison with the conventional process.

Reaction kinetics of the iron solution from consumable anode was reported (Dikusar, A. L., 1993) to be of third to first order. The mechanism was reported to be the adsorption of various trace metal ions (like Cr, Fe, Zn, Bi and Sb) on ferrihydrite produced by the hydrolysis of the electrolytic iron. Wastewater samples containing heavy metals, suspended solids, oils, colloids and organics are subjected to direct current to neutralize the ionic and other charged particles before coagulation (Dalrymple, C. W., 1995). A microprocessor-based system was developed (Kim, H. D., 1993), where the waste stream from electroplating industry was treated continuously. In-situ generation of FeS removed Cr(VI) at 97 to 99% efficiency from electroplating wastewater (Mudakavi, J. R., 1995) which had potential for commercial application.

A bipolar packed bed electrolytic cell for generation of Fe^{2+} ion, was used to remove Cr(VI) from solution (Ogutveren, U. B. 1994). Cr(VI) containing solution from electroplating industries were treated by applying oxidation-reduction potential (Zhu, H. W., 1992). A vertical electrochemical coagulator was used to reduce Cr(VI) (Shingarev, A. M., 1992) to Cr(III) by using graphite and iron anode (Shi, G. 1992).

Cr(VI) containing wastewater was treated in a fluidized bed electrochemical reactor and the overall efficiency of the process was reported by Flack et al (Flack, T. M., 1991). Zhu et al (Zhu, G., 1991) used iron scraps as electrode to treat chromium contaminated water. Photo-catalytic reduction of Cr(VI) by titanium pillared zirconium phosphate and titanium phosphate under solar radiation was reported by Das et al (Das, D. P., 2006). This process was favorable in acidic conditions and followed pseudo

second order kinetics. It is seen from the above accounts that the electrolytic process is applied to all kinds of industrial wastewaters to remove Cr(VI). The main mechanism of the total process is the in-situ generation of Fe(II) which reduces Cr(VI) to Cr(III) followed by the precipitation of Fe(III) as hydroxide, popularly known as ferrihydrite. The freshly precipitated ferrihydrites have high surface activity and thereby adsorb the chromium thus reducing concentration of the contaminant. As per solubility product, Cr(III) concentration in water after reduction is higher than the permissible limit for drinking water. Thus the process must have a built-in mechanism for achieving a very low level of overall chromium concentration

2.5.3. Biological/microbial methods using live microorganisms

The use of biological process to treat wastewater containing heavy metal ions is a recent development although the technique has been extensively used in chemical and pharmaceutical industries in a commercial scale. The knowledge gained in these industries is now being extended to address various problems related to environment. The use of biotechnology is slowly gaining importance due to the advanced knowledge as well as sufficient availability of waste biomass for further use. A chromium resistance *Shwanella algae bry* was reported to remove Cr(VI) from wastewater under anaerobic conditions (Caccavo, F. Jr., 1996). Verma et al (Verma, N., 1996) reported the use of microorganisms to remove Cr(VI) from solution. Chromate bearing cooling tower wastewater was purified in 20 L continuous stirred tank reactor using *Psedominant mendocina*. The process efficiency was found to be more than 99.9% in when the Cr(VI) concentration varied in the range 25 to 100 mg/L and the retention time varied between 4.5 to 8 h. The microorganism efficiently withstood wide variation in pH (6.5-9.5) and heat (25-40 ^{0}C). Batch reduction and adsorption of Cr(VI) from aqueous solutions by Corncob under highly acidic conditions (pH~1) was reported (Bosinco, S., 1996). A two-stage process was developed (Shen, H., 1995) to treat Cr(VI) contaminated water using *E. coli* strain. In the first step, the microorganisms were grown in a chemostat and after the growth, the bacterial solution was pumped into a

plug flow reactor operated under anaerobic condition. The flow rate and retention time was regulated to maximize the conversion.

Peat moss was also used to treat Cr(VI) contaminated water. The peat moss was found to adsorb Cr(VI) at a pH of 2.0 (Sharma D.C., 1995). Initially the Cr(VI) was reduced to Cr(III) followed by biosorption and the total process was carried out at pH 2.0. Bio-sorption of heavy metal ions under acidic conditions from industrial wastewater using the green algae *Cladophora crispate* was also reported (Ozer, D., 1994). The optimum conditions for adsorption also have been established. Fude et al (Fude, L., 1994) reported sulphate reducing bacterial strains isolated from a metal finishing waste to treat Cr(VI) contaminated water. Li et al (Li, F., 1993) also used sulfate reducing microorganisms to treat Cr(VI) contaminated solutions.

The microbial/biological processes are inexpensive and pollution free. But the technique is relatively new and requires special skill in handling the microbe strains for treating the metal contaminated solution. Since long-term impacts of most of the strains are not yet known, many are skeptical and advocate further intensive studies before employing such microorganisms in environmental processes.

2.5.4. Adsorption methods

Among other processes for removal of Cr(VI) from industrial/mining wastewater, adsorption process is an economically feasible alternative. Adsorption is a process in which a single or a group of ions/compounds get accumulated on the surface of another solid or liquid. The substance on which the adsorption takes place is known as adsorbent and the substance, which gets adsorbed, is called adsorbate. Based on the extent of attraction between the adsorbent and adsorbate, the adsorption process can be classified into two types:

- Physical adsorption or vanderWaal's adsorption
- Chemisorption

Adsorption, which can result from the vanderWaal's force of interaction, is known as physical adsorption or vanderWall's adsorption. In this type of adsorption, the process heat is of the order of 20-40 kJ/mol. Physical adsorption process is reversible and established rapidly. Physical adsorption can be of two types, i.e., monolayer adsorption and multi-layer adsorption. In chemisorption, the chemical interaction/electrostatic force of attraction occur between the adsorbent surface and adsorbate molecules. In this process, the heat of adsorption usually varies from 40 to 400kJ/mol. It is associated with appreciably high activation energy and therefore termed as activat ed adsorption. It is a relatively slow process.

Physical adsorption is a reversible process that occurs at a temperature lower or close to the critical temperature of an adsorbed substance. On the other hand chemisorption, in general, is an irreversible process because of strong electrostatic force of interaction between the adsorbent and adsorbate molecules. Physical adsorption is very effective, particularly at a temperature close to the critical temperature of a given fluid. Chemisorption occurs usually at temperatures much higher than the critical temperature and by contrast to physical adsorption, is a specific process, which can only take place on some solid surface for a given fluid. Contrary to physical adsorption, chemisorption leads to monolayer adsorption (Maron, S. H). Under favorable conditions, both the processes can occur simultaneously or alternately. Physical adsorption is accompanied by a decrease in free energy and entropy of the adsorption system and, there by, this process is exothermic in nature.

Most of the adsorbents in industrial possess have a complex porous structures that consist of pores of different sizes and shapes. The total porosity is usually classified into three groups: micro pores (diameter, $d<2$ nm), meso pores ($2<d<50$ nm) and macro pores ($d>50$ nm). The significance of pore size in the adsorption process is well known. Because the size of micro pores are comparable to those of adsorbate molecules, all atoms or molecules of the adsorbent can interact with the adsorbate species. This is the fundamental difference between adsorption in micro, meso and macro pores. Consequently, the adsorption in micro pore is essentially a pore filling process in which

the pore volume is the main controlling factor (Dubinin, M. M., 1975). In case of mesopores whose walls are formed by a large number of adsorbent atoms or molecules, the boundary of the inter-phase has a distinct physical meaning. That means the adsorbent surface area has a physical meaning. The adsorption forces do not occur throughout the void volume in macro pores but at a close distance from their walls. Therefore, the mono and multilayer adsorption take place successively on the surface of meso-pores and their final fill proceeds according to the mechanism of capillary adsorbent condensation (Oscik, J., 1982). The basic parameters characterizing meso-pores are: specific surface area, pore volume and pore size or pore-volume distribution. The mechanism of adsorption on the surface of macro pores does not differ from that of the flat surfaces. The specific surface area of macro-porous solid is very small; that is why adsorption on this surface is usually neglected. The capillary adsorbate condensation does not occur in macro pores.

Various forms of chemical adsorbents and materials of biological origin or biosorbents have been shown to be effective metal removers from the industrial and mining wastewater (Leyva, R, R., 1994, Panchanandikar, V. V., 1994, Crusberg, T. C., 1991, Lo, S. L., 1989, Schindler, P. W., 1981, Benjamin. M. M., 1981, Devis, J. A., 1978, Benjamin. M. M., 1982). The adsorption process has many advantages such as:

- Low cost of adsorbent
- Easy availability of adsorbent
- Utilization of industrial, biological and domestic wastes as adsorbent
- Low operational cost
- Ease of operation compared to other processes
- Re-use of adsorbent after regeneration
- Capacity of removing heavy metal ions over a wide range of pH and to a much lower level
- Ability to remove complex form of metals that is generally not possible by other conventional method
- Environment friendly, cost effective and technically feasible alternative due to utilization of biomaterials.

Due to ease of operation, the adsorption techniques have been used widely to treat metal ion containing wastewater. Sawdust, being cheap and easily available, is used widely either as such or in treated from to remove metal ions from wastewater (Argun, M. E., 2007; Gaballah, I., 1998; Dakiky, M., 2002; Chanah, T. G., 2005). Sorption studies were carried out mostly in batch scale and various adsorption parameters affecting the overall process were studied. Use of activated carbon was also reported (Zhao,N., 2005; Bailey, S. E., 1999; Toley, C. A., 1997) to remove metal ions from wastewater. The activated carbon were made from various raw materials having high carbonaceous materials, including wood, saw dust, coconut shell etc. They can be activated by thermal decomposition in a high-temperature oxidation or lower temperature chemical dehydration reaction. The activated carbon is being used widely to treat wastewater to remove organic or inorganic pollutants because of their large specific surface area, high adsorption capacity and special surface chemical properties (Park, S. J., 1999; Park, S. J., 2002). These physical and chemical properties of the activated carbon depend on pore size, pore distribution and number of surface oxygen groups. The pore size and pore volume can be controlled during the activation process such as activation time, activation agent and temperature. The surface oxygen also can be changed by using suitable oxidizing agents and thermal treatment in order to get the surface functional groups such as carboxyl, phenolic and lactonic group attached to carbon (Toles, C. A., 1999, Barton, S. S., 1999). These groups can improve the adsorption capacity and selectivity on a certain adsorbate in the gaseous or liquid phase (Pradhan, B. K., 1999, Cimino, G., 2000).

Waste microorganisms usually in the form of dead cells are also used as an alternative adsorbent for the treatment of heavy metal containing wastewater. In this process biological materials accumulate heavy metals from wastewater by either metabolically mediated or purely physico-chemical pathways of uptake (Fourest, E., 1992). The major advantages of biosorption over other conventional treatment methods are:

- Low cost,
- High efficiency of metal removal from dilute solution,
- No additional nutrient requirements

- Regeneration and recycling of the biosorbent and
- Possibility of metal recovery

The microorganisms can take up metal ion in numerous pathways. The mechanisms of biosorption have been discussed by Veglio and Beolchini (Veglio, F., 1997). Gadd (Gadd, G. M., 1988) and Brierley (Brierley, C. L., 1990) reviewed the unknown ways in which bacteria, fungi and algae can take up toxic metals. The uptake of heavy metal ions can take place by entrapment in the cellular structure and subsequent sorption on to the binding sites present in the cellular structure.

Prakasham et al (Prakasham, R. S., 1999) used *Rhizophus arrhizus* biomass for the treatment of Cr(VI) contaminated wastewater. *R. arrhizus* was immobilized in 2% alginate solution. The prepared material was used further to establish the optimum conditions for removal of Cr(VI) from solution. Sag et al reported (Sag, Y., 2000) equilibrium parameters for the single and multicomponent biosorption of Cr(VI) and Fe(III) ions on *R. arrhizus* in a packed bed column. In the above study, breakthrough curves for Cr(VI) adsorption in column were established. The Cr(VI) adsorption capacity decreased in presence of Fe(III), a common contaminant in Cr(VI) containing wastewater. Methylated yeast biomass was also reported (Seki, H., 2005) to remove Cr(VI) from solution efficiently. The Cr(VI) adsorption was negligible at neutral pH but increased with the increase of degree of methylation. The optimum pH of adsorption varied in the range 4-6. A metal binding model was used to describe the adsorption. *Mucor hiemalis* was also reported (Tewari, N., 2005) to remove Cr(VI) from solutions. The detailed studies were made with regards to its kinetics and mechanism of adsorption. The competitive biosorption of Fe(III) and Cr(VI) on *C. vulgaris* from binary mixtures was investigated (Aksu, Z., 2000) in a single stage batch reactor by varying the solid/liquid ratio at an initial pH of 2.0. The batch adsorption was assumed to be a single stage equilibrium operation. The separation process was mathematically defined. For this purpose, the individual Langmuir constants evaluated from the non-competitive isotherms were used to find the competitive Langmuir model describing multi-component adsorption equilibrium and thus predicting the equilibrium concentration at a given

solid/liquid ratio. Biosopriton of Cr(IV) from aqueous solutions on *Aeromonas caviae* particles was investigated (Louhido, M. X., 2004) in a well-stirred batch reactor. Equilibrium and kinetic studies were performed at various initial bulk concentrations, biomass loads, temperatures and ionic background. The kinetics was observed to follow pseudo-second order rate. A number of fresh water macrophytes like *Myriophyllum specatus, Potamogeton luceus, Salvinia herzogin, Ceratophyllum demersum, Eichhorria crassipes* (Schneider, I. A. H., 1999, Mohanty, K., 2006) were reported to remove Cr(VI) from solution. In these cases the hydrophytes were dried, powdered, sieved and then used for biosorption purpose. Biosorption studies were carried out in a batch reactor to evaluate the various adsorption parameters. Loukidon et al (Loukidon, M. X., 2004) used *Aeromonas caviae* to treat Cr(VI) contaminated wastewater. The adsorption studies were carried out in a stirred reactor. Equilibrium and kinetic experiments were carried out for various parameters like bulk concentration, biomass load, temperature and ionic background. The isotherm followed monolayer Langmuir model. The adsorption process followed chemical sorption controlled. The brown seaweed, *Ecklonia s*p., was reported (Park, D., 2005) to reduce Cr(VI) to Cr(III). The Cr(VI) reducing capacity was enhanced by various chemical treatment methods. The Cr(VI) reducing capacity was enhanced by modifying the amino and carboxyl group.

Adsorption studies were also carried out using various agricultural wastes like grape stalk waste (Fiol, N., 2006), neem leaf powder (Sharma, A., 2004), maple saw dust (Yu, L. J., 2003), waste acron (Malkoc, E., 2006), pine sawdust (Ozacar, M., 2005), rice husk (Guv Y., Qi, 2002), wheat straw (Chun, L., 2004) etc. In all these reports, adsorption studies were carried out either in stirred or up-flow reactor. Various adsorption parameters were studied to evaluate their effects on Cr(VI) removal efficiency. Among the adsorption parameters, pH was observed to be an important factor in determining the adsorption efficiency. Adsorption kinetics was observed to be reasonably faster and followed dual rate, i.e. initial faster rate followed by slower one. The initial faster and latter slower rates might be due to surface and intra particle diffusion processes respectively.

Chitin, the waste polymer from fishery industry, was reported to be a good adsorbent for Cr(VI) (Li, Q., 1997). It is white, hard inelastic material containing nitrogenous polysaccharides derived from the outer skeleton of insects, crabs, shrimps and other marine animals. Chitin is the second most abundant natural polymer i.e. polysaccharide and its estimated annual production is almost equal to cellulose (Li, Q., 1997). Chitin is converted to chitosan by alkaline hydrolysis using 50% (W/W) aqueous NaOH solution. Chitosan has many applications due to the presence of reactive $–NH_2$ group at position 2 and two hydroxyl groups at position 3 and 6. Due to the presence of the functional groups, chitosan is a good chelator (Li, Q., 1997) and forms complexes with almost all heavy metal ions. Further, due to its cationic nature, it adsorbs various anionic species. The solubility of chitoson in aqueous acids is a limiting factor for many such applications. It is therefore necessary to crosslink chitosan to render it insoluble in acid media. Chitosan is generally cross-linked using chemical reagents such as glutraldehyde and epichlorohydrin (Rorrer, G. A. F., 1993). Ramani and Sabharmal (Ramani, S. P., 2006) developed a Gamma radiation based method for cross-linking chitosan in the presence of carbon tetrachloride sensitizer. The cross linking facilitated the desorption process. Hydrogel chitosan beads were reported to adsorb Cr(VI) (Modrzejewska, Z., 2006). The adsorbent was prepared by phase inversion method. The process followed pseudo second order rate. The uptake capacity of the adsorbent was observed to be high (1.1 g/g of chitosan). Cr(VI) adsorption studies were carried out (Hassan, S., 2003) by using chitosan coated perlite beads and under equilibrium as well as dynamic conditions. The uptake capacity was 452 mg/g of chitosan. Desorption studies were carried out by using alkali.

Apart from biomaterials, a number of chemical adsorbents were used to treat Cr(VI) contaminated water. Stannous hydroxide was reported (Goswami, S., 2005) to have good Cr(VI) adsorptive capacity. The adsorbent was prepared by adding hydrochloric acid to a solution of sodium stannate. Various adsorption parameters were studied to evaluate their effect. The adsorption process followed first order kinetics. Hydrotalcite was also used to treat Cr(VI) contaminated water (Lazaridis, N. K., 2003). Hydrotalcite, $Mg_6Al_2(OH)_{16}\ CO_3,\ 4H_2O$ (HT), is a double layered mixed metal

hydroxide. Due to positive charge of HT, it is a potential adsorbent for various anions. Cr(VI) adsorption studies were carried out by using manganese nodule leach residue (Mallick, S., 2006). Since the leached residue is having high surface area, it was a potential adsorbent. Its adsorption behavior was studied as a function of time, pH, temperature, concentrations of adsorbate and adsorbent dose. The adsorption process was endothermic in nature. Metallurgical wastes like red mud was also reported (Pradhan J., 1999) to be a good adsorbent for Cr(VI). Activated red mud was prepared by acid dissolution followed by ammonia precipitation and drying at 110 ^{0}C. The process was optimized by varying the adsorption parameters. Adsorption studies were also carried out using Wollastonite (Sharma, Y. C., 2001). Wollastonite is a clay mineral whose surface area was increased by heat treatment. The rate of adsorption was a function of temperature and pH. Ferrihydrite being a active adsorbent, was employed (Lehmann, M., 2001) for Cr(VI) adsorption. Various other chemical adsorbents were used to treat Cr(VI) contaminated water such as clay (Lazaridis, N. K., 2001), zeolite (Tahir, H., 1998), feldspar (Singh, D. K., 1994), hydrated zirconium oxide (Ghosh, U. C., 2001), hydrous titanium oxide (Ghosh, U. C., 2003) and ion exchange resins (Rangaraj, S., 2001).

Apart from process development in small scale, adsorption studies were also carried out in different reactors, which helped in scaling up the laboratory/bench scale data to pilot or industrial scale. The main requirement of a large scale sorption process is that the sorbent should be used in a suitable reactor configuration such as packed or fluidized bed or stirred tank reactor. Such large scale adsorption in reactors requires suitable adsorbent in granulated or pellet form. The size, density and shape of the particles should prevent clogging or large pressure drops across the adsorbent bed (in case of packed bed column) and at the same time, should permit optimum flow. Continuous adsorption of metal ions from solution can be accomplished by employing different types of reactor configurations. The reactors commonly employed for wastewater treatment include packed bed, fluidized bed, expanded bed, stirred tank reactor and moving column reactor etc. Bai et al (Bai, S. R., 2005) reported the treatment of Cr(VI) containing wastewater in different types of reactors. Chang et al(Chang, H., 2006) used the measured isotherm in designing fixed-bed reactor for breakthrough curve.

The effective diffusivity was calculated, which was used to predict breakthrough under other adsorption conditions. The performance of packed bed is usually described through the concept of break through curve. The time for breakthrough appearance and the shape of the breakthrough curve are very important characteristics for determining the operation and the dynamic response of an adsorption column. The breakthrough curve shows the loading behavior of the metal to be removed from solution from a fixed bed and is usually expressed in terms of adsorbed metal concentration. Using the inlet and out let concentrations of the up-flow solution, Malkoe et al (Malkoe, E., 2006) designed rector.

2.6. Conclusions and work done

From the literature cited, it was clear that there was a need to find a low cost process for the removal of toxic heavy metal contaminants from water. The process should have ease of operation so that the rural people can use it with least technical knowledge. Adsorption is universally accepted as the latest method of treating industrial/mine wastewater for removal of soluble toxic components. The treatment process is also simple and convenient.

Keeping in view the importance of treatment of Cr(VI) contaminated water from industrial and mining establishments, the present study reports the feasibility of Cr(VI) adsorption by using different low cost, environment friendly adsorbents. Five different adsorbents were used in the study, such as:

- Treated bauxite
- Treated Sawdust
- Fresh water weed
- Acid treated weed
- Heat activated weed

In this study, an attempt was made to increase the adsorption capacity of these adsorbent by using different activation methods. The bauxite used for the adsorption of Cr(VI) was activated in two ways: one, by heating up the bauxite to 450 ^{0}C for 4 hours and the second one, by treating it with 0.5 N H_2SO_4. To increase the physical and

chemical characteristics of sawdust, it was treated with 1% formaldehyde solution at room temperature. Similarly, the weed *Salvinia cucullata* used in the present study was activated in two ways: one, by heating it at 500 ^{0}C for 1 hour in an inert (nitrogen) atmosphere to prevent oxidation and complete combustion and the second one, by treating it with 0.1 N acetic acid solutions at room temperature. The physico-chemical properties of the adsorbents were analyzed by Malvern particle size analyzer, XRD, XRF, FT-IR, SEM and EDAX. For all the five adsorbents, adsorption efficiency was studied as a function of contact time, pH, temperature, stirring speed, particle size, adsorbent dose and adsorbate concentration. Different adsorption isotherms were employed in order to evaluate the optimum adsorption conditions. Different adsorption model equations for kinetics, isotherm and rate mechanism of all the process were used to find out the best model, which fitted well to the experimental data. Different statistical parameters, such as regression coefficient and average absolute percentage deviation were employed to find out the validity of the best-fit model equation. Thermodynamic parameters such as standard enthalpy (H^0), standard Gibbs energy (G^0), activation energy (E) and standard entropy (S^0) were calculated for each process using the experimental data. From the experimental results, the best adsorbent was chosen considering the metal loading capacity and kinetics. A full factorial design of n^k type was used to find out the mathematical relationship between the percentage adsorption and variables affecting adsorption process such as pH, temperature, time and adsorbate concentration. From the adsorption isotherm developed, the adsorption conditions such as number of stages and amount of adsorbent required to treat the waste were also established. Up-flow column studies were carried out under optimum conditions such as retention time, pH, and temperature obtained from the factorial design method to evaluate Cr(VI) removal efficiency using the chosen adsorbent. It was found that the adsorption capacity of the adsorbent studied was well compared to the other adsorbents reported in literature.

A part of the work in this thesis has been published or accepted for publication in different international journals and some more papers would be communicated in due course of time. The reprints of papers published/ accepted have been appended at the end.

CHAPTER-3

THEORETICAL CONSIDERATIONS

Theoretical considerations

This chapter describes the various theories based on which our experimental results are interpreted.

3.1. Adsorption isotherm model equations

Adsorption isotherm helps in determining the properties of the adsorbents such as pore volume, pore size or energy distribution and specific surface area. The isotherm curve can also be utilized to obtain information concerning the desorption mechanism strictly connected with interaction between the adsorbent and adsorbate molecules. Therefore, the efficiency of an industrial adsorbent can be assessed through this curve. The correct interpretation of experimental adsorption isotherm can be realized in terms of some mathematical equations called adsorption isotherm model equations. Such equations are derived assuming an ideal physical model for the adsorption system. The model assumptions are usually a result of experimental observations. The experimental results allow for the formulation of a hypothesis about the character of the adsorption process. This hypothesis can be tested experimentally and if found suitable, could be developed into a theory, i.e., a suitable adsorption isotherm equation. The adsorption isotherm thus developed provides useful information for estimating performance in a full-scale process stream. Firstly, they help to determine, the possibility to reach a desired purity level for a given adsorbent. This is important when multiple impurities are present and one or more impurities are poorly adsorbed. Secondly, the isotherm allows calculation of uptake (q_e) at equilibrium, which has a major impact on the process economy. It can also be used to predict the relative performance of different types of adsorbents.

Prior to 1914 only a few theoretical interpretations of adsorption isotherms were in use. But thereafter, a number of isotherm equations were proposed by different investigators. Some of those in frequent use are:

- Freundlich adsorption isotherm
- Langmuir adsorption isotherm
- Brunneuer-Emmeth-Teller adsorption isotherm
- Temkin adsorption isotherm

3.1.1. Freundlich isotherm

Freundlich adsorption isotherm was proposed by Boedecker in 1895 (Dabrowski, A., 2001) as an empirical equation. Later Freundlich (Freundlich, H., 1926) made some useful modifications as a result of which, it assumed great importance. The Freundlich adsorption equation can be written as:

$$\frac{x}{m} = q_e = kc^{\frac{1}{n}} \tag{3.1}$$

Taking the logarithm of both sides,

$$\log q_e = \log k + \frac{1}{n}\log C_e = K_f + \frac{1}{n}\log C_e \tag{3.2}$$

where 'q_e' is equilibrium adsorption capacity (mg/g), 'C_e' is the equilibrium concentration of the adsorbate in solution, 'K_f', and 'n' are constants related to the adsorption process such as adsorption capacity and intensity respectively.

3.1.2. Langmuir adsorption isotherm

The Langmuir adsorption isotherm (Langmuir, I., 1918) was based on the following assumptions:

- Fixed number of adsorption sites: at equilibrium, at any temperature, a fraction of the adsorbent surface sites (θ) is occupied by adsorbed molecules and the rest (1-θ) is free.

- All sorption processes are homogeneous.
- There is only one sorbate
- One sorbate molecule reacts with only one active site.
- No interaction between the sorbate species.
- A monolayer surface phase is formed.

The equation proposed by Langmuir was universally applicable to chemisorption with some restrictions involving physical adsorption. This equation is applicable to the physical or chemical adsorption on solid surface with one type of adsorption active center. As long as its restrictions and limitations are clearly recognized, the Langmuir equation can be used for describing equilibrium conditions for sorption behavior in different sorbate-sorbent systems or for varied conditions within any given system. The Langmuir equation is given by:

$$\frac{C_e}{q_e} = \frac{1}{Q_0 b} + \frac{C_e}{Q_0} \qquad (3.3)$$

Where 'C_e' is the equilibrium concentration and 'q_e' is the amount of adsorbate adsorbed per gram of adsorbent at equilibrium (mg/g); 'Q_0' and 'b' are Langmuir constants related to the sorption capacity and intensity respectively.

3.1.3. Brunauer-Emmett-Teller (BET) isotherm

Langmuir adsorption isotherm, although simple, had limited application. Therefore, attempts were made to generalize the Langmuir equation by taking into account lateral interaction among adsorbed molecules, their mobility and the energetic surface homogeneity of the solid. At first the BET equation was derived from the kinetic considerations analogous to those proposed by Langmuir while deriving the monomolecular adsorption isotherm. While the Langmuir adsorption model is valid for a single layer adsorption, the BET model represents sorption isotherm reflecting apparent multi-layer adsorption. Both models may be deduced from either kinetic or

thermodynamic consideration of adsorption (Langmuir, I., 1918, Brunauer, S., 1938, Adamson, A., 1967).

The BET model assumes that a number of layers of adsorbate molecules form at the surface and that the Langmuir equation applies to each layer. A further assumption of BET model is that a given layer need not complete formation prior to initiation of subsequent layers. The equilibrium conditions will therefore involve several types of surfaces or number of molecular layers in each surface site. The BET isotherm is given by;

$$q = \frac{BQC_f}{(C_s - C_f)[1 + (B-1)(C_f / C_s)} \tag{3.4}$$

where 'C_s' is the saturation concentration of the solute, 'C_f' final concentration at time 't', 'B' is a constant relating to the energy of interaction with the surface, 'Q' is the number of moles of solute adsorbed per unit weight of adsorbent in forming a complete mono-layer on the surface.

3.1.4. Temkin adsorption isotherm

Temkin and Pyzhev suggested that due to the indirect adsorbate/adsorbent interaction, the heat of adsorption of all the molecules in the layer would decrease linearly with coverage (Aksu, Z., 2005). The linear form of Temkin isotherm can be written as:

$$q_{eq} = B \ln A + B \ln C_{eq} \tag{3.5}$$

where B=RT/b, 'T' is absolute temperature in Kelvin and 'R' is the universal gas constant. The constant 'b' is related to heat of adsorption. C_{eq} = equilibrium concentration of the adsorbate

3.2. Adsorption kinetic models

The study of adsorption kinetics in wastewater is significant as it provides valuable insight into the reaction pathways and into the mechanism of the reaction. Further, it is important to predict the time at which the adsorbate is removed from aqueous solution in order to design an appropriate sorption treatment plant. Any adsorption process is normally controlled by three diffusive transport processes for the adsorbate:

- From bulk solution to the film surrounding the adsorbent.
- From the film to the adsorbent surface
- From the surface to the internal sites followed by binding of the metal ions onto the active sites.

But in kinetic modeling, all these three steps are grouped together and it is assumed that the difference between the average solid phase concentration and equilibrium concentration is the driving force for adsorption. Further, it is established from the experimental observations that at optimum agitation speed, the external boundaries have hardly any effect. So application of the kinetic model depends only on the initial and final concentrations of the solution at different time intervals. It is incorrect to apply simple kinetic model such as first and second order rate equations to a sorption process with solid surface, which is rarely homogenous. Secondly, the effects of transport and chemical reaction are often experimentally inseparable.

Several kinetic models have been proposed to clarify the mechanism of a solute sorption from aqueous solution onto an adsorbent:

- Pseudo first order/Lagergren kinetic model
- First order reversible kinetic model
- Ritchie's second order kinetic model
- Pseudo second order kinetic model

3.2.1 Pseudo first order or Lagergen kinetic model

The Pseudo first order or Lagergen kinetic rate equation for the sorption of liquid-solid system was derived based on solid adsorption capacity. It is one of the most widely used sorption rate equations for sorption of a solute from a liquid solution (Taqvi, S. I. H., 2006, Sudhodan, P., 2006, Ho, Y. S., 1999, Lagergren, S., 1898). According to the authors, the overall adsorption rate is directly proportional to the driving force, i.e., the difference between initial and equilibrium concentrations of the adsorbate (q_e-q). Therefore, the pseudo first order kinetic equation can be expressed as:

$$\frac{dq_e}{dt} = k(q_e - q_t) \tag{3.6}$$

where 'q_e' is the amount of solute adsorbed at equilibrium per unit mass of adsorbent (mg/g), 'q' is the amount of solute adsorbed at any given time 't' and 'k' are the rate constant. By using the boundary conditions and simplifying, the equation 3.6 becomes

$$\log(q_e - q) = \log q_e - \frac{k}{2.303}t \tag{3.7}$$

'k' can be calculated from the slope of the linear plot between $\log(q_e-q_t)$ vs. 't' for different adsorption parameters such as pH, temperature, adsorbate concentration, adsorbent dose, particle size and agitation speed

3.2.2. First order reversible kinetic model

The sorption process may be considered as a first order reversible reaction (Hamid, N. K., 2001, Arun, K. 1984), which can be expressed as

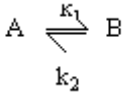

The rate equation for the reaction is expressed as

$$\frac{dC_B}{dt} = -\frac{dC_A}{dt} = k_1 C_A - k_2 C_B = C_{A0}\frac{dX_A}{dt} = k_1(C_{A0} - C_{A0}X_A) - k_2(C_{B0} - C_{A0}) \qquad (3.8)$$

where 'C_A' (mg/L) and 'C_B' (mg/g) are the concentrations of the adsorbate in solution and sorbent respectively at a given time 't'; 'C_{A0}' and 'C_{B0}' are the initial concentrations of adsorbate and adsorbent respectively, 'X_A' is the fractional conversion of the adsorbate, 'k_1' and 'k_2' are the first order rate constants. At equilibrium conditions:

$$\frac{dC_B}{dt} = -\frac{dC_A}{dt} \qquad (3.9)$$

and

$$X_{Ae} = \frac{K_c - (C_{B0}/C_{A0})}{K_c + 1} \qquad (3.10)$$

where 'X_{Ae}' is the fractional conversion of the adsorbate at equilibrium and 'K_c' is the equilibrium constant which is defined as:

$$K_c = \frac{C_{Be}}{C_{Ae}} = \frac{C_{B0} - C_{A0}X_{Ae}}{C_{A0} - C_{A0}X_{Ae}} = \frac{k_1}{k_2} \qquad (3.11)$$

where 'K_c' is the equilibrium constant and 'C_{Ae}' and 'C_{Be}' are the equilibrium concentrations of adsorbate in the solution and adsorbent, respectively. Applying the equilibrium conditions, equation 3.8 becomes:

$$\ln(1 - U_t) = -(k_1 + k_2)t\,; \qquad (3.12)$$

where 'U_t' is the fractional attainment of equilibrium and is given by

$$U_t = \frac{C_{A0} - C_A}{C_{A0} - C_{Ae}} \tag{3.13}$$

The values of rate constant were calculated from the equilibrium conditions from the plot between $\ln(1-U_t)$ vs. 't' .

3.2.3. Pseudo second order kinetic model

A pseudo second order reaction model (Ho, Y. S., 1998, Ho, Y. S., 1999) can also be applicable to kinetics of sorption and the equation for this reaction can be shown as:

$$\frac{dq}{dt} = k(q_e - q)^2 \tag{3.14}$$

On integration for boundary conditions when t=0 to t>0 and q=0 to q>0 and further simplifications, equation 3.14 becomes,

$$\frac{t}{q} = \frac{1}{kq_e^{\,2}} + \frac{1}{q_e}t = \frac{1}{h} + \frac{1}{q_e}t \tag{3.15}$$

where $h=kq_e^2$ is known as initial sorption rate where 'k' is rate constant.

The plot of t/q_t vs. 't' at different adsorption parameters will give a linear relationship, which allows for computation of 'q_e', 'k' and 'h'.

3.2.4. Ritchie second order kinetic model

Ritchie second order equation can be expressed as (Ritchie, A. G.,1997, Cheung, C. W., 2001)

$$\frac{q_e}{q_e - q_t} = 1 + k_2 t \tag{3.16}$$

where q_t= uptake (mg/g) at time 't', q_e= equilibrium uptake capacity and k_2=rate constant have their usual meanings.

3.3. Rate controlling mechanism

The adsorption process for porous solid can be devided into three stages, i.e. (a) mass transfer (boundary layer/film diffusion), (b) sorption of ions on to sites and (c) intra-particle diffusion. In many cases there is a possibility that intra-particle diffusion will be the rate-limiting step and is given by (Karthikeyen, T., 2005) :

$$q_t = k_{id} t^{1/2} \tag{3.17}$$

The plot between q vs. $t^{1/2}$ gives the values of coefficient of intra particle diffusion (k_{id}) for different adsorption parameter. Again the plot between time (t) vs. percentage adsorption at different adsorption parameters may not be linear over the entire time range. In that case, more than one step may affect the adsorption process. So the adsorption process can be divided into two distinct steps, the initial curved portion relates to film diffusion (D_1) and the latter linear portion relates to the diffusion within the adsorbent. The equation for 'D_1' and 'D_2' are given by;

$$\frac{q_t}{q_e} = 6\left(\frac{D_1}{\pi a^2}\right)^{\frac{1}{2}} t^{\frac{1}{2}} \tag{3.18}$$

$$\ln\left(1 - \frac{q_t}{q_e}\right) = \ln\left(\frac{6}{\pi^2}\right) - \left(\frac{D_2 \pi^2 t}{a^2}\right) \tag{3.19}$$

'D_1' can be calculated from the slope of the plot between q_t/ q_e vs. $t^{1/2}$ for the initial curved portion. 'D_2' can be calculated from the slope of the curve between ln(1-q_t/q_e) vs. 't'.

3.4. Thermodynamic equations

Temperature dependence of the adsorption process is associated with several thermodynamic parameters. The standard Gibbs free energy is calculated by using the following equation:

$$\ln \frac{1}{b} = \frac{\Delta G^0}{RT}; \tag{3.20}$$

where b = Langmuir constant

T = absolute temperature

R = universal gas constant

The other thermodynamic parameters such as change in standard enthalpy (ΔH^0) and standard entropy (ΔS^0) are determined using the following equation

$$\ln k = \Delta S^0/R - \Delta H^0/T \tag{3.21}.$$

ΔS^0 and ΔH^0 are obtained from the slope and intercept of the vant Hoff's plot of lnk verses 1/T

The isosteric heat of adsorption (ΔH_r) is also calculated using the following equation:

$$\Delta H_r = \frac{R \ln \frac{C_2}{C_1}}{1/T_2 - 1/T_1} \tag{3.22}$$

where 'C_1' and 'C_2' are the equilibrium concentrations at temperatures 'T_1' and 'T_2', respectively.

The activation energy can be calculated by using the Arrhenius equation:

$$\ln k = \ln A - E_a/RT \quad (3.23)$$

where 'k' is the rate constant at temperature 'T' (in Kelvin), 'A' pre-exponential factor, 'R' the universal gas constant and 'E_a' (J/mol) is the activation energy for the process. The slope of the plot between lnk versus 1000/T, gives the activation energy.

3.5. Statistical parameters

The estimated values of the model parameters can be reported along with other statistical parameters such as correlation coefficient 'R^2' and the average absolute percentage deviation (% Dev) between $q_{e(cal)}$ and $q_{e(exp)}$ is calculated by using the following equation;

$$\%Dev = 100 \times \frac{1}{N} \sum_{i=1}^{N} \left| \frac{(q_e)_{\exp} - (q_e)_{pred}}{(q_e)_{\exp}} \right|_i \quad (3.24)$$

3.6. Experimental design and evaluation of optimum parameters

3.6.1. Experimental design method

Practical experiments are carried out to prove the validity of the theories and hypotheses. In order to develop a process, a number of influencing parameters are needed to be studied. But the process of studying each and every variance separately is quite tedious as well as time consuming. Thus, the optimization of parameters by using a design experimental model can minimize the above difficulties. With the availability of complete information relating to the process parameters with the help of thermodynamics, kinetics studies etc, one can develop a deterministic mathematical model to establish a process. This mathematical model may be a set of ordinary differential equations or partial differential equations. Once the model is established, the

variables coefficients of the equation can be determined with the progress of experiment. In other words, designing of an experiment means deciding how the observations or measurements should be taken to answer a particular question in a valid, efficient and economical way (Gun, A. M., 2002). Another feature of the design of experiment is to conduct a series of experiments in which purposeful change are made to the input variable of a process or system so that the reasons for changes in the output response may be observed and identified.

Generally there are three types of variables affecting a process, those are;

- Measurable or controllable input variable
- Uncontrollable or random input variable
- Response or output variable

The process guides the transfer of an input into an output that has one or more observable responses. The objectives of designing the experiments are:

- To determine those variables which are the most influential on the response
- To develop an empirical model based on the independent variable so that the response is almost always near the desired maximal/minimal value
- To minimize the effect of uncontrollable variables input
- To find out the optimal process parameters

Experimental design plays an important role in process development and process troubleshooting to improve performance.

3.6.2. Application of the method

Experimental design methods can be applied to many disciplines. In this method, experimentation is viewed as a part of the scientific process and as one of the ways to learn about how the system or process works. In general, knowledge is gathered through a series of activities in which conjectures are made about a process. Experiments are

carried out to generate data for the process and then the information from the experiments are used to establish new conjectures which lead to new experiment and so on. Experimental design method is an important tool in the engineering science for improving the performance of the process. It has also been applied extensively in the development of new processes. Application of this method in the process development can result in:

- Improved yield
- Reduced variability and closer conformance to nominal or target requirements
- Reduced development time
- Reduced overall cost

Engineering design plays a major role in optimising the process parameters, where new products are developed and existing ones are improved. Some applications of engineering design are;

- Evaluation and comparison of basic design configuration
- Evaluation of material alteration
- Selection of designing parameters so that the product will work well under a wide variety of field conditions
- Determination of key product design parameters which have impact on the product performance

3.6.3. Guidelines for designing of experiments

Application of statistical approach in designing and analyzing an experiment requires that every one involved with the experiment should have a clear idea about the parameters to be studied, collection of data and at least a qualitative understanding of how the data are to be analyzed. An outline of the recommended procedure is stated in brief (Montgomery, D. C., 1991)

- *Recognition and state of the problem*: Clear statements of the problem often contribute substantially to a better understanding of the phenomena and the final solution of the problem.
- *Choice of factors and levels:* At the beginning of a study, choice should be made about the factors to be varied in the experiments, the ranges over which this factors will be varied, and a specific level at which runs will be made. Consideration must also be given to how these factors are to be controlled at the desired values and how these are to be measured.
- *Selection of the response variable*: In selecting the response variables, it must be ascertained that this variable really provides useful information about the process.
- *Choice of experimental design*: If the first three steps are performed correctly this step becomes relatively easy. Choice of design involves consideration of sample size (number of replicates) and selection of a suitable number of trials. In selecting the design, it is important to keep experimental objectives in mind.
- *Performing the experiment:*. While running the experiments, it is essential to monitor the process carefully to ensure that everything is being done as per plan. Errors in experimental procedure at this stage will usually destroy experimental validity.
- *Data analysis*: Statistical method should be used to analyze the data so that the results and conclusions are objectives rather than conclusive in nature. If the experiments have been designed correctly and if it has been performed according to the design, then the statistical methods required are not elaborate.
- *Conclusion and recommendation*: Once the data have been analyzed, practical conclusions about the results are drawn and a course of action is recommended.

3.6.4. Using statistical methods in experimentation

Much of the research in engineering, basic science and industry are empirical and make extensive use of experimentation. Statistical methods can greatly increase the efficiency of these experiments and often strengthen the conclusion so obtained. Intelligent use of statistical methods in experimentation requires the following points to be considered (Mentgomery, D.C., 1991):

- Non-statistical practical knowledge of the problem.
- Design and analysis of sample.
- Recognition of the difference between practical and statistical significance.
- Iterative experiments..

Generally, there are three different engineering designing methods:

- Response surface methodology.
- Box –Behnken design.
- Factorial design.

Since the thesis covers only factorial design, the same would be discussed.

3.6.5. Factorial design

In factorial designing, the major input variables are noted as x_1, x_2, ….. x_k which form the basis of set of variables, as they control the entire range experiments. The output response variable is designated as y_1, y_2, ……, y_k. Applying regression correlation to the experimental data, various relationships can be established among the variables present in the process and the optimum condition can be well established. A typical mathematical model is:

$$y = \phi(x_1, x_2, ..., x_k) \tag{3.25}$$

In which y is represented as a function of x (input). Here y is a dependent variable and x is an independent variable, which include all input parameters. Approaching equation 3.25 by statistical method, the mathematical model becomes a polynomial. From the Taylor expansion series the equation 3.25 becomes:

$$y = \beta_0 + \sum_{j=1}^{k} \beta_j x_j + \sum_{u,j=1}^{h} \beta_{uj} x_u x_j + \sum_{j=1}^{k} \beta_{jj} x_j^2 \qquad (3.26)$$

where $\beta_j = \frac{\partial \phi}{\partial x_j}$ $\beta_{uj} = \frac{\partial^2 \phi}{\partial x_u \partial x_j}$ $\beta_{jj} = \frac{\partial^2 \phi}{2\partial x_j{}^2}$

In the actual process there are certain uncontrollable variables, which make the random variation of response variable. Thus, the experimental data are obtained in the form of simple regression coefficients like b_0, b_1, b_2, ….., b_j, b_{uj}, b_{jj} and thus the regression equation becomes:

$$y = b_0 + \sum_{j=1}^{k} b_j x_j + \sum_{u,j=1}^{h} b_{uj} x_u x_j + \sum_{j=1}^{k} b_{jj} x_j^2 \qquad (3.27)$$

where 'b_0' is regression free coefficient, 'b_j' is linear term, 'b_{jj}' is quadratic terms, and 'b_{uj}' is interaction term representing the interaction among the input variables.

During any experimental designing, certain fixed levels are assigned to each variable, which is deliberately varied from one experiment to the other. In case of full factorial design, all possible combination of the factors at all levels involved in the experiments is studied. The number of experiments to be performed (N) is given by:

$$N = n^K \qquad (3.28)$$

where 'n'=number of levels used during design of experiment, and 'k'= number of factors involved in the study. For example, in a two level full factorial experiment, each

factor has to be varied within two fixed levels and during the study, all possible combinations of the 'k' factors are used.

For optimization of a process, the investigator has to carry out some experiments on the process to generate certain data. The information obtained from the results are called as prior information, i.e., obtained before the beginning of the designed experiment. The prior information reveals the particular points, which can be utilized for optimization of the process parameters. It also gives an idea about the variant factor and how to optimize the parameters which vary with small variations in the values of the factors. Thus, for the selection of an experimental region, the prior information has to be analyzed in detail so as to get a perfect orientation of the trial run.

The secondary criterion is the selection of a base level. For any statistical experiment, the factor space chosen is a combination of levels corresponding to the best condition determined from an analysis of the prior information. The base level of an experiment is considered as the initial point in the factor space, which contributes maximum to the design of an experiment. It is also termed as the zero level or base level of the experiment. During experimental designing, the selection of the experimental point is symmetrically related to the base level. Once the zero level has been selected, the variation interval has to be chosen. For example, in case of a two level experiment, an upper and a lower levels are selected with similar intervals from the base level. For simplification of the experimental data, the scale along the axis is so selected that the upper level corresponds to +1 and the lower one to –1 and the base level as zero. This relationship can be represented as:

$$x_j = \frac{\bar{x}_j - x_j^0}{\Delta J_j} \tag{3.29}$$

where, x_j= Coded value of the factor,

$\bar{x}_j$ = Natural value of the factor,

x_j^0= Natural value of the base level,

ΔJ_j= variation interval and

J= Number of factors under consideration

In experimental designing, to get a linear model, the factors are varied in two levels. In qualitative approach, the upper level is coded as +1 and lower as –1. If the total numbers of factors are known, it is immediately possible to find the number of trial experiments needed for realization in all possible combinations by using the simple formula:

$$N = 2^k \tag{3.30}$$

where N=number of trial experiments, k=number of factor varies and 2=number of levels.

Once the experimental levels are chosen, the condition can be mentioned in the form of a table with rows and columns, where the rows correspond to different trials and columns as values of the factors. Such a representation is called experimental by designed matrix. Here, each column is termed as column factor and row factors as shown in Table 3.1.

Table 3.1: Experimental designing matrix with coded values

Trial runs	x_1	x_2	y
1	-1	-1	y_1
2	+1	-1	y_2
3	+1	+1	y_3
4	-1	+1	y_4

3.6.6. Establishment of a mathematical model to design factorial experiments

In designing an experiment, the first step is to get a model that should be nearer to the optimum point. In order to establish a factorial experiment mathematically, some

unknown terms named as factorial coefficient denoted by b_0, b_1, b_2 or b_1b_2 for different factors appear in the model frequently. The estimated value of these coefficients depends on the experimental results obtained from the trial runs.

The term b_0 is called the free term in the experiment and the other terms like b_1, b_2, etc. are calculated from the matrix multiplication. The interaction term b_1b_2 appears due to the fact that the effect of one factor depends on the level of influence of the other factor.

A factorial experiment is the only source to make it possible to quantitatively assess the individual independent term as well as interaction effects of different coefficients and factors. A possible way to calculate the factorial coefficient in a statistical design is shown in Table 3.2. For example: a two level of design experiment with three factors of influence are shown in Table 3.2

Table 3.2: Design of experiment for three factors

Trial runs	x_1	x_2	x_3	y
1	+	+	+	y_1
2	-	+	+	y_2
3	+	-	+	y_3
4	-	-	+	y_4
5	+	+	-	y_5
6	-	+	-	y_6
7	+	-	-	y_7
8	-	-	-	y_8

Using the least square method coefficient of the regression equation can be determined in the way of matrix calculus.

$$B = \begin{vmatrix} b_0 \\ b_1 \\ b_2 \\ b_3 \end{vmatrix} = (x^T x)^{-1} x^T . y \tag{3.31}$$

where this matrix corresponds to another experimental matrix of Table 3.3

Table 3. 3: Design of experiment for four factors

Trial No.	x_0	x_1	x_2	x_3	y
1	0	+	+	+	y_1
2	0	-	+	+	y_2
3	0	+	-	+	y_3
4	0	-	-	+	y_4
5	0	+	+	-	y_5
6	0	-	+	-	y_6
7	0	+	-	-	y_7
8	0	-	-	-	y_8

As a consequence, any coefficient say 'b_j' of the estimated regression equation is defined by the scalar product of any column by the respective 'x_j' column divided into the number of experiments 'N' in the design matrix

$$b_j = \frac{1}{N} \sum_{i=1}^{N} x_{ji} y_i \tag{3.32}$$

Using the design matrix presented in Table 3.3, the coefficients of the estimated linear regression equation are found to be:

$$y = b_0 + b_1 x_1 + b_2 x_2 + b_3 x_3 + ... \tag{3.33}$$

3.6.7. Student 't' test

The student't' distribution has simplified the statistical matrix calculation. When the systematic errors are absent in an experiment, the expected values of random

variables coincide with the true results of observation. Therefore, the estimation of the mean values is important in processing an observation data.

The mean or zero level value is the easiest value to estimate the variance in the population. However, no observation can lead to the population variance 'σ^2' in a designed experiment. The population variance can only be estimated in terms of the simple variance, 'S^2', represented by the relation:

$$\sigma^2 = S^2 \tag{3.34}$$

The error resulting from the replacement of the population variance by sample variance gradually decreases as the sample size increases. When the sample size is small, in order to ignore the corresponding error, a confidence interval is assumed for the expected value using student 't' distribution.

The student 't' distribution holds for a random variable:

$$t = \frac{x - \mu}{S / \sqrt{n}} \tag{3.35}$$

Where x=sample mean

$\sqrt{n}$ =sample size variation

t= deviation of the estimated mean from that of the population measured in terms of $S/\sqrt{n}$ unit and

μ= the confidence level

The denominator, $S/\sqrt{n}$ is a useful quantity estimating $\sigma/\sqrt{n}$ i.e. the standard error in the sample. In large samples, the standard error can be avoided with μ=0 and σ= 1. But when the sample size is less than 50, the distribution becomes obvious. The student 't' distribution is symmetrical about the mean.

3.6.8. Test to signify the coefficients

The significance of individual coefficient of a regression equation can be tested separately by two different ways, i.e. using student 't' test or by constructing the confidence interval. For a full factorial design, the confidence intervals for all variable coefficients including interacting terms are equal.

The degree of variance is first found out for the regression coefficient S^2b_j. This regression coefficient can be determined with the formula:

$$S^2 b_j = S_e^2 / N \tag{3.36}$$

This formula indicates that the variances for all the coefficients are equal as they depend on the error of the trial experiment.

Thus, for constructing the confidence level,

$$b_j = \pm t Sb_j \tag{3.37}$$

where, 't' is the tabulated degree of freedom. Here, S^2_e was determined at selected significance level, usually 0.05.

Sb_j is the quadratic error of the regression coefficient represented as

$$Sb_j = +\sqrt{S_e^2} \tag{3.38}$$

Let us consider as an example that three replicated observations have been made at the base level or center point and the designed matrix yield the following values,

y_1^0=8.0, y_2^0=9.0, y_3^0=8.8

Thus, $\overline{y_0} = \frac{1}{3}\sum_{u=1}^{3} y^0 = 8.6$

$S_e^2 = \frac{1}{2}\sum_{u=1}^{3}\left(y_u^0 - \overline{y_0}\right)^2 = 0.28$

S_e=0.55

Sb_j=0.55/8=0.2

The significance of individual parameters and their coefficients can be tested using student 't' test.

$$t_0 = \frac{b_0}{S_{b0}} = \frac{8.5}{0.2} = 42.5 \quad t_1 = \frac{b_1}{S_{b1}} = \frac{2.5}{0.2} = 12.5$$

For the significance level of α =0.05 and ν =2 (degree of freedom), the tabulated value of student't' distribution is t_α (ν) = 4.3.

Thus, t_α (ν) represents a level and coefficient of regression equation having value less then 4.3 are considered to be insignificant and those values can be deleted from the main regression equation. After the deletion of the insignificant coefficient from the regression equation, it is then verified using Fisher's adequacy test.

3.6.9. Test of adequacy of a model

In order to test whether the coefficient of the equations are fitting to its model, an adequacy test has to be carried out. This type of test is known as testing of the adequacy of a model.

Let us consider two experimental models containing two illustrations with an identical arrangement of the experimental points and consequently with an identical scatter relative to regression line, best with a different mean scatter at a point (with a

different variance of reproducibility). The scatter points are shown by lengths of the straight line forming the confidence interval equal to +2 S_e.

Out of these two models first model is adequate because in the given case the scatter at the points is of the same order as that related to the lines. This short of observation can explain the qualitative estimations but quantitative measurement is essential for testing adequacy of the model. The residual sum of square is quite suitable for characterizing the mean scatter related to the line of regression. This residual sum of the equation depends on the number of coefficient present in that equation and sometimes the sum becomes zero. This is the reason for which it is preferred to relate this term to one free trial. The number of such trial is called the number of degrees of freedom. The difference between the number of trial and the number of coefficients, that have already been calculated according to the results of trials, independent of one another, which is called the number of degrees of freedom.

If a 2^3 factorial experiments is designed, number of degrees of freedom (f) is expressed:

$$f = N - (k+1) = 8 - (3+1) = 4 \tag{3.39}$$

This residual sum of squares divided by the number of degree of freedom is called the variance of adequacy. The modified regression equation is then tested to see how it fits the observations using Fisher's test. The variance ratio is given by:

$$F = S_{res}^2 / S_e^2 \tag{3.40}$$

where $$S_{res}^2 = \frac{\sum^{8} \left(y_i - \hat{y}_i\right)^2}{N - m} = \frac{6}{4} = 1.5 \tag{3.41}$$

If S_e^2=0.28 and m (number of significant coefficients in the regression equation)=4, then F=1.5/0.28=5.3

The tabulated value of Fisher's variance ratio (F) for $\alpha=0.05$, $\nu_1=4$ and $\nu_2=2$ is

$$F_{1-\alpha} \propto (\nu_1, \nu_2) = 19.3 \tag{3.42}$$

Thus, $F_{\alpha}<F_{1-\alpha}(\nu_1, \nu_2)$ and the estimated regression equation given above fits the experimental data adequately.

3.6.10. Level of significance

Sample parameters are random variables and their deviation from the respective population parameters are likely to be random. These deviations can only be estimated by giving the probability of particular deviation. For these estimations, mathematical statistic can be used with the following two concepts:

(i) Confidence interval

(ii) Level of significance

Let an experiment yield a^* of a, i.e. population parameter 'a' has an unbiased estimate a^*. In order to determine the probability of an error in this estimation, a sufficiently high probability level $P=1-\alpha$ has been taken for consideration.

Thus, the probability (ε) is given by

$$\varepsilon = f(P) = \varepsilon_{1-\alpha} \tag{3.43}$$

Thus, $$P\left(a^* - a / \leq \varepsilon_{1-\alpha}\right) = 1-\alpha \tag{3.44}$$

The range of errors arises due to replacement of a by a^* is $\pm\varepsilon_{1-\alpha}$ and the value of 'α' can be determined by the relationship, $\alpha=1-P$, which is called the level of significance and in statistical designing this significance level is expressed in term of percentage.

This expression can also be expressed as the probability that the values of parameter ‘a’ can be found between

$$a^{*} - \varepsilon_{1-\alpha} \leq a \leq a^{*} + \varepsilon_{1-\alpha} \quad (3.45)$$

The probability (1- α) is called the confidence level of the designed experiments and this coefficient characterizes the degree of assurance in the estimate obtain the interval, $1=a^{*}+ \varepsilon_{1-\alpha}$ is called the confidence interval and the limits of these values lies between $a'=a^{*}- \varepsilon_{1-\alpha}$ and $a''=a^{*}+ \varepsilon_{1-\alpha}$ where a’ and a” are called the confidence limit. At a given confidence level, the interval between the lower and upper limits define the certainty of the estimated values.

The magnitude of confidence interval depends on the confidence coefficient with which the parameter ‘a’ is guaranteed to lie inside the confidence interval, i.e. greater the value of 1- α, higher the value of $\varepsilon_{1-\alpha}$.

Thus, the more we guarantee the standardization of the result, the larger the confidence interval within which it lies. As the number of observation increases, the confidence interval gradually decreases. For practice, it is very unusual to fix the confidence coefficient at 0.9 (90%), 0.95 (95%) or 0.99 (99%) and the confidence interval $\varepsilon_{1-\alpha}$ is then found accordingly.

3.7. Breakthrough curve modeling

The performance of a packed bed reactor is obtained through the concept of breakthrough curve. The time for breakthrough appearance and the shape of the breakthrough curve are very important characteristics for determining the operation and the dynamic response of a adsorption column. Again, successful design of an adsorption column requires prediction of the concentration-time profile or breakthrough curve for the output. In many cases, kinetics of adsorption in column has been tested for Bohart-Adams model. However, it has also been shown that Bed Depth Service Time (BDST),

Thomas and Yoon-Nalson model can sometimes provide a better description of the adsorption kinetics. So in this study, attempt has been made to find out the best model describing the adsorption kinetics in column.

3.7.1. Bohart-Adams model

Bohart and Adams derived a fundamental equation describing the relationship between C/C_0 and 't' in a continuous flowing system for the adsorption of chlorine on charcoal. This model was established based on the surface reaction theory and it assumed that equilibrium is not instantaneous. Therefore the rate of adsorption was proportional to both the residual capacity of the activated carbon and the concentration of the sorbing species (Goel, J., 2005; Malc, E., 2006;). The Bohart-Adams model was used for the initial part of the breakthrough curve (Aksu, Z., 2004; Liao, X., 2004). Its overall approach is now being applied successfully in quantitative description of other systems. The mathematical equation of the model can be written as:

$$\ln \frac{C_t}{C_0} = k_{AB} C_0 t - k_{AB} N_0 \frac{z}{U_0} \tag{3.46}$$

where 'C_0' and 'C_t' are the inlet and outlet adsorbate concentrations respectively, 'Z' (cm) is the bed height, 'U_0' is the superficial velocity (cm/min), 'N_0' is the saturation concentration (mg/L) and 'k_{AB}' is the mass transfer coefficient (l/mg min). In the present study the range of time was considered from the beginning to the end of the breakthrough curve.

3.7.2. The Bed Depth Service Time (BDST) model

The Bed Depth Service Time model which is a modified form of Bohart-Adams model (Tan, T. W.,1993; Bohart, G. C., 1920; Muralidharan, T. R., 1994) was used to compare the uptake capacity of the adsorption columns. This model was derived based on the assumption that intra-particle diffusion and external mass transfer resistance are

negligible and that the adsorption kinetics is controlled by surface chemical reaction between solute in the solution and the unused adsorbent. This model also serves as a useful tool for comparing the performance of columns operating under different process variables. The BDST model is expressed as

$$C_o = \frac{N_0 h}{u} - \frac{1}{k}\ln\left(\frac{C_0}{C_t} - 1\right) \tag{3.47}$$

where 'C_0' and 'C_t' are inlet and output concentration respectively, 'k' is the adsorption rate constant (mg/min), 'N_0' is the adsorption capacity (mg/g), 'h' is the bed depth (cm) and 't' is the service time to breakthrough (min).

3.7.3. Thomas model

Thomas model is one of the most general and widely used models in the column performance theory. Thomas or reaction model assumes Langmuir kinetics of adsorption-desorption with no axial dispersion and is derived with the assumption that the rate driving force obeys second order reversible reaction kinetics. Thomas model also assumes a constant separation factor but is applicable to either favorable or unfavorable isotherms. The expression developed by Thomas (Thomas, H. C., 1944), calculates the maximum solid phase concentration of the solute on the sorbent and the adsorption rate constant for a continuous adsorption process in the column. The linearised form of the model is given as:

$$\ln\left(\frac{C_0}{C_t} - 1\right) = \frac{k_{Th} q_0 m}{Q} - \frac{k_{Th} C_0 V_{eff}}{Q} \tag{3.48}$$

where 'K_{Th}' is the Thomas rate constant (mL/mg min), 'q_0' is the equilibrium adsorbate uptake (mg/g) and 'm' is the amount of adsorbent in the column.

3.7.4. Yoon-Nelson model

Yoon and Nelson developed a relatively simple model addressing the adsorption and breakthrough of adsorbate gases with respect to activated charcoal. This model was derived based on the assumption that the rate of decrease in the probability of adsorption for each adsorbate molecule is proportional to the probability of adsorbate adsorption and the probability of adsorbate breakthrough on the adsorbent (Yoon, Y. H., 1984). The linearised model for a single component system is expressed as:

$$\ln\left(\frac{C_t}{C_0 - C_t}\right) = k_{YN}t - \tau k_{YN} \tag{3.49}$$

where 'k_{YN}' is the rate constant (min^{-1}), 'τ' is the time required for 50% adsorbate breakthrough.

3.7.5. Error analysis

In order to find out the best model from the goodness of fit with the experimental values it is necessary to analyze the data using error analysis. So in the present study a number of error analysis methods such as the sum of the square of the error (SSE), the sum of the absolute error (SAE), average relative error (ARE) and the average relative standard error (ARS) were used to find out the model which was best fit to the experimental observations. The expressions for some error functions are as follows (Lazaridis, N. K., 2003; Leyva, R. R, 2005; Aksu, Z., 2005; Kundu, S., 2006):

$$SSE = \sum_{i=1}^{n} (y_c - y_e)_i^2 \tag{3.50}$$

$$SAE = \sum_{i=1}^{n} \left| y_c - y_e \right|_i \tag{3.51}$$

$$ARE = \frac{1}{n}\sum_{i=1}^{n}\left|\frac{y_c - y_e}{y_e}\right| \tag{3.52}$$

$$ARS = \sqrt{\frac{\sum_{i=1}^{n}[(y_c - y_e)/y_e]^2}{n-1}} \tag{3.53}$$

where 'n' is the number of experimental data points, 'y_c' is the predicted (calculated) data, 'y_e' is the experimental data and 'y' represents the ratio of C_t/C_0. The above statistical error expressions were applied to all the breakthrough curve model equation.

CHAPTER-4

ADSORPTION OF Cr(VI) ON CALCINED BAUXITE

Adsorption of Cr(VI) on calcined bauxite

4.1. Adsorbent preparation

Bauxite is abundantly available in the earth crust. India ranks fourth in the world amongst the bauxite-producing nations. Bauxite is the only ore from which aluminimum is extracted commercially. The bauxite ore used in this study was collected from the captive mines of National Aluminium Company (NALCO), Pachpatmali, Koraput, Orissa. Aluminium in bauxite is mainly present in the form of gibbsite and it contains other iron bearing minerals. The ore is used as feed material for extraction of alumina in the NALCO refinery situated at Damanjodi. The lumpy sample collected was crushed and ground to powder form. The powdered bauxite sample was sieved to different size fractions. The smallest size fraction (–125 μm) was used for further treatment before using as an adsorbent. The adsorbent was treated in two ways:

- Heating up the bauxite at 450 ^{0}C for 4 h and the
- Treating with 0.5 N HCl solution.

For acid treatment, 60 mL of 0.5 N HCl was added to 25 gm of bauxite and refluxed for one hour. Then the residue was filtered and washed several times with distilled water to remove acidic solution adhering to it and dried at 100 ^{0}C.

4.2. Characterization of material

4.2.1. Specification of physical parameters

Bulk density

The bulk density of the sample was studied in a Jolly's spring balance using a liquid of known density. Weight of the sample was first measured in air. Then the material was completely immersed in the liquid and weighed carefully. From these two weights, the bulk density of the sample was calculated using the following equation:

$$\text{Bulk density } D = \frac{A}{A-B}\rho_T \qquad (4.1)$$

where A= weight of the solid in air

B= weight of the solid when immersed in the test liquid.

ρ_T= density of the test liquid at the operating temperature T.

The results are shown in Table 4.1

Specific gravity

The specific gravity of the sample was determined using specific gravity bottle. The sample was first weighed in the specific gravity bottle. It was then immersed in water inside the specific gravity bottle and then weighed accurately. The specific gravity was then calculated using the following formula and the value is given in Table 4.1

$$\text{Specific gravity } S = \frac{A}{A-B}\rho_T \qquad (4.2)$$

Porosity

The porosity of the material was calculated from the bulk density obtained from the volume displacement of material in water using the following formula

$$\% \text{ Porosity } = \frac{w_2 - w_1}{w_2 - w_3} \times 100 \qquad (4.3)$$

Where w_1= weight of the sample

w_2= weight of the water saturated sample

w_3= sample weight under immersed conditions

The results are shown in Table 4.1

4.2.1.1. Particle size analysis by Malvern particle size analyzer

Particle size was analyzed by Malvern make Particle Size Analyzer (model 2000). It was found that 95% of the particle belonged to 25 μm size range as shown in Fig.4.1.

4.2.1.2. Analysis of specific surface area by BET method

The specific surface area of the powder was analyzed by nitrogen adsorption at 77 K applying BET method in Quantaserb (Quanta Chrom-USA). Degassing at 100 ^{0}C and 2 to 10 mm Hg for 2 h was performed prior to measurement. The specific surface area of bauxite, acid treated bauxite and calcined bauxite are given in Table 4.1

4.2.2. Chemical characterization

4.2.2.1. Chemical composition of adsorbent by XRF analysis

To determine the chemical composition of bauxite, X-ray fluorescence (XRF) analysis was carried out on Philips spectra 300T equipped with Ti-target X-ray tube. The tube voltage was set at 24 kV with current of 81 A. The count and warm-up time were 40 and 4 sec respectively. The region of interest (ROI) was between 7 and 11 keV, while a back correction was done between 12 and 17 keV. The chemical composition of the adsorbents are shown in Table 4.2

4.2.2.2. X-ray diffraction analysis

X-ray diffraction (XRD) analysis was carried out using Cu Kα radiation on a computer controlled Philips make 1050 defractometer. The scan speed was 0.5^0 2θ per minute and step size was 0.02 ^{0}2θ. XRD Patterns were recorded from 10 to 70^{0}2θ . The XRD patterns for untreated and calcined bauxite are shown in Fig.4.2. The characteristic peaks at 4.82, 2.42, 1.95 and 1.65 for the untreated sample indicated gibbsite ($Al(OH)_3$) as the main constituent. Some characteristic peaks at 3.5, 2.69, 2.51, 1.91, 1.8, 1.694 and

1.41 show the presence of goethite (FeOOH). However, on calcination the characteristic peaks for gibbsite disappeared and new peaks appeared at 2.51, 2.24, 1.84, 1.48 and 1.45, which indicated the conversion of gibbsite to bohemite (Al_2O_3). Also the peaks for goethite disappeared partly on calcined bauxite and new peaks appeared at 2.72, 2.34, 2.17, 1.66 and 1.46 corresponding to hematite. The disappearance of lines corresponding to gibbsite and goethite indicated the dehydration of the ore on calcination.

4.2.2.3. Scanning Electron Microscope (SEM) analysis

Powdered uncalcined bauxite and calcined bauxite after adsorption were analyzed by Scanning Electron Microprobe (SEM JXO-8100) at 300X magnification and the results are presented in Figs.4.3-4.5. It can be seen from the figures that the bauxite after calcination has irregular porous structures, which may be due to the change in lattice structure on heating. Due to evaporation of water of crystallization as well as free water molecule on heating, additional cleavages in the lattice structure were created thereby increasing the porosity in the adsorbing material. A comparison of the SEM images before and after adsorption also showed change of morphology and the grain size increase due to adsorption on the surface. EDAX results showed (Figs.4.6-4.8.) the increase of Cr count after adsorption, which unequivocally proved the adsorption of the said ion on the adsorbent.

4.2.2.4. FTIR studies

FTIR analysis of the adsorbents was carried out using JASCO make FTIR-3500 spectrophotometer. Pellets (press disk) were used for measuring absorption spectra. The samples were ground with 200 mg of KBr (spectroscopic grade) in a mortar and pressed into 10 mm diameter disks under 10 tons of pressure and high vacuum for FT-IR analysis. The conditions used were 16 scans at a resolution of 4 cm^{-1} measured between 600 and 4000 cm^{-1}. The results are shown in Fig.4.9.

4.3. Adsorption experiments

The stock solution of Cr(VI) having concentration 1000 mg/L was prepared by using dried crystalline $K_2Cr_2O_7$ (Analytical grade). Experimental solutions of the desired concentrations were obtained by successive dilution. The pH of the solution was maintained at desired value by adding dilute HCl or NaOH solution before adsorption.

Adsorption experiments were carried out in 100 mL stoppered conical flasks using 25 mL Cr(VI) solution with required amount of adsorbent. The flasks were continuously shaken for the required time period in Yorko thermostatic water bath-cum-shaker. The mixture was filtered through Whatman 42 filter paper and the volume was finally adjusted to 25 mL. The residual Cr(VI) concentration after filtration was determined spectrophotometrically using a Chemito 2500 double beam recording type spectrophotometer (Chun, L., 2004). All experiments were carried out using AR/GR grade E Merck chemicals.

4.4. Results and discussion

4.4.1. Effect of treatment of bauxite

The following bauxite samples were used to determine the efficiency of Cr(VI) adsorption from solution:

- Untreated bauxite
- Acid treated bauxite
- Calcined bauxite

0.5 g of the adsorbent was taken in 100 mL conical flask and shaken for different time intervals at ambient temperature after adding 25 mL of 10 mg/L synthetic Cr(VI) solution. The samples were filtered and Cr(VI) content of the filtrates was estimated.

The percentage of adsorption were calculated and plotted against the contact time as shown in Fig.4.10. All the three adsorbents showed very fast kinetics initially followed by a slower one. From the figure it is concluded that the adsorption efficiency of calcined bauxite in removing Cr(VI) was the highest as compared to bauxite as such and acid treated bauxite. Since the calcined bauxite was found to be the best amongst the three samples tested under identical conditions, further adsorption studies were carried out with the calcined bauxite only. The surface area of bauxite, acid treated bauxite and calcined bauxite were 18.83, 112.5 and 167.53 m^2/g respectively. The higher efficiency of adsorption for calcined bauxite was due to higher surface area as adsorption efficiency depends on surface area. Similar observation was reported for Cu adsorption (Das, L., 2005). The progressive increase of surface area from bauxite to acid treated bauxite and finally to calcined bauxite may be due to change in crystal structure. As discussed earlier, the bauxite as such showed XRD peaks confirming the presence of gibbsite and goethite. The calcined bauxite showed the lines corresponding to bohemite and hematite. Calcination of bauxite resulted in the loss of water and other inorganic impurities. The loss might have initiated the cracking in crystal structure resulting in increase of surface area. Details of the XRD peak and assigned groups are listed in Table 4.3

4.4.2. Effect of contact time

Effect of contact time between the adsorbate and adsorbent particles is one of the important parameters in the adsorption studies. To find out the effect of contact time on Cr(VI) sorption process, adsorption experiments were carried out over different contact time for varying concentrations of the adsorbent (Fig.4.11) as well as adsorbate (Fig.4.12). Aqueous Cr(VI) solution with initial concentration of 10 mg/L was kept in contact with different amounts of adsorbent (0.5, 1.0, 1.5 g/25 mL) for 4 h. The residual concentration of Cr(VI) beyond 2 hours showed hardly any adsorption. Further, it was observed that the adsorption kinetics increased slowly upto 1 h at low adsorbate concentrations (10 mg/L) and beyond that the increase was marginal. For high adsorbate concentration (30 mg/L), the adsorption kinetics increased upto 10 min. Therefore, after 1 h of contact time a steady state approximation was assumed and a quasi-equilibrium

situation was attained for Cr(VI) concentration of 10 mg/L and the same assumption is valid after 10 min for Cr(VI) concentration of 30 mg/L. In other words, the equilibrium time is very less (10 min) for higher adsorbate concentrations while it is more (1 h) for low adsorbate concentrations. Hence, time has very little effect on percentage adsorption since adsorption was fast. This is one of the advantages of using bauxite. Accordingly, all the batch experiments were conducted with a contact time of 10 to 60 min under vigorous shaking conditions.

The rate of Cr(VI) removal was found to be very rapid during the initial 10 min, and thereafter, the rate of removal decreased considerably. No significant change in metal ion removal was observed after 1 h. During the initial stage of sorption, a large number of vacant surface sites are available for adsorption. After a lapse of time, the remaining vacant surface sites are difficult to be occupied due to repulsive forces between the adsorbate molecules on the solid surface and in the bulk phase. Besides, the metal ions are adsorbed into the meso-pores that get almost saturated during the initial stage of adsorption. Thus the driving force for the mass transfer between the bulk liquid phase and the solid phase decreases with the passage of time. Further, the metal ions have to traverse farther and deeper into the pores encountering much larger resistance (Srivastava, V. C., 2006). This results in the slowing down of the adsorption during the later phase.

4.4.3. Effect of pH

The pH is an important parameter in adsorption process, especially for treatment of wastewater since their initial pH varied widely. The variation of pH affects the efficiency as hydrogen ion itself is a strong competing adsorbate, and the chemical speciation of the cations and anions depend on the same. Fig.4.13 shows the effect of pH on Cr(VI) adsorption. It is observed that the adsorption efficiency decreased with the increase of pH upto 3.8 and on further increase the adsorption efficiency slowed down and beyond 7.4 the pH hardly had any effect. The effect of pH on the adsorption may be attributed due to the combined effect of the nature of surface and the presence of acid and

base used to adjust the pH of the solution. To explain the observed behavior of Cr(VI) adsorption with respect to pH, it is necessary to examine various mechanisms such as electrostatic attraction/repulsion, chemical interaction and ion exchange, which are responsible for adsorption on sorbent surfaces.

From the Eh-pH diagram (Benefield, L. D., 1992), it is evident that the most prevalent forms of Cr(VI) in aqueous solution are acid chromate ($HCrO_4^-$),chromate(CrO_4^{2-}), dichromate ($Cr_2O_7^{2-}$) and other oxy-anions. From the stability diagram of Cr(VI)-H_2O system, it is evident that at low pH, acid chromate ion ($HCrO_4^-$) is the dominant species. As the pH increased, there was a slight increase in the percentage adsorption and attained a peak was attained at 3.8. When the pH further increased, a sharp decrease in percentage of adsorption was observed. This may be due to weakening of electrostatic force of atraction between the adsorbate and the adsorbent, and it ultimately led to the reduction in sorption capacity. When the pH increased beyond 6.0, a gradual decrease in the percentage adsorption may be due to the competition between OH^- and the dichromate ions ($Cr_2O_7^{2-}$), the former being the dominant species at higher pH values. The net positive surface potential of sorbent, decreased resulting in weakening of electrostatic force between the sorbate and the sorbent, which ultimately leads to lowering the sorption capacity. Similar results were also observed with fly ash (Dermatas, D., 2003) and coal (Arslan, G. 2007). The point of zero charge (pzc) was found to be at pH 7.4. This is in agreement with our experimental observation showing very low adsorption at pH>7

The FT-IR spectra for the bauxite as such, calcined bauxite and calcined bauxite after adsorption are shown in Fig.4.9**.** The details of the FT-IR peaks and the assigned groups are listed in Table 4.4. The absorption bands at 3650, 3520 and 3380 cm^{-1} may be assigned to the –OH stretching frequencies of gibbsite. Bands found at 1100, 1020, 915 and 743 cm^{-1} correspond to the –OH bending deformation in calcined bauxite. Two sharp peaks obtained at 1160 and 1080 cm^{-1} correspond to –OH stretching for bohemite. Similarly, peaks at 1713, 1560, 1640, 1340, 1324 and 1240 cm^{-1} correspond to the –OH vibration in goethite. These results are similar to the ones reported earlier (Frost, R. L.,

1999, Ruan, H. D., 2002). These peaks were either shifted or not detectable in non-calcined bauxite as well as calcined bauxite after adsorption. From these observations it can be concluded that the bauxite after treatment had different phases as compared to untreated and used samples. These corroborated from similar observations from XRD analysis.

4.4.4. Effect of initial adsorbate concentration

The percentage adsorption with different adsorbate concentrations was studied by varying Cr(VI) concentration from 10 mg/L to 30 mg/L keeping adsorbent dose at (1 g/25 mL), stirring speed (400 rpm), pH (3.8), and temperature (25 ^{0}C) constant. Fig.4.14 shows the effect of initial adsobate concentration vis-à-vis the adsorption efficiency. It is observed that the percentage of adsorption decreased with the increase of adsorbate concentration whereas the reverse trend is observed in case of Cr(VI) uptake. This may be due to the fact that at a fixed adsorbent dose, the number of active adsorption sites to accommodate the adsorbate ions remained unchanged while with higher adsorbate concentrations, the adsorbate ions to be accommodated increased. Thus, the loading was faster with higher initial concentrations of adsorbate.

4.4.5. Effect of adsorbent dose

To find out the effect of adsorbent dose for the adsorption of Cr(VI) from aqueous solution, adsorption studies were carried out at an initial Cr(VI) concentration of 10 mg/L with different adsorbent doses at different time intervals. The percentage of adsorption increased from 60.7 to 88.67 for an increase in adsorbent dose from 20 to 100 g/L as shown in Fig.4.15, whereas the Cr(VI) uptake decreased from 3.04 to 0.88 mg/g for the same adsorbent dose. Higher percentage of adsorption with the increase of adsorbent concentration can be attributed to increase in surface area and the availability of more binding sites for adsorption (Garg, U. K., 2004). The decrease in uptake with increase in adsorbent dose may be due to overlapping of adsorption sites as a result of over-crowding of adsorbent particles (Namasivayam, C., 1998). Since the slope of the line is < 1, the

increase in adsorption may not be directly proportional to adsorbent concentration. Similar trend has also been reported by other authors relating to Cr(VI) sorption (Garg, U. K., 2006) using other materials.

4.4.6. Effect of temperature

Temperature dependence of the adsorption process is associated with several thermodynamic parameters. Adsorption studies were carried out at different temperatures taking the same adsorbate (100 mg/L) and adsorbent concentrations (2 g/50 mL), which were equilibrated for 1h (Fig.4.16). Initially the percentage adsorption increased up to 46 ^{0}C and then decreased steadily. Hence, the optimum adsorption took place at 46 ^{0}C. The decrease in percentage adsorption beyond 46 ^{0}C might be due to the increase in desorption rate. The standard Gibbs free energy (ΔG^0) was calculated by using equation 3.20. The calculated ΔG^0 value is 3.26 kJ/gmol. The isosteric heat of adsorption (ΔH_r) is also calculated using equation 3.22. The ΔH_r values were calculated for the temperature range 34 ^{0}C to 46 ^{0}C and found to be +553.32 J/mole. The positive heat of adsorption indicates that the process is endothermic in nature.

4.5. Adsorption isotherms

At a fixed initial concentration of the adsorbate (10 mg/L), the adsorbent dose was varied. Different adsorption isotherms were tested for the adsorption process. It was found that the data fitted well into the linearized Freundlich adsorption isotherm, whose mathematical expression is given in equation 3.2. The plot of log (x/m) vs. log (C_e) (Fig.4.17) shows a linear curve and hence the adsorption obeys the Freundlich adsorption isotherm. Freundlich constant 'n' from the 'Y' intercept and 'K_f' from the slope of the curve was found to be 0.429 and –0.2878 respectively.

The Langmuir adsorption isotherm whose mathematical expression is given in equation 3.3 was applied for the equilibrium adsorption data. The linear plot of C_e/q_e vs. 'C_e' (Fig.4.18) shows that the adsorption obeys the Langmuir adsorption isotherm also.

'Q_o' and 'b' are determined from the slope and intercept of the curve and found to be 2.021 and 0.2742 respectively.

4.6. Study of rate constant

Adsorption of Cr(VI) from liquid phase into the solid phase can be considered as a reversible process with equilibrium established between the two phases. An attempt was made to study the rate constant for adsorption of Cr(VI) on calcined bauxite in the light of Lagergrens first order equation, which is given in equation 3.7. The plot log (q_e – q) vs. 't' at fixed adsorbent (1 g) and adsorbate (15 mg/L) doses is given in Fig.4.19. The value of the correlation coefficient (R^2) and specific rate constant (K_{ad}) is found to be 0.9396 and 0.0417 sec^{-1} respectively.

A pseudo second order kinetic model may also be applicable to this sorption process, the mathematical expression of which is given in equation 3.15. The t/q_t vs. 't' are plotted and shown in Fig.4.20. The correlation coefficient (R^2) and rate constant (k) are found to be 0.9999 and 9.097 respectively. From the R^2 values it can be concluded that the adsorption process follows pseudo second order kinetics.

4.7. Conclusions

The calcined bauxite has been found to be effective for removal of Cr(VI) from aqueous solutions. The efficiency of adsorption increased by heating the adsorbent at 450 ^{0}C for 4 h. The increase in adsorption may be due to the change in the lattice structure of adsorbent. This is amply proved from various physical structure analyses like XRD, SEM and FTIR. The uncalcined and calcined bauxite samples after adsorption were quite different in structure as compared to the calcined bauxite, which show different phases with higher number of holes or sites available for adsorption. The adsorption process follows pseudo second order kinetics and obeys the Freundlich and Langmuir isotherms. Low concentration Cr(VI) in solution promoted its efficient removal from the solution and it increased with increase in the adsorbent doses. Due to easy availability and high

efficiency of the removal of Cr(VI) from solution, the calcined bauxite shows promise for practical application. Applicability of different isotherms was also tested to arrive at the adsorption constants.

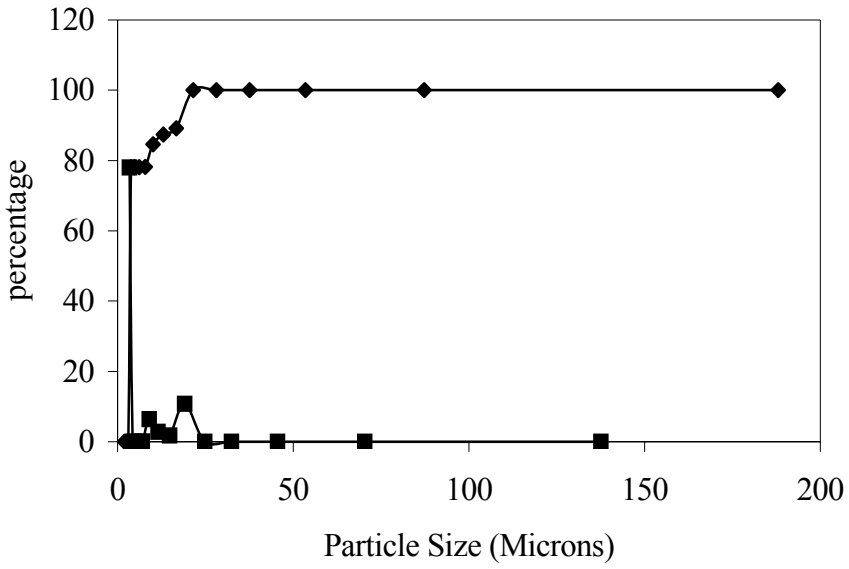

Fig.4.1. Particle size distribution of powdered and sieved bauxite

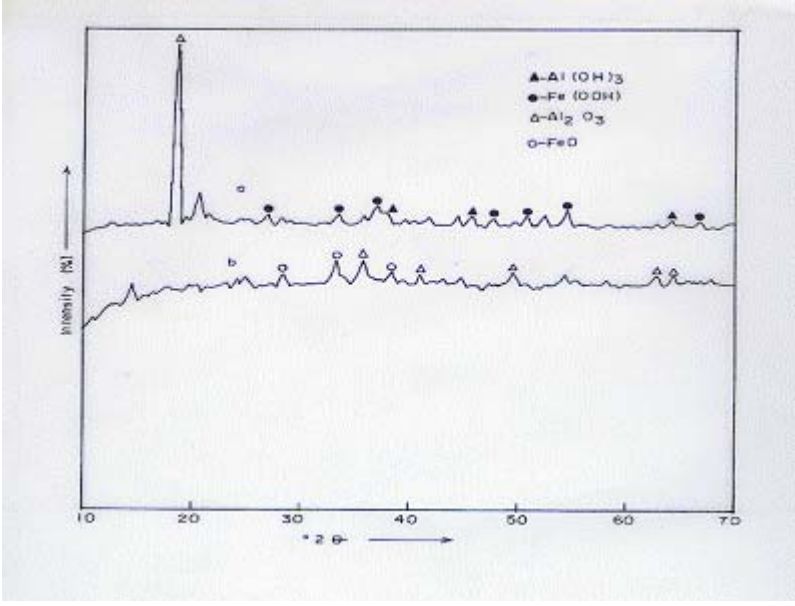

Fig.4.2. X-ray diffraction patterns of (a). Bauxite, (b). Calcined Bauxite

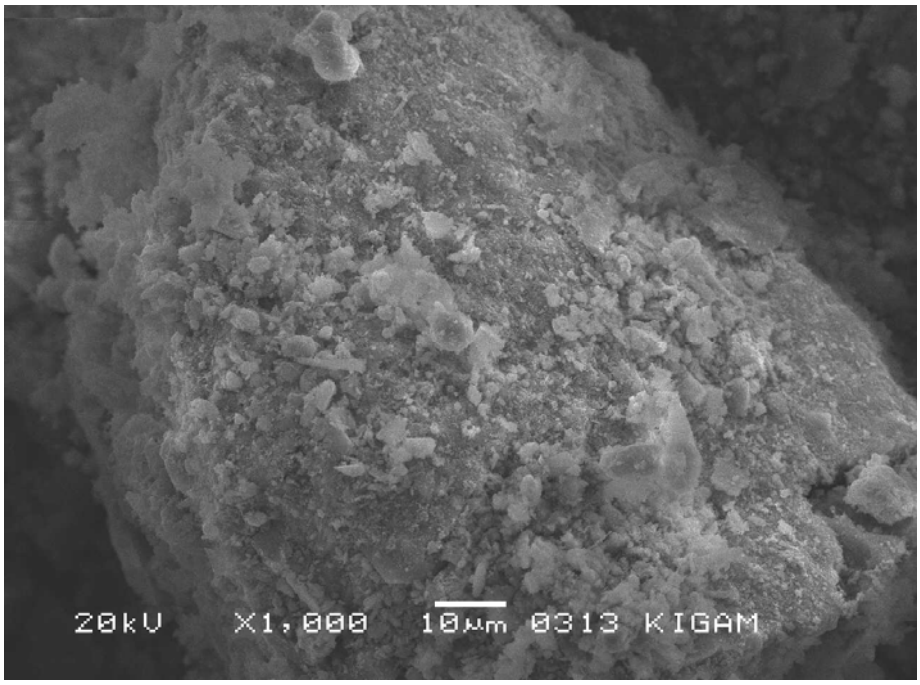

Fig.4.3. SEM image of bauxite before treatment

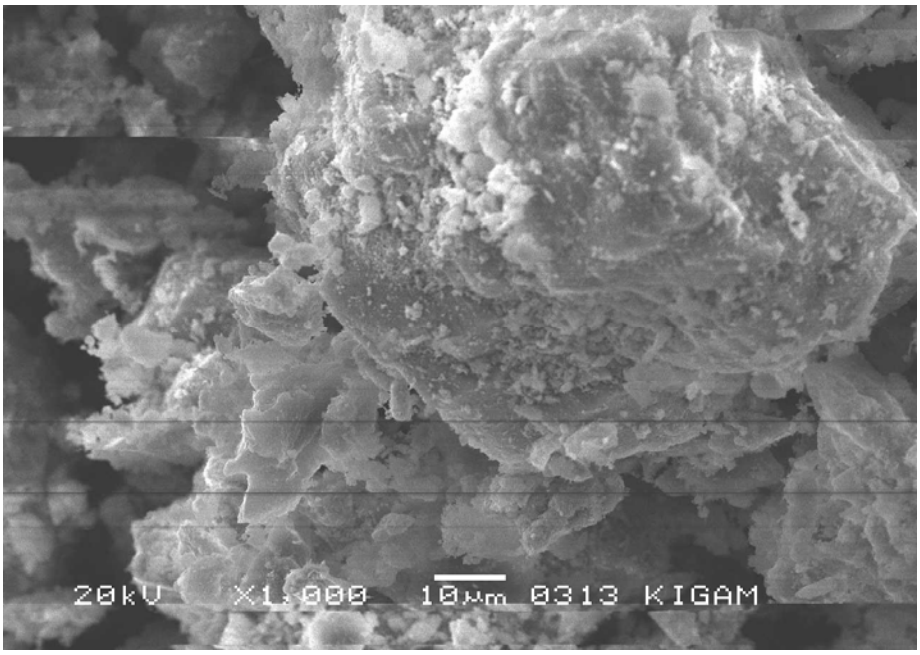

Fig.4.4. SEM image of calcined bauxite

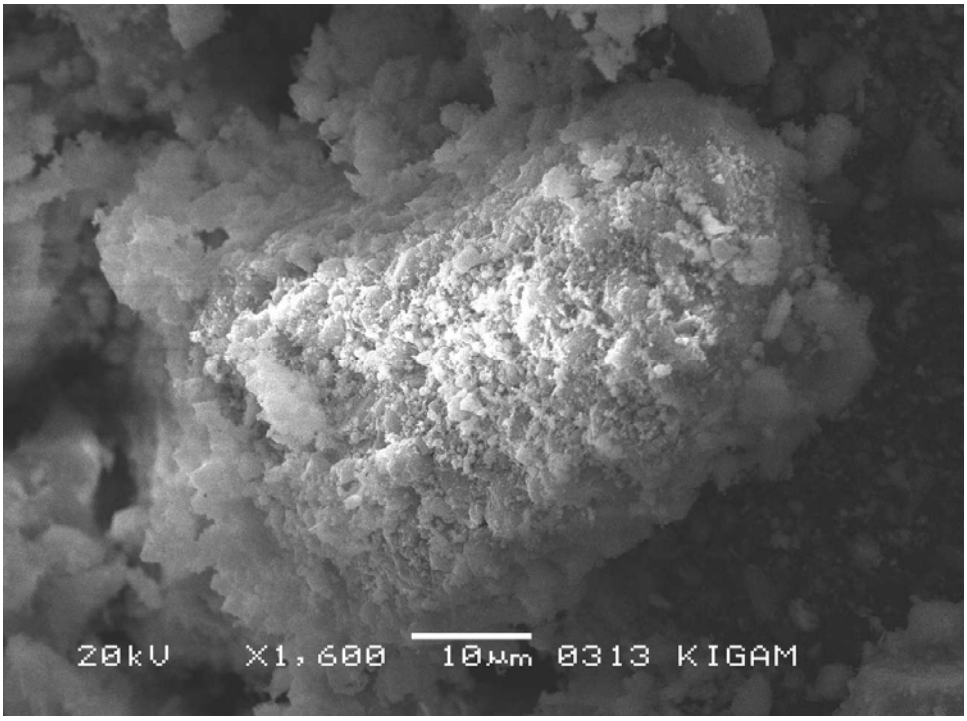

Fig. 4.5. SEM image of calcined bauxite after adsorption

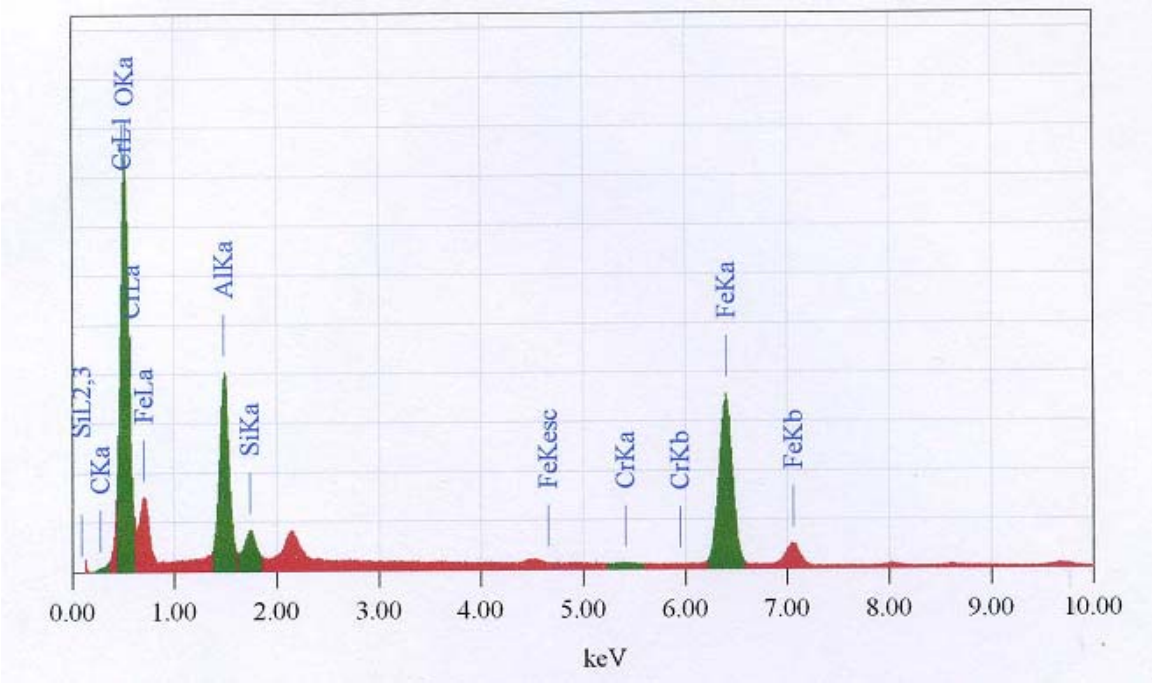

Fig. 4.6. EDAX image for bauxite as such

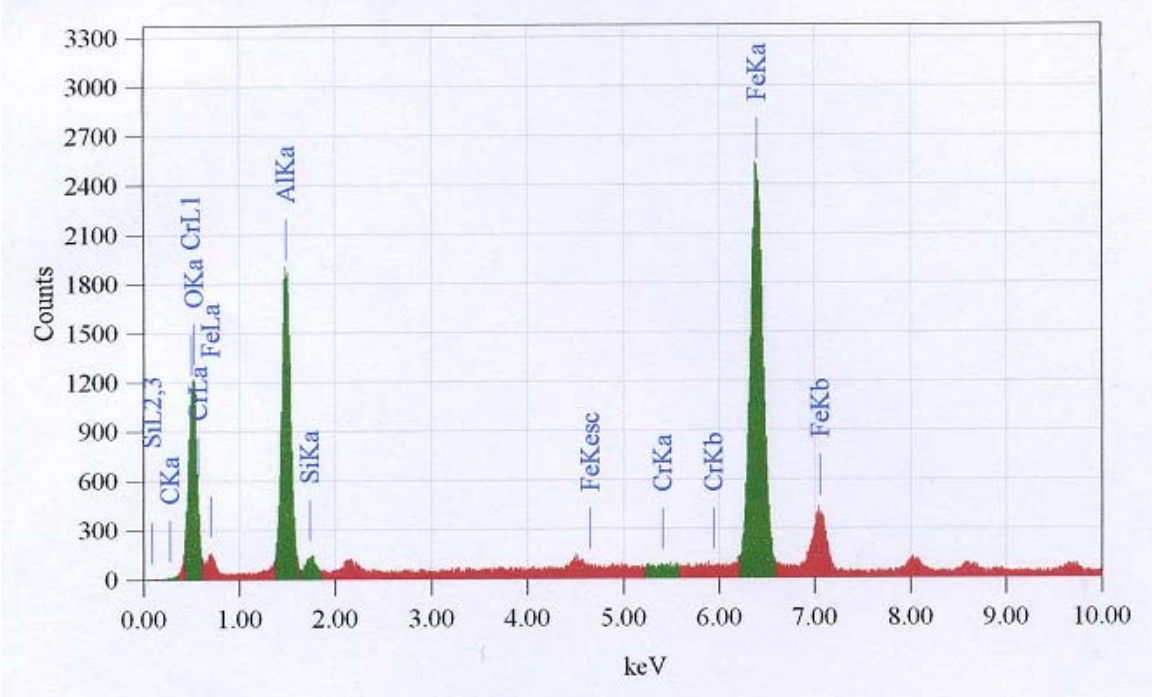

Fig. 4.7. EDAX image for calcined bauxite

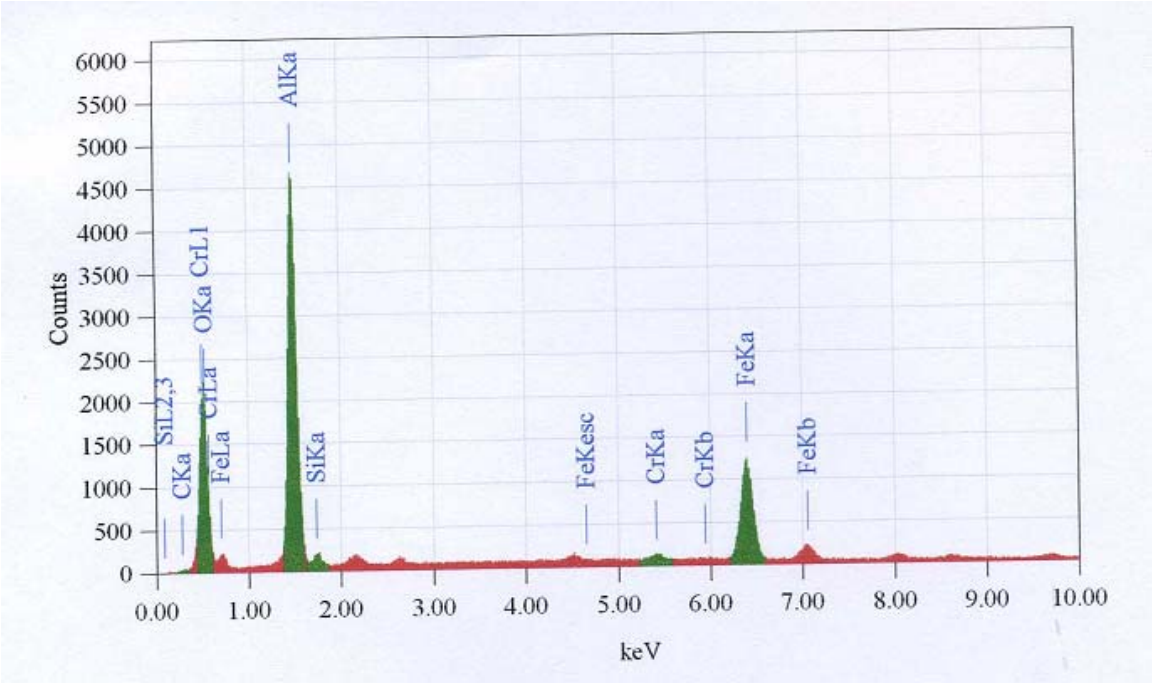

Fig.4.8. EDAX image for calcined bauxite after adsorption

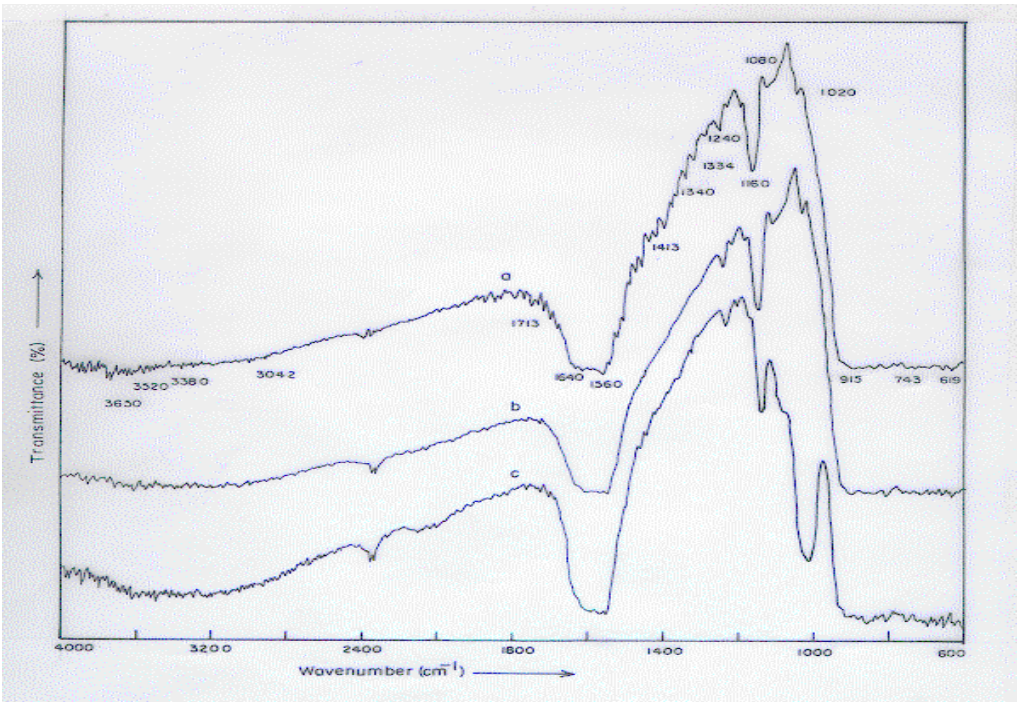

Fig.4.9. FTIR microscopic spectra of (a) Calcined Bauxite (b) Bauxite (c) Calcined Bauxite after adsorption

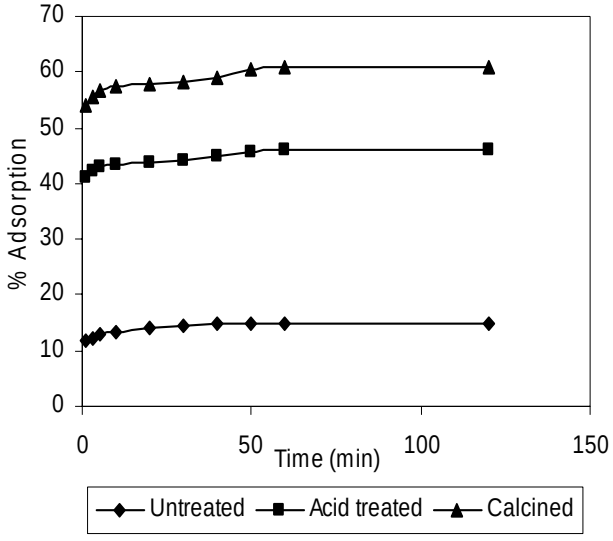

Fig.4.10. Effect of treatment of bauxite on adsorption of Cr(VI). [Conditions: pH 4.6, temperature 30 ^{0}C, Cr(VI) 100 mg/L, Adsorbent 0.5 g]

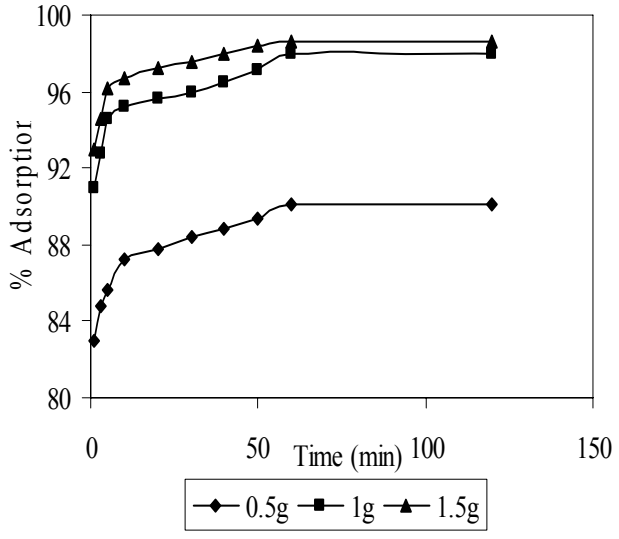

Fig.4.11. Effect of contact time on adsorption at different adsorbent concentrations. [Conditions: pH 3.8; temperature 30 ^{0}C; Cr(VI) 10 mg/L].

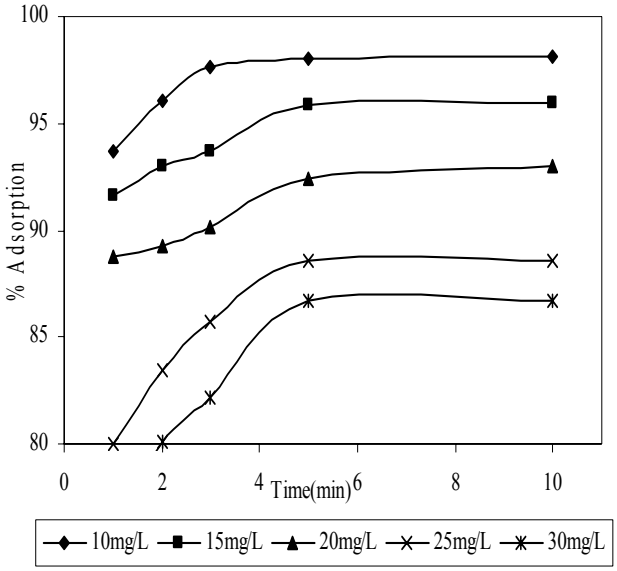

Fig.4.12. Effect of contact time on adsorption at different adsorbate concentrations. [Conditions: pH 3.8; temperature 30 ^{0}C; adsorbent 1g/25 mL].

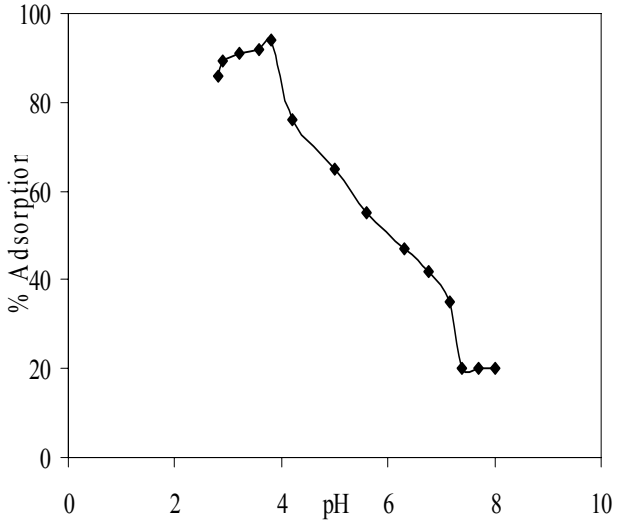

Fig.4.13. Effect of pH on adsorption. [Conditions; temperature 30 ^{0}C, adsorbent 0.1 g/50 mL].

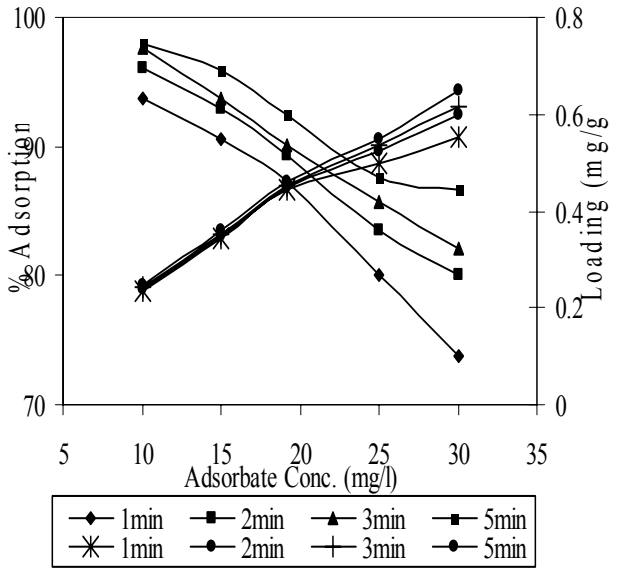

Fig.4.14. Effect of initial adsorbate concentration on adsorption at different time. [Conditions: pH 3.8; temperature 3 0^{0}C; adsorbent 1 g/25 mL].

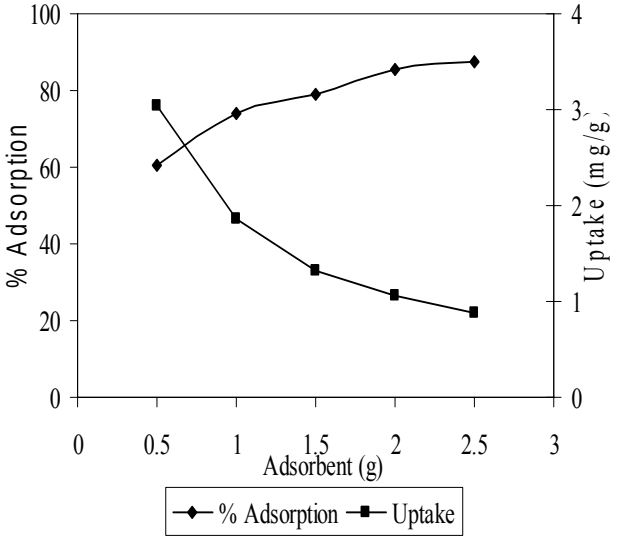

Fig.4.15. Effect of adsorbent dose on adsorption. [Conditions: pH 3.8; temperature 30 ^{0}C; time 1h; Cr(VI) 100 mg/L].

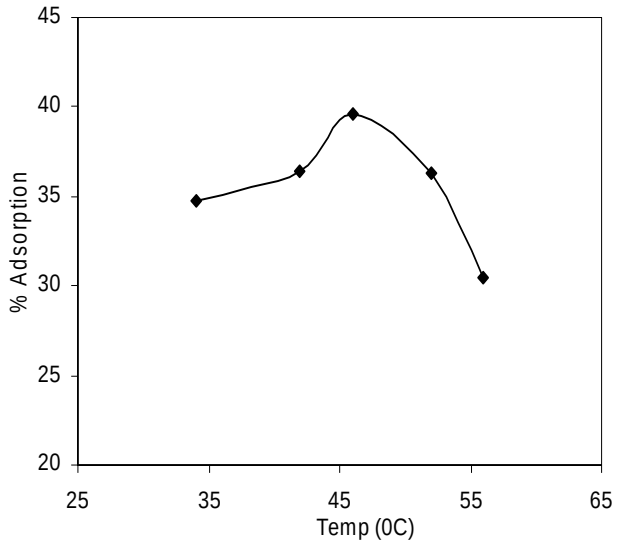

Fig.4.16. Effect of temperature on adsorption. [Conditions: pH 7.4; time 1h; Cr(VI) 10 mg/L; adsorbent 2 g/50 mL].

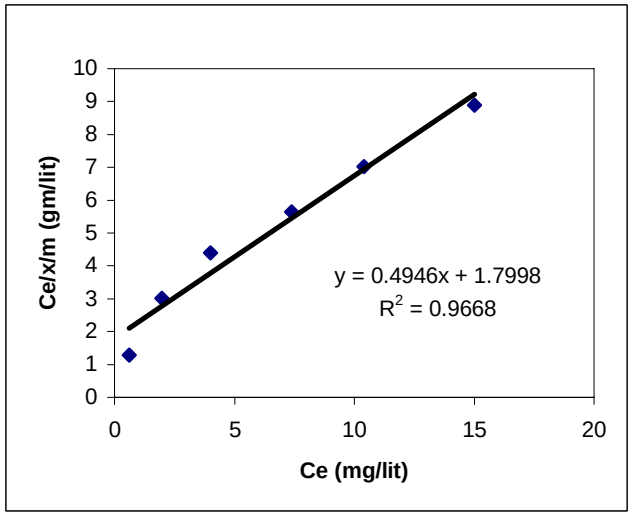

Fig.4.18. Langmuir adsorption isotherm. [Conditions: pH 3.8; temperature 33 ^{0}C; adsorbent 0.5 g/25 mL]

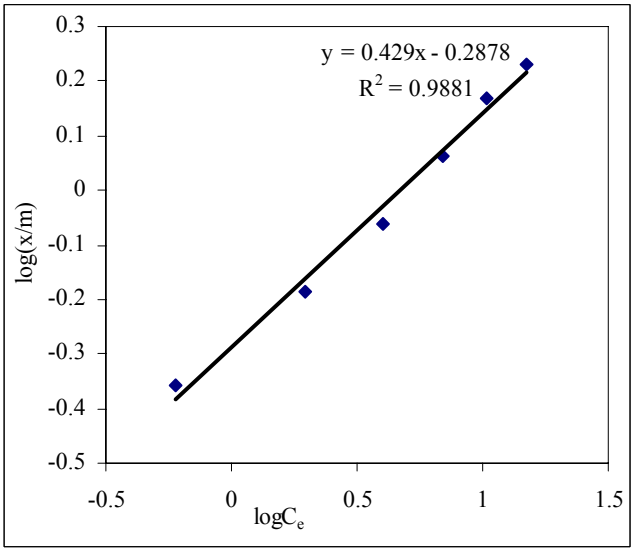

Fig. 4.17. Freundlich adsorption isotherm. [Conditions: pH 3.8; temperature 33 ^{0}C; adsorbent 0.5 g/25 mL].

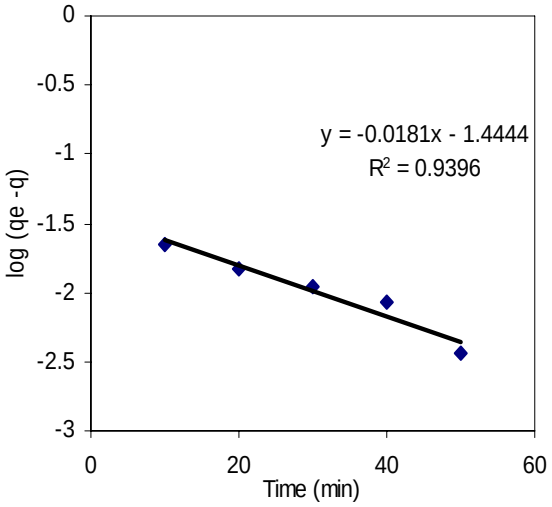

Fig.4.19. Lagergrens kinetics. [Conditions: pH 3.8; temperature 30 ^{0}C; adsorbent 1 g/25 mL].

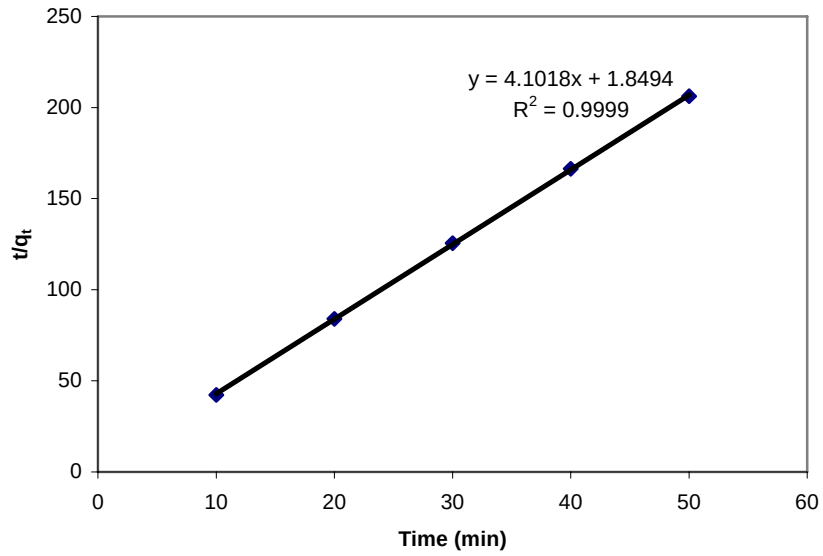

Fig. 4.20. Pseudo second order kinetics. [Conditions: pH 3.8; temperature 30 ^{0}C; adsorbent 1 g/25 mL].

Table 4.1: Physical properties of the adsorbents

Physical parameters	Bauxite as such	Acid treated bauxite	Calcined bauxite
Specific gravity	2.05	1.98	1.8
Bulk density (gm/cc)	1.97	1.8	1.68
Porosity (%)	35	51	65
Surface area (m^2/g)	18.63	112.5	167.5
Average particle size (microns)	53	53	53

Table 4.2: Chemical composition of bauxite from the XRF analysis

Constituent	w/w %	Constituent	w/w %
Al_2O_3	52.2	TiO_2	1.67
SiO_2	3.1	V_2O_5	0.05
FeO_2	20.96	Cr_2O_3	0.056
MgO	0.04	ZrO_2	0.057
MnO	0.045	L.O.I	22.0
P_2O_5	0.092		

Table 4.3: XRD peaks

Sl. No.	Peak for bauxite as such	Assigned to	Peak for calcined bauxite	Assigned to
1	4.82, 2.42, 1.95, 1.65	Gibbsite ($Al(OH)_3$)	3.5, 2.69, 2.51, 1.91, 1.8, 1.694 ,1.41	Goethite (FeOOH)
2	2.51, 2.24, 1.84, 1.48 , 1.45	Bohemite (Al_2O_3)	2.72, 2.34, 2.17, 1.66 , 1.46	Hematite (Fe_2O_3)

Table 4.4: FT-IR peaks and group assignment

Peak at wavelength cm^{-1}	Assigned to
3650	OH stretching for gibbsite
3520	OH stretching for gibbsite
3380	OH stretching for gibbsite
1100	–OH bending deformation in calcined bauxite
1020	–OH bending deformation in calcined bauxite
915	–OH bending deformation in calcined bauxite
743	–OH bending deformation in calcined bauxite
1160	–OH stretching for bohemite
1080	–OH stretching for bohemite
1713	–OH vibration for goethite
1560	–OH vibration for goethite
1640	–OH vibration for goethite
1340	–OH vibration for goethite
1324	–OH vibration for goethite
1240	–OH vibration for goethite

CHAPTER-5

ADSORPTION OF Cr(VI) ON TREATED SAWDUST

Adsorption of Cr(VI) on treated sawdust

5.1. Adsorbent preparation

Sawdust is a major waste material in wood processing units. The waste material are either stockpiled near the sawmills or used to make fuel aggregates by mixing with coal dust and other combustible materials. The availability of sawdust is quite high and has practically very little commercial value. The sawdust contains various organic functional groups, which are good chelating agents and thus good binder for various metal ions. Therefore, it has the potential to treat wastewater containing heavy metal ions. Interest in the use of sawdust as an adsorbent has been stimulated by the good results obtained by other investigators (Sukla, A., 2002). This sawdust of *Shorea robusta (*Sal), a common wood for making door and window frames, has been used in this experiment. It is available in plenty and was collected from a local sawmill. The sawdust is particularly interesting in India because of its high availability and low cost as compared to the other sawdusts reported earlier. In addition, it is a renewable source since plantations in depleted forests are practiced by the local Governments in this region.

The collected sawdust was dried in sunlight until almost all the moisture evaporated. It was ground to a fine powder and sieved to +125 to -250 micron size. Sawdust contained water-soluble compounds like tannin, which give brown color to the effluents during the treatment. Treatment of wastewater with sawdust is also likely to create a high BOD in the wastewater. Therefore chemical treatment of the sawdust is required before using it for the treatment of heavy metal contaminated wastewater. Chemical treatment with formaldehyde leads to polymerization of the compounds responsible for colorization. Sawdust (50g) was washed repeatedly with distilled water and subsequently dried for 24 h at 60 ^{0}C to get rid of tannin and other soluble organic compounds. To improve the stability, it was treated either with 1% formaldehyde in the ratio of 1:4 (sawdust: formaldehyde, w/v) or 0.2 N H_2SO_4. The mixture was boiled at 100 ^{o}C for 6 hours. The product was cooled, filtered and washed several times with distilled water and finally dried at 60 ^{0}C.

5.2. Characterization of the adsorbent

The physical characteristics such as specific gravity, bulk density, porosity, surface area, average particle size etc. along with the chemical composition of the sawdust as such and the treated sawdust are shown in Table 5.1. The FTIR spectra of sawdust, treated sawdust and the sawdust after adsorption are shown in Fig.5.1 and the absorption bands are given in Table 5.2. The spectra of sawdust showed peaks at 3240, 3015, 1650, 1540, 1450, 1420 1250 and 1160 cm^{-1} which may be assigned to OH group, aliphatic C-H group, unsaturated groups like alkenes, amide, CH deformation, OH deformation, aromaticity and OH stretch respectively. The intensity of the peaks were either minimized or shifted slightly in case of treated and adsorbed sawdust respectively. These results are similar to the ones reported earlier (Huang, G. F., 2005). Due to the limitation of the instrument, we could not undertake the spectral analysis in the far IR, which might have showed the evidences of Cr-N, Cr-S or Cr-O bonding in samples after adsorption to establish the mechanism by which Cr(VI) binds to the adsorbent.

The adsorption of Cr(VI) on the surface of the treated sawdust was analysed by SEM. The SEM images for the treated sawdust before and after adsorption are shown in Figs.5.2 and 5.3 respectively. From Fig.5.2 it is observed that the adsorbent surface is smooth. But in case of sawdust after adsorption some of the surface of the sawdust are found to be coated with a thin layer which, confirms the adsorption of Cr(VI) on the surface of sawdust. Further adsorption of Cr(VI) on the surface of the sawdust was confirmed by the elemental analysis by EDAX method. The EDAX images for treated sawdust and treated sawdust after adsorption are shown in Figs.5.4 and 5.5 respectively. From the EDAX analysis it was observed that the weight percentage of Cr is higher in case of treated sawdust after adsorption which confirms the adsorption of Cr(VI).

5.3. Adsorption experiments

Adsorption experiments were conducted by varying contact time, pH, adsorbent dose and adsorbate concentration. Experiments were carried out in 100 mL conical flasks and the total volume of the reaction mixture was kept at 50 mL. The pH of solution was

maintained at a desired value by adding 0.1 M NaOH or HCl. The conical flasks were shaken for the required time period in a Yorko thermostatic water bath. The mixture was filtered through Whatman 42 filter paper and the final volume made to 50 mL. The Cr(VI) analyses were carried out as described in Chapter-4.

5.4. Results and discussion

5.4.1. Effect of contact time

A plot of percentage adsorption versus adsorption time is shown in Fig.5.6. It is evident from the figure that the equilibrium time is dependant on the adsorbate concentration. The equilibrium time was varied from 2 h at higher adsorbate concentration (40 mg/L) to 5 h at low adsorbate concentration (5 mg/L). All the curves obtained were smooth indicating formation of monolayer on the surface of the sorbent. In the initial stage, the slope of the plot was 1 and it decreased with time. The rate of uptake was rapid in the early stages but gradually decreased and became constant when equilibrium was reached.

5.4.2. Effect of pH

The adsorption experiment was carried out in the concentration range of 2.72 mg/L (chromite mine water) to 10 mg/L (synthetic solution) of Cr(VI) as a function of equilibrium pH and is shown in Fig.5.7. It is evident from this figure that the percentage adsorption is higher at lower pH, reaching maximum in the pH range 4.5 to 6.0. As the pH increased, there was little increase in the percentage of adsorption and it was maximum at pH 4.5. When the pH was further increased, a sharp decrease in percentage of adsorption was observed. This might be due to the weakening of electrostatic force of attraction between the oppositely charged adsorbate and adsorbent and ultimately led to the reduction in sorption capacity. When the pH was increased beyond 6.0, a gradual decrease in the percentage adsorption was observed. This might be due to the competition between OH^- and chromate ions (CrO_4^{2-}), where the former was the dominant species. But it decreased with increase in pH and became constant at pH > 9.0. The effect of pH on the adsorption capacity of treated sawdust can be best explained in terms of pH_{pzc} (pH

at the point of zero charge) of the adsorbent. The pH_{pzc} of sawdust was found to be 9.0 and below this pH, the surface charge of the adsorbent was positive. At pH less than pH_{pzc} (pH<9.0) the predominating metal ion species (M^{n+}, $M(OH)^{(n-1)+}$) are positively charged (Yu, L. J., 2003); therefore, uptake of metal ions in the pH range 4.5 to 6.0 is a H^+-M^{n+} exchange process.

The possible sites on the sawdust for specific adsorption included H^+ ions in phenolic (-C_6H_4OH) andacid (–COOH) functional groups in which H^+ ion can be exchanged for a cation in solution as shown below:

$$S\text{-}COOH + M^{n+} \longrightarrow S\text{-}COOM^{(n-1)+} + H^+$$

$$S\text{-}C_6H_4\text{-}OH + M^{n+} \longrightarrow S\text{—}C_6H_4\text{-}OM^{(n-1)+} + H^+$$

$$S\text{-}COOH + MOH^{(n-1)+} \longrightarrow S\text{-}COOM(OH)^{(n-2)+} + H^+$$

$$S\text{-}C_6H_4\text{-}OH + M(OH)^{(n-1)+} \longrightarrow S\text{-}C_6H_4\text{-}OM(OH)^{(n-2)+}$$

where ‘S’ denotes the activated sawdust surface. Along with those groups, other sites on the modified sawdust can also contribute to the adsorption process. In acidic medium, the electromeric effect of amide groups in sawdust leads to surface protonation and a net positive charge on the surface. These H^+ ions on the surface are also exchanged with the positively charged sorbate species with subsequent coordination of a metal ion. The decrease in removal of ions at lower pH (<4.5) is apparently due to the higher concentration of H^+ ions present in the reaction mixture, which, compete with the M^{n+} ions for the adsorption sites of sawdust. Decrease in adsorption at higher pH is due to the formation of soluble hydroxyl complexes. Similar observations are reported by Li, Yu., et al. (Yu, L. J., 2003).

5.4.3. Effect of initial adsorbate concentration

Analysis of percentage adsorption and loading capacity versus initial concentration (Fig.5.8) studied at varying contact time showed that the percentage adsorption decreased with increase in initial concentration of the adsorbate. But the

uptake capacity increased with increase in initial concentration. The extent of adsorption increased from 47.75 to 91% when the concentration of the adsorbate decreased from 40 to 5 mg/L and the uptake increased from 1.14 to 4.8 mg/g when the adsorbate concentration increased from 5 to 40 mg/L. The increase in uptake may be due to the availability of more number of Cr(VI) ions in solution for sorption. Moreover, higher initial adsorbate concentration provided higher driving force to overcome all mass transfer resistances of the metal ions from the aqueous to the solid phase resulting in higher probability of collision between Cr(VI) ions and the active sites. This also resulted in higher uptake of Cr(VI) for the given amount of treated sawdust.

5.4.4. Effect of adsorbent dose

The percentage adsorption increased with increase in adsorbent dose. This is evident from Fig.5.9, where the percentage adsorption was plotted against adsorbent dose. The percentage adsorption increased from 20 at lower adsorbent dose (0.2 g/L) to 100 at higher adsorbent dose (1.6 g/L). However, the Cr(VI) uptake capacity of the sawdust was found to have reduced from 2.72 mg/g at low adsorbent dose (0.2 g/L) to 1.7 mg/g at high adsorbent dose (1.6 g/L). Other investigators on Cr(VI) sorption (Donmez, G. C., 1999) have also reported similar trend. The decrease in Cr(VI) uptake at higher adsorbent dose may be due to competition of the Cr(VI) ions for the sites available.

5.4.5. Effect of temperature

Temperature has an important effect on the process of adsorption. The percentage of Cr(VI) adsorption was studied as a function of temperature in the range of 30 to 45 ^{0}C. The results obtained are presented in Fig.5.10. When the temperature was raised from 30^{o}C (303K) to 45^{o} (318K), the percentage of adsorption and uptake decreased from 91 to 52% and from 1.14 to 0.65 mg/g respectively. The decrease in percentage of adsorption with rise in temperature might be due to desorption caused by an increase in the available thermal energy. Higher temperature induced higher mobility of the adsorbate causing desorption.

5.5. Adsorption kinetics modeling

The adsorption kinetic models are important in the process of removal of toxic heavy metals from the aquatic environment. Different reversible models were tested in this batch reaction.

5.5.1. First order reversible kinetics

The sorption of Cr(VI) on treated sawdust may be considered as a first order reversible reaction (Arun, K., 1984). The plot for the first order reversible kinetics as shown in equation 3.4 was drawn for sawdust at different temperatures (Fig.5.11). The correlation coefficients 'R^2', rate constant 'K_c', 'k_1' and 'k_2' were calculated using equation 3.3 and 3.4 for different plots and are shown in the Table 5.3. It is observed that the values of 'k_1' and 'k_2' decrease from 5.06 to 0.542 and 0.4769 to 0.2047 respectively when the temperature was increased from 30 to 45 ^{0}C. 'K_c' values increased from 0.9609 to 0.3776 when the temperature was increased from 30 to 45 ^{0}C. The correlation coefficient (R^2) varied from 0.9978 to 0.9601 for the first order reversible plot at different temperatures.

5.5.2. Pseudo first order kinetics

The sorption kinetics may also be described by the pseudo first order reaction model (Ho, Y.S., 1998). The plot of log (q_e-q) vs t as shown in equation 3.7 was plotted at different temperatures (Fig.5.12). The correlation coefficient and rate constants were calculated and are given in Table 5.4. From the table it is observed that the 'k' values decreased from 0.59 to 0.57, when the temperature increased from 30 to 45 ^{0}C. The correlation coefficients are in good agreement with the pseudo first order kinetics.

5.5.3. Pseudo second order kinetics

A pseudo second order reaction model (Ho, Y.S., 1998) may also be applicable to the kinetics of sorption. The kinetics plots of 't/q' vs. 't' as per equation 3.15 were made at different temperatures (Fig.5.13) and the values of correlation coefficients, 'h' and 'k',

were calculated from the plot as shown in the Table 5.5. It is observed that the 'k' values decreased from 250 to 69, when the temperature was increased from 30 to 45 ^{0}C. But the 'h' values decrease from 0.12 to 0.9, when the temperature was increased from 30 to 45 ^{0}C.

From the above discussion, it can be concluded that the process of Cr(VI) adsorption in treated sawdust is best fitted to pseudo second order kinetics since the 'R^2' values matched very well.

5.6. Adsorption isotherm and thermodynamic parameters

5.6.1. Langmuir adsorption isotherm

Adsorption studies were carried out with a fixed initial adsorbent dose (0.1 g) and varying adsorbate concentration. The data were tested for the applicability to the Langmuir adsorption isotherm. The data obtained fitted well into the linearised Langmuir adsorption isotherm, by using equation 3.3. The values of 'Q_0' and 'b' were calculated from the slope and intercept of the plot (Fig.5.14) and were found to be 3.6 (mg/g) and 2.36 respectively.

5.6.2. Thermodynamic parameters

The activation energy could be calculated by using the Arrhenius equation (equation 3.23). The lnk values were plotted against 1000/T (Fig.5.15) and the activation energy was calculated to be 18.357 kJ/mol. This low value of activation energy suggests that the adsorption process was governed by the process of diffusion.

The standard Gibbs free energy was calculated by using equation 3.20. The calculated ΔG^0 value was -746 Jg/mol. The negative value of Gibbs energy indicated the spontaneity and the feasibility of the adsorption process.

The isosteric heat of adsorption (ΔH_r) was also calculated using the equation 3.22. The value of ΔH_r calculated over the temperature range 30 to 45 ^{0}C was found to

be -2.068 kJ/mole. The negative value of heat of adsorption (ΔH_r) indicated that the process was exothermic in nature.

5.7. Mass transfer model

The adsorbent used in the present case is saw dust which is a porous material. So the adsorption phenomenon may be either surface or intraparticle diffusion or a combination of both. The contact time experiment can be used to study the rate-determining step in the adsorption process. Since adsorption studies were carried out under agitated condition, the bulk diffusion coefficient, i.e., transfer from adsorbate ion from the bulk to the surface of the adsorbent, could be negligible if not nil. Therefore, the rate determining step might be either film or intra-particle diffusion as both the processes act in series. The slower of the two will be the rate determining step (Karthikeyan, T., 2005). Rate constant for intra particle diffusion can be evaluated using

$$Q = k_{id}\, t^{0.5}$$

The 'k_{id}' value was determined from the slope of the linear plot between 'q_t' vs. '$t^{0.5}$' (Fig. 5.16) and was found to be 0.0298 mg/g $min^{0.5}$.

5.8. Conclusions

The studies on adsorption of hexavalent chromium over sawdust were conducted by varying various parameters such as contact time, pH, amount of adsorbent, concentration of adsorbate and temperature. Treated sawdust has been shown to be an effective adsorbent for removal of Cr(VI) from aqueous solutions. The optimum adsorption capacity of the treated sawdust was compared with other adsorbents reported in literature (Table 5.6). The equilibrium time was 3 h for the adsorbent concentration of 30 mg/L. The maximum adsorption takes place in the pH range 4.5 to 6.0. The adsorption data fitted well to the Langmuir adsorption isotherm and pseudo second order reaction model. The rate constant was calculated at 30, 35, 40 and 45 ^{0}C and the activation energy (E_a) was calculated using the Arrhenius equation. Thermodynamic parameters such as standard Gibbs energy (ΔG^o) and heat of adsorption (ΔH_r) were calculated. Decrease in

percentage of adsorption with increase in temperature indicated the process to be exothermic in nature and so low temperatures favored the adsorption process. Due to easy availability and high efficiency for removal of Cr(VI), the treated sawdust can be considered as an ideal adsorbent for removal of Cr(VI) from aqueous solutions.

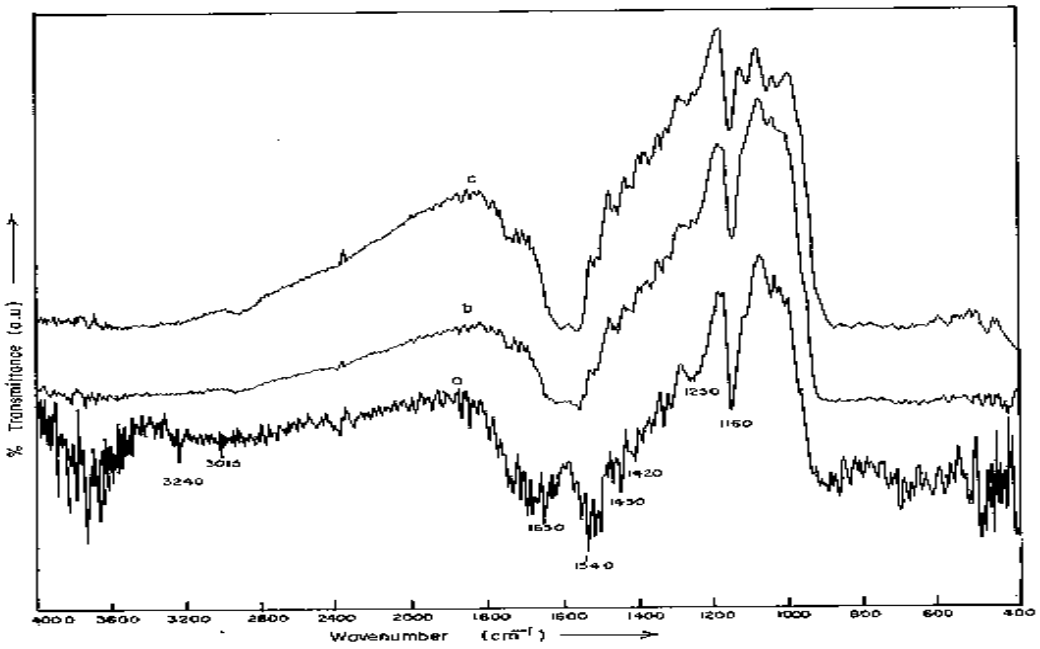

Fig.5.1. FTIR Spectra of (a) Untreated sawdust (b) Treated sawdust (c) Treated sawdust after adsorption

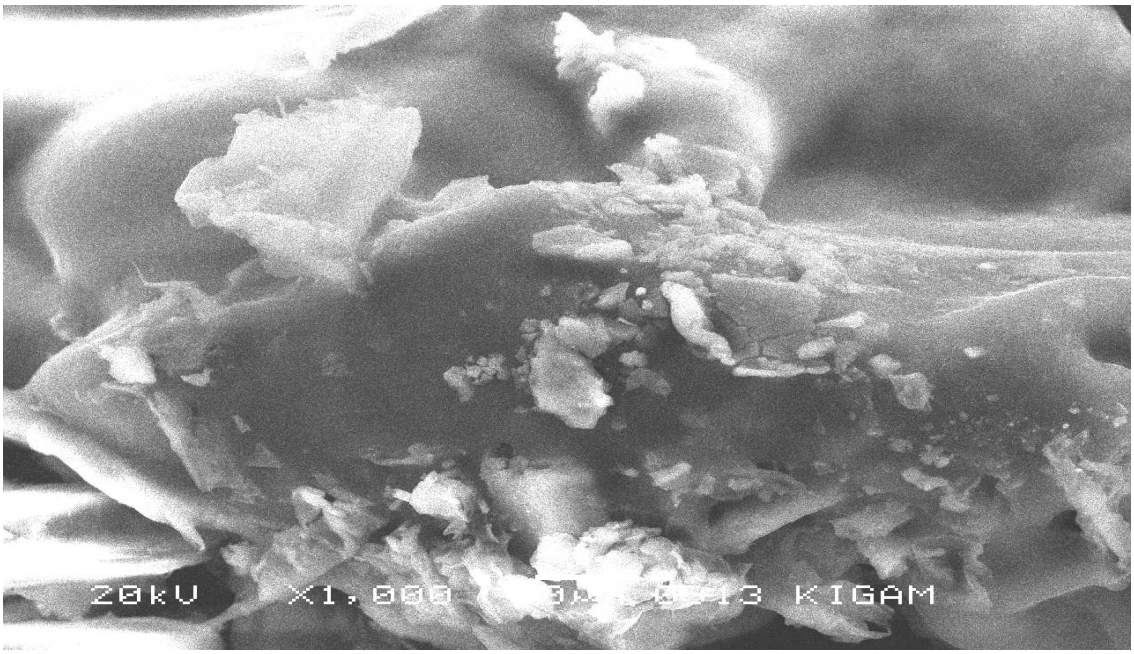

Fig.5.2. SEM image for treated sawdust

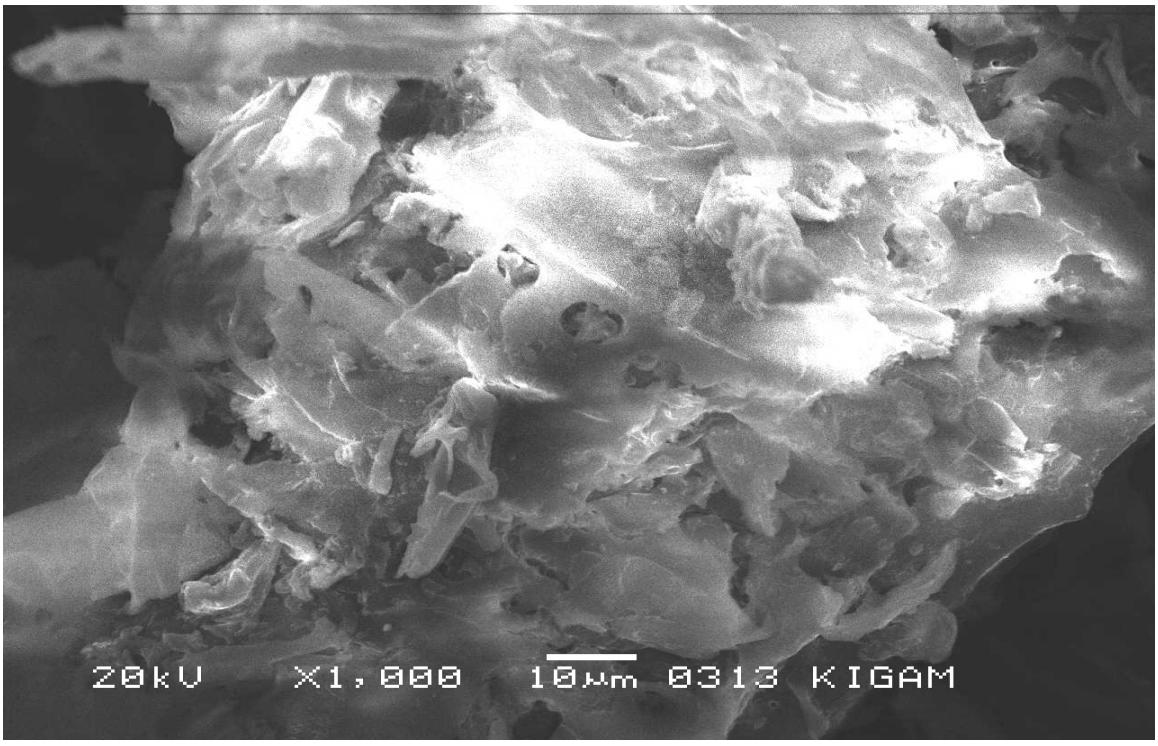

Fig.5.3. SEM image for treated sawdust after adsorption

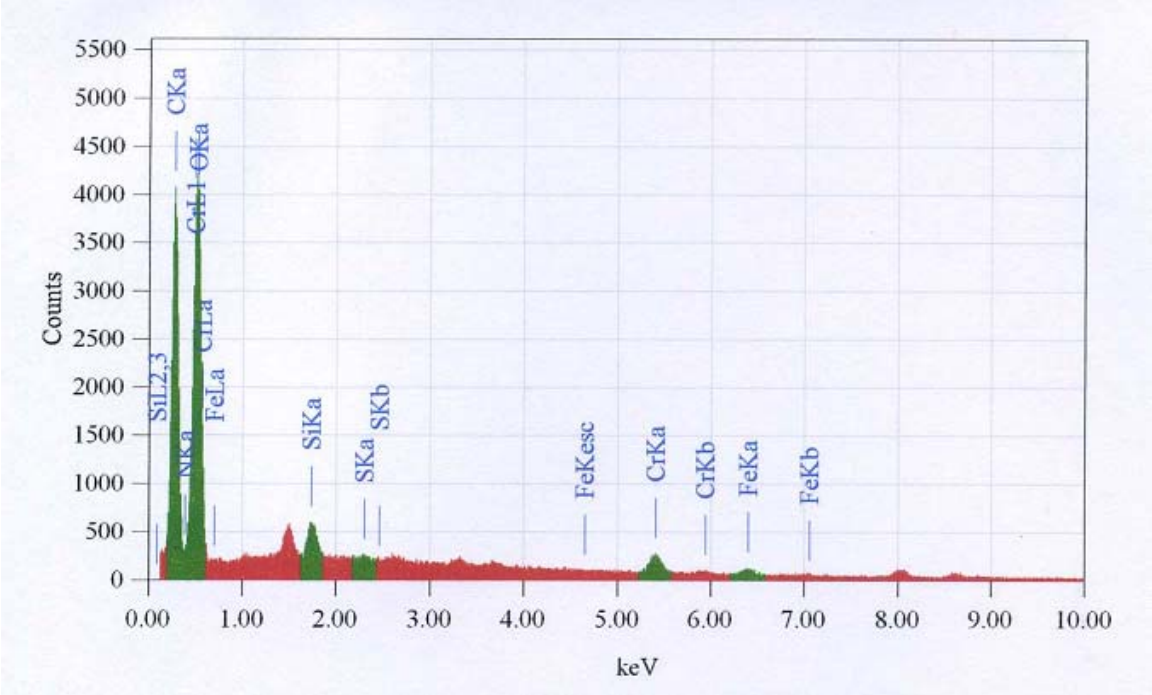

Fig.5.4. EDAX image for treated sawdust

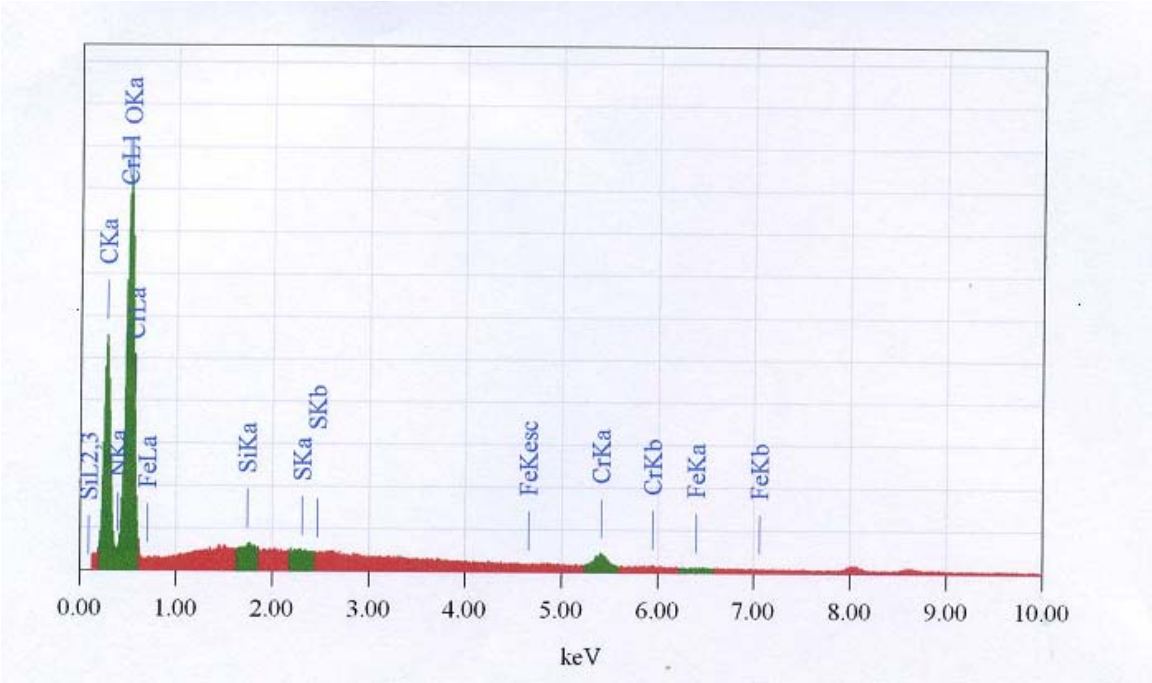

Fig.5.5. EDAX image for treated sawdust after adsorption

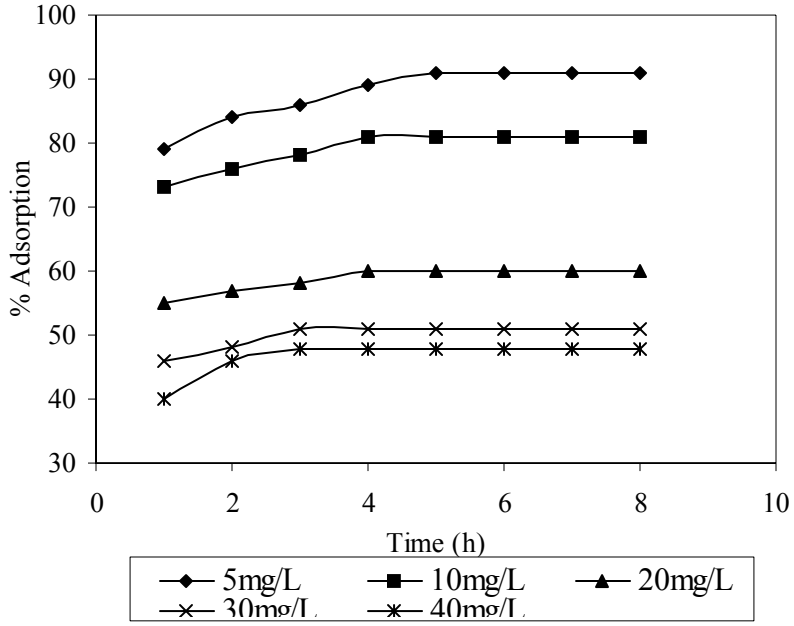

Fig.5.6. Effect of contact time on adsorption at different adsorbate concentrations. [Conditions: Adsorbent 0.1 g, pH 3.5, Temp 30 ^{0}C]

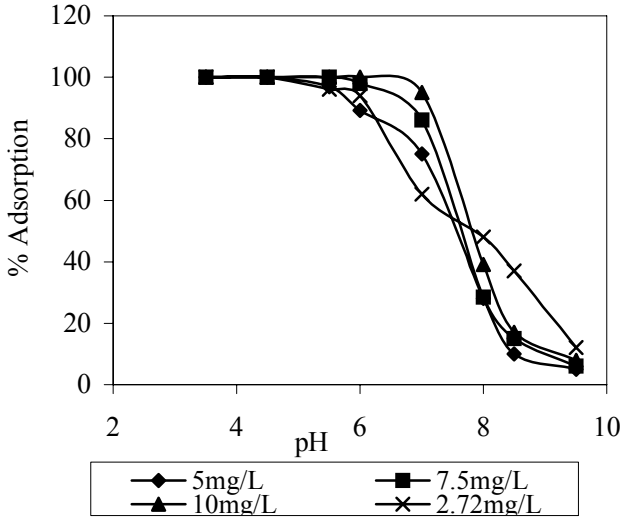

Fig.5.7. Effect of pH on adsorption at different adsorbate concentrations [Conditions: Adsorbent 0.6 g, Time 1 h, Temp 30 ^{0}C,]

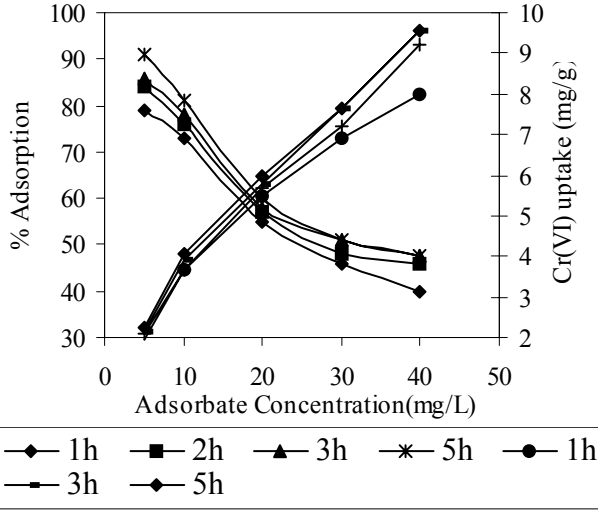

Fig.5.8 Effect of adsorbate concentration on adsorption at different time [Conditions: Adsorbent 0.1 g, pH 3.5, Temp 30 ^{0}C]

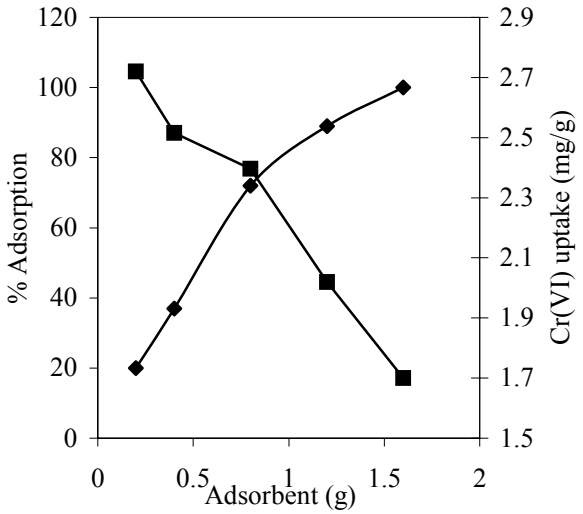

Fig.5.9. Effect of adsorbent dose on adsorption [Conditions: Time, 1 h. Adsorbate 2.72 mg L^{-1}. Temp 30 ^{0}C. pH 3.5]

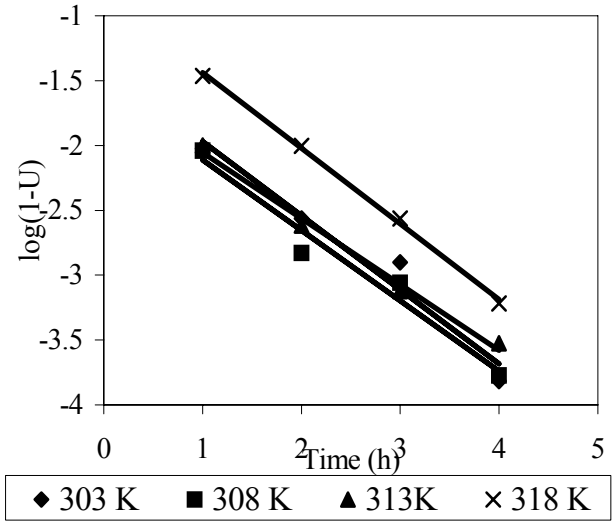

Fig.5.11. First order reversible reaction kinetics for different temperatures [Conditions: Adsorbent 0.1 g, Adsorbate 5 mg/L, pH 3.5]

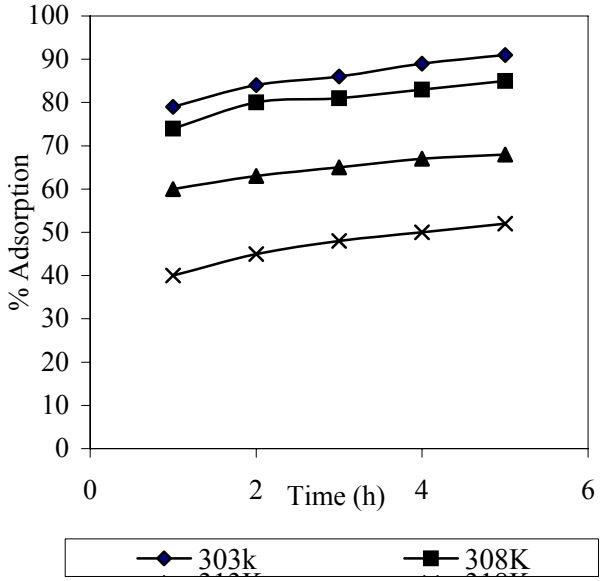

Fig.5.10. Effect of temperature on adsorption at different time. [Conditions: Adsorbent 0.1 g, Adsorbate 5 mg/L, pH 3.5.]

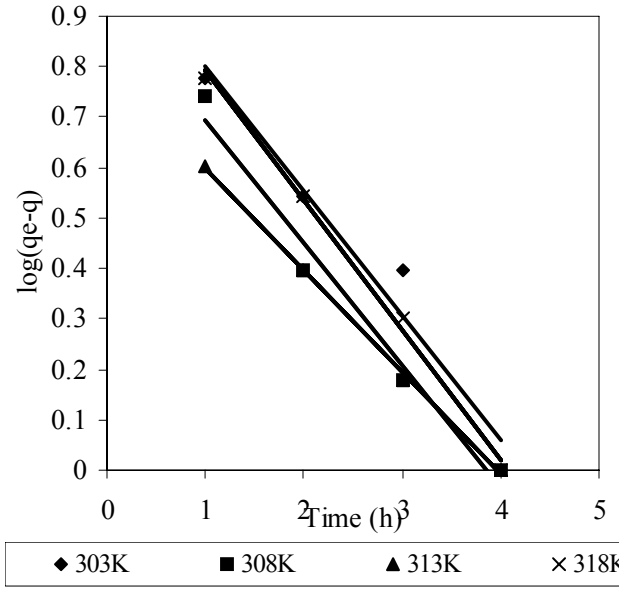

Fig.5.12. Pseudo first order reaction kinetics plot for different temperatures [Conditions: Adsorbent 0.1 g, Adsorbate 5mg/L, pH 3.5.]

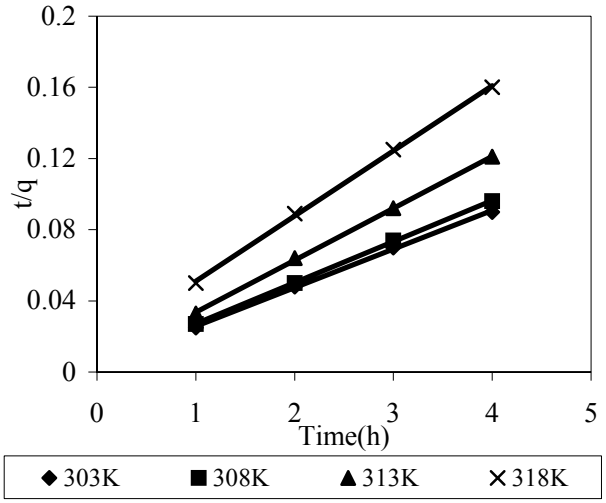

Fig.5.13. Pseudo second order reaction kinetics for different temperatures [Conditions: Adsorbent 0.1 g, Adsorbate 5 mg/L, pH 3.5.]

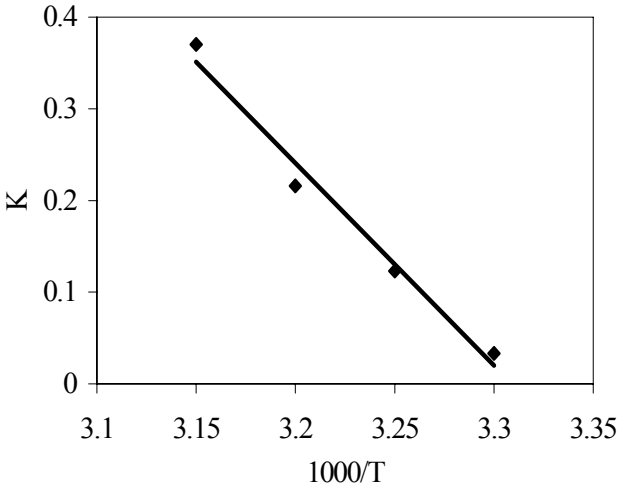

Fig.5.15. Arrhenius plot for evaluation of activation energy

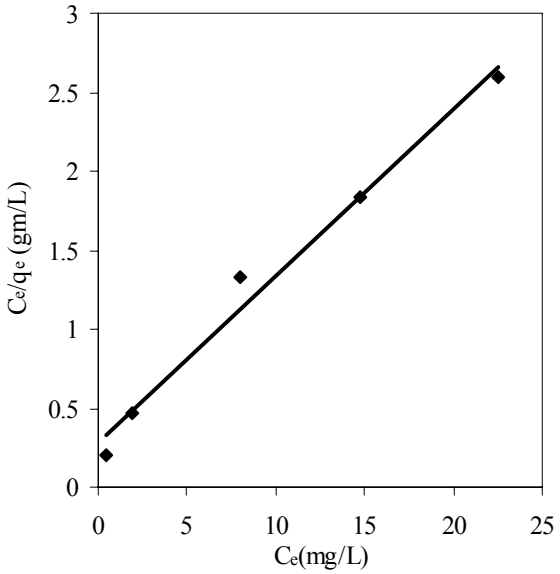

Fig.5.14. Langmuir adsorption isotherm

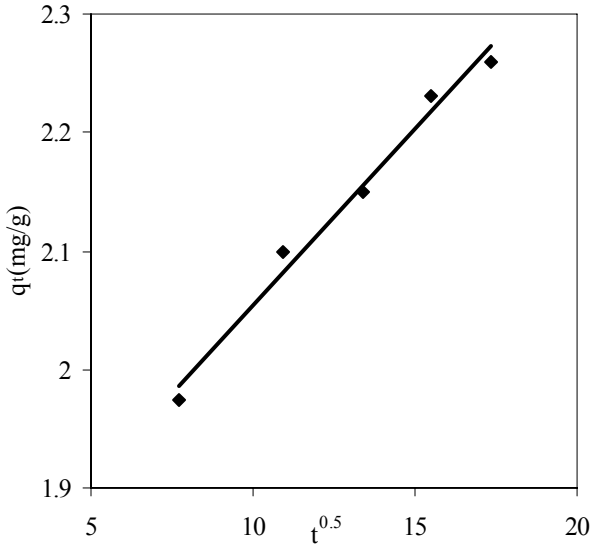

Fig.5.16. Mass transfer model. [Conditions: Adsorbent 0.1 g, Adsorbate 5 mg/L, pH 3.5.]

Table 5.1: Physical properties of adsorbents

Parameters	Sawdust as such	Treated sawdust
Specific gravity	0.65	0.61
Bulk density (g/cc)	0.61	0.59
Porosity (%)	68	72
Surface area (m^2/g)	17	19
Average particle size (micron)	0.7micron	0.65micron
Moisture content (%)	53.9	50.1
Loss on ignition	96.22(w/w %)	96.12
Al_2O_3	2.38(w/w %)	2.38(w/w %)
SiO_2	1.17(w/w %)	1.17(w/w %)
FeO_2	0.23(w/w %)	0.23(w/w %)

Table 5.2: FT-IR peaks and group assignment

Peak wavelength, cm^{-1}	Assigned to
3240	OH group
3015	Aliphatic C-H group
1650	Alkenes group
1540	Amide group
1450	CH deformation
1420	OH deformation
1250	Aromatic stretch
1160	OH stretch

Table 5.3: First order reversible kinetic rate constants with regression coefficients for different temperatures

Temperature (K)	k_1 (min^{-1})	K_2 (min^{-1})	K_C	R^2
303	5.06	0.4769	0.0943	0.9609
308	2.833	0.4324	0.1527	0.9911
313	1.063	0.4208	0.2266	0.9978
318	0.542	0.2047	0.3776	0.9978

Table 5.4: Pseudo first order kinetic rate constants with regression coefficients for different temperatures

Temperature (K)	K (min^{-1})	R^2
303	0.5711	0.9609
308	0.5622	0.9769
313	0.4668	0.9982
318	0.5935	0.9963

Table 5.5: Pseudo second order kinetics rate constants with regression coefficients for different temperatures

Temperature (K)	k (g/mg min)	h (mg/g min)	R^2
303	0.1177	250	0.9994
308	0.1334	250	0.9997
330	0.1895	222.22	0.9996
318	0.0924	68.97	0.9994

Table 5.6: Comparison of the adsorption capacity of the treated sawdust with the other adsorbents

Adsorbents	Adsorption Capacity (mg/g)	pH	C_0(mg/L)	Reference
Leaf mould	43.1	2	1000	(Karthikeyan, T., 2005)
Coconut shell carbon	10.88	4	25	(Karthikeyan, T., 2005)
Beech sawdust	16.1	1	200	(Karthikeyan, T., 2005)
Sugarcane bagasse	13.4	2	500	(Karthikeyan, T., 2005)
Treated sawdust of Indian Rosewood	10	3	100	(Karthikeyan, T., 2005)
Coconut tree sawdust	3.6	3	20	(Karthikeyan, T., 2005)
Sawdust activated carbon	44.05	2	200	(Karthikeyan, T., 2005)
Treated sawdust of Sal tree	9.55	3.5	40	Current studies

CHAPTER-6

ADSORPTION OF Cr(VI) ON WASTE WEED

Adsorption of Cr(VI) on waste weed

6.1. Adsorbent preparation

In this chapter a waste weed, *Salvinia cucullata*, growing profusely in sweet water ponds and lakes was used to treat Cr(VI) contaminated water. The adsorbent, *Salvinia cucullata*, was collected from a lake at Nandan Kanan situated about 15 km from Bhubaneswar, the capital city of Orissa. The weed was washed with distilled water followed by sun drying and finally drying in an oven at 70 ^{0}C for 4 hours. The dried weed was ground and sieved to obtain different sieve fractions and size analysis was carried out using Malvern Particle Size Analyzer model-2000.

The physical characteristics such as specific gravity, bulk density, specific surface area, porosity and average particle size along with the chemical constituents of the adsorbent are listed in Table 6.1. The SEM images of the weed before and after adsorption are shown in Figs.6.1 and 6.2 respectively. From the images it was observed that in case of weed before adsorption the surface is smooth and uninterrupted. But in case of weed after adsorption a thin layer was found on the surface of the adsorbent. From this change in the morphology, it can concluded that Cr(VI) was adsorbed on the surface of the weed, forming a number of thin layers over it. Further, to confirm the above conclusion, elemental analysis by the EDAX was carried out. The EDAX plots for the weed before and after adsorptions are shown in Figs.6.3 and 6.4 respectively. From the elemental analysis, it was observed that the weight percentage of Cr in the weed was higher after adsorption, which conformed the adsorption of Cr(VI) on the surface of the adsorbent.

6.2. Adsorption experiments

Adsorption experiments were carried out in 100 mL flasks using 50 mL of synthetic Cr(VI) solution. Aqueous solution of Cr(VI) was prepared by dissolving requisite amount of $K_2Cr_2O_7$ in de-ionised water. A stock solution having concentration 1000 mg/L of Cr(VI) was prepared and subsequently diluted to the required strengths to

carry out the adsorption studies. The mixtures were agitated by a Remi make mechanical stirrer with speed regulator. Adsorption studies were carried out at different temperatures using an automatic temperature controlled water bath with an accuracy of ± 1 ^{0}C. For higher temperatures, the adsorption studies were carried out in a sealed unit to avoid loss due to evaporation. The pH of the solution was adjusted before mixing the adsorbent, by using dilute HCl or NaOH, as the case may be. Unless other wise mentioned, all adsorption studies were carried out under following conditions:

- pH: 1.7
- agitation speed: 600 rpm
- adsorbent concentration: 2 g/L
- adsorbate concentration: 500 mg/L
- temperature: 30 ^{0}C
- contact time: 12 h

After adsorption, the mixture was filtered through Whatman No.42 filter paper. The residual Cr(VI) concentration was determined by diphenylcarbazide method, using an UV/Visible spectrophotometer (Perkin Elmer Lambda-35) (Chun, Li., 2004). The equilibrium adsorption uptake was calculated using the following equation:

$$q_e = \frac{(C_0 - C_e)V}{M} \qquad (6.1)$$

where 'q_e' is the equilibrium adsorption capacity (mg/g), 'C_0', 'C_e' are initial and equilibrium concentrations (mg/L) of Cr(VI) in the solution, 'V' is the volume (L) of solution taken, and 'M' is the mass (g) of adsorbent used.

The FT-IR spectra of the weed as such and weed after adsorption were taken as discussed in the previous section. All experiments were carried out using AR/GR grade EMerck chemicals. De-ionised water was used in all the experiments. All experiments were carried out in duplicate and the results reported are average of the two. The differences between duplicate experimental values were in the range of ±3%.

6.3. Results and discussion

6.3.1. Effect of agitation speed

Adsorption studies were carried out at varying agitation speeds: 100-800 rpm. It was observed that the percentage of adsorption increased with the increase of stirring speed up to 600 rpm (Fig.6.5**)** and thereafter, the adsorption efficiency was independent of agitation speed. The increase of adsorption efficiency with the increase of agitation speed could be mainly due to resistance to mass transport in the bulk solution at lower agitation speeds. A thin liquid film surrounding the adsorbent particles offered resistance to mass transport by diffusion. As the agitation speed increased, there would be decrease in the thickness of the boundary film, thereby decreasing the effect of film diffusion. Since beyond an agitation speed of 600 rpm, there was hardly any increase in adsorption efficiency, further studies were carried out with this agitation speed. Under these experimental conditions, it could be safely assumed that the solution homogeneity can be maintained and simultaneously there might not be appreciable attrition of the adsorbent particle during adsorption process.

6.3.2. Effect of contact time

Contact time is an important parameter to determine the process kinetics as well as equilibrium time. To determine the minimum contact time required for maximum adsorption, studies were carried out for 12 h. and the results are shown in Fig.6.6. It was observed that the kinetics could be divided into two parts: the initial faster rate of reaction followed by a slower one. The initial transfer rate usually lasted for 15 minutes, which accounted for > 50% of total adsorption. As the equilibrium was achieved in 12 h, all further studies were carried out for 12 h.

6.3.3. Effect of pH

pH is another important parameter to determine the efficiency of adsorption. A number of experiments were carried out by varying the initial pH from 1.7 to 4.5 and the

results are shown in Fig.6.7. It was observed that in all cases, the equilibrium pH was higher than initial pH, which indicated acid neutralization effect and proton adsorption of hydroxylated mineral surface, popularly known as ligand exchange mechanism (Goldberg, S., 2003, Attundogar, H. S., 2002, Attundogar, H. S., 2003). It is widely believed that the mechanism for the adsorption of anions onto adsorbent surface involved surface complexation. There are two types of surface complexation such as inner and outer complexation. Formation of these types of complexation depends on the degree of surface protonation or dissociation as shown below:

$$\equiv SOH(s) + H^{+} \Leftrightarrow \equiv SOH^{+}{}_{2}(s) \qquad (6.1)$$

$$\equiv SOH(s) \Leftrightarrow \equiv SO^{-}(s) + H^{+} \qquad (6.2);$$

where , ≡ SOH(s) is surface of the adsorbent.

If the numbers of protonated surface groups are more than that of dissociated groups, the surface would be positively charged, thus facilitating the anion adsorption. On the other hand, if the amounts of both the species were equal, then the net charge would be zero. Thus the complex formation reaction can be shown as:

Outer sphere complex

$$\equiv SOH^{+}{}_{2}(s) + A^{-n} \Leftrightarrow \equiv SOH^{+}{}_{2}(s) \text{—} A^{-n} \text{—} \quad (6.3)$$

Inner sphere complex

$$\equiv SOH^{+}{}_{2}(s) + A^{-n} \Leftrightarrow \equiv SA^{(n-1)}(s) + H_2O \text{ —} \quad (6.4)$$

where, A^{-n} is the anion and Cr(VI) in the present case.

As reported in Chapter-4, the most dominant species in the aqueous solution are $HCrO_4^-$, CrO_4^{-2} and $Cr_2O_7^{-2}$, whereas the dominant species in pH range 1.7-4.5 (as in case of the present studies) is $HCrO_4^-$. Increase in the initial pH would convert $HCrO_4^-$ to CrO_4^{-2}. It was observed that the lower initial pH facilitated the adsorption of Cr(VI). The

percentage of adsorption decreased slightly when the initial pH increased from 1.7 to 2.0 but on further increase, the adsorption efficiency decreased sharply. The increase of equilibrium pH was considerably lower at lower initial pH compared to higher initial pH, which pointed towards protonation of the adsorbent. The lower adsorption efficiency at higher initial pH might be due to decrease in net positive charge and competition between OH^- and $HCrO_4^-$ ions. Therefore, at higher pH values, there was a minor change in equilibrium pH as shown in Fig.6.7. The equilibrium time increased with pH as the efficiency of adsorption increased, while at lower pH, the efficiency of adsorption was very high.

Again, the adsorption might be due to formation of complex with the chelating agent present in the adsorbent. Evidence of complex formation was obtained from Fourier Transform Infrared spectroscopy. The details on the peak intensity with the group assigned are listed in Table 6.2. Results showed that the adsorbent contained two or more functional groups. The main absorbance bands for weed as such were: two sharp peaks at 3350 cm^{-1} (H bonds, OH group) and 2930 cm^{-1} (aliphatic), three broad bands at 1630 cm^{-1} (unsaturated C=C), 1420 cm^{-1} (C-O streach) and 1020 cm^{-1} (C-O stretch, Si-O stretch) and two small peaks at 1560 cm^{-1} (amide double bond) and 880 cm^{-1} (aromatic CH). The Cr(VI) adsorbed material showed either shift or reduction in absorption peak suggesting the vital role played by the functional group.

From the pH variation it was observed that at higher pH (4.5) the adsorption capacity was 32.48 mg/g, which compared quite satisfactorily to the other adsorbents reported in literature (vide Table 6.8). So the adsorbent can be used to treat mine discharge water for domestic uses which is in generally at high pH,. The industrial water generally is at low pH and high Cr(VI) concentration. So this adsorbent can also be used to treat Cr(VI) contaminated industrial water because of its high adsorption capacity (164 mg/g) at lower pH, i.e.,1.7.

6.3.4. Effect of initial adsorbate concentration

Initially adsorption experiments were carried out with low adsorbate concentration (5 to 50 mg/L), but it was observed that within very short time the concentration reached non-detectible limit. So to interpret results kinetically and to get the maximum adsorption capacity, the initial Cr(VI) concentration was varied from 400 to 700 mg/L. It was observed that with the increase in initial concentration, the percentage of adsorption decreased, as is generally expected in the equilibrium process. When the initial concentration was increased from 400 to 700 mg/L, the percentage of adsorption decreased from 72 to 47% as shown in Fig.6.8**.** The metal uptake capacity increased from 144 to 171 mg/g when the initial concentration was increased from 400 to 600 mg/L. It decreased slightly when the initial metal ion concentration was increased beyond 600 mg/L. This may be attributed to higher availability of Cr(VI) ions in the solution. Moreover, higher initial concentration provided increased driving force to overcome mass transfer resistance of metal ions between the aqueous and solid phases resulting in higher probability of collision between Cr(VI) ion and the adsorbent. The decrease of uptake capacity beyond the Cr(VI) concentration of 600 mg/L might be due to saturation.

6.3.5. Effect of adsorbent dose

The adsorbent concentration was varied from 0.8 to 2.4 g/L in order to find out the adsorption efficiency. It was observed that the uptake decreased from 188 to 145 mg/g when the adsorbent concentration was increased from 0.8 to 2.4 g/L. The percentage adsorption increased from 30 to 70% when the adsorbent concentration was increased from 0.8 to 2.4 g/L. The results are shown in Fig.6.9.

6.3.6. Effect of temperature

Temperature is also an essential parameter in determining the kinetics as the wastewater temperature varies widely. The temperature was varied from 30 to 60 ^{0}C and

the results are shown in Fig.6.10. The uptake and the percentage adsorption increased almost parallel with increase in the adsorption temperature. The percentage of adsorption and uptake increased from 65 to 84% and 164 to 212 mg/g respectively when the temperature was raised from 30 to 60 ^{0}C. The increase in efficiency with increase in temperature indicated that the reaction followed endothermic pathway.

6.3.7. Effect of particle size of adsorbent

The particle size of the adsorbent was varied from 53 to 221 µm in order to find out the optimum particle size for maximum of Cr(VI) removal. The results are shown in Fig.6.11. The percentage of adsorption decreased from 65 to 51% with increase in particle size from 53 to 221 µm, whereas the uptake decreased from 164 to 128 mg/g. The decrease in percentage of adsorption and uptake with increase in particle size might be attributed to the decrease in specific surface area of the adsorbent.

6.4. Adsorption kinetic modeling

In order to determine a suitable kinetic model, the adsorption data was fitted into the following three kinetic equations (Hamid, N. K., 2001):

- irst order reversible:
- Pseudo first order
- Pseudo second order

6.4.1. First order reversible kinetics

The plot for the first order reversible rate as shown in equation 3.8 was drawn for Cr(VI) adsorption on weed under different adsorption parameters such as pH, adsorbate concentration, adsorbent dose, temperature and size of the particle. The values of the first order reversible kinetic parameters such as 'K_c', 'k_r', 'k_1'and 'k_2' were calculated using equations 3.10-3.12 and are given in Table 6.3. From Table 6.3 it is observed that the 'K_c' and 'k_1' values changed from 0.0747 to 0.9571 and 0.0003 to 0.0024 with decrease

of pH from 4.5 to 1.7 respectively; whereas, the 'k_2' values decreased from 0.0046 to 0.0025 when pH was decreased from 4.5 to 1.7. From the 'k_1' and 'k_2' values it can be concluded that the lower pH favored the forward reaction, or the adsorption process. With increase in adsorbate concentration from 400 to 700 mg/L, the 'K_c' and 'k_1' values decrease from 1.385 to 0.444 and 0.0041 to 0.0016 respectively and the 'k_2' values increased from 0.0025 to 0.0036. Similarly, with increase in adsorbent dose and temperature, 'K_c' and 'k_1' values increased and the 'k_2' values decreased. But with increase in particle size, the 'K_c' and 'k_1' values decreased and 'k_2' values showed a reverse trend. From the above discussions, it can be concluded that the higher adsorbent dose and temperature as well as lower pH, adsorbate concentration and particle size favored forward reaction or the adsorption process.

6.4.2. Pseudo first order kinetics

The pseudo first order equation (equation 3.7) was plotted at different adsorption parameters such as pH, adsorbate concentration, adsorbent dose, temperature and particle size. The values of rate constant 'k' and regression coefficient 'R^2' are given in Table 6.4. From the table it is observed that the 'k_2' values decreased from 0.0046 to 0.0025 when the pH value increased from 1.7 to 4.5. With variation in adsorbate concentration from 400 to 700 mg/L, the value of 'k' did not follow any specific trend. Similarly 'k' value decreased with increase in temperature and particle size whereas it increased with increase in adsorbent dose. The regression coefficient 'R^2' value varied between 0.78 to 0.98.

6.4.3. Pseudo second order kinetics

Pseudo second order kinetic model was also tried to evaluate the goodness of fit with the experimental data. Using the experimental data at different adsorption parameters kinetic plots were made for the pseudo second order kinetic equation (Eqn.3.15). The values of initial adsorption rate 'h', rate constant 'k' and regression coefficient 'R^2' are given in Table 6.5. The 'h' and 'k' values decreased from 0.2108 to

0.0801 and 0.0045 to 0.0005 respectively when pH decreased from 4.5 to 1.7. With increase in adsorbate concentration from 400 to 700 mg/L, the 'h' and 'k' values decreased from 0.0845 to 0.0872 and 0.0005 to 0.0004 respectively. Similarly the values of 'h' and 'k' increased with increase in adsorbent concentration and temperature but decreased with increase in particle size.

Since three kinetic models were used to fit the experimental data, different statistical analysis such as regression coefficient and absolute percentage deviation were used to find out the best fit for the curve. The absolute percentage deviation between the experimental data point and predicted data point from the model was calculated by using equation 3.24. The absolute percentage deviation provides a numerical value to interpret the goodness of fit of the given mathematical model to the data. Table 6.3 – 6.5 show different kinetic parameters along with 'R^2' values. From 'R^2' values it can be concluded that the adsorption followed pseudo second order kinetics.

6.5. Evaluation of thermodynamic parameters

As discussed earlier, the adsorption process is more favorable at higher temperatures. Using Arrhenius equation (equation 3.23) the energy of activation was calculated to be 1.2 kJ/mol. From the activation energy, it appears that Cr(VI) adsorption on the weed was physical adsorption as the activation energy was less than 6 kJ/mol (Tewari, N., 2005).

The standard free energy change (ΔG^0) was calculated by using the equation 3.20. The other thermodynamic parameters such as change in standard enthalpy (ΔH^0) and standard entropy (ΔS^0) were determined using the equation 3.21. ΔS^0 and ΔH^0 were obtained from the slope and intercept of the vant Hoff's plot of lnk verses 1/T. The calculated ΔH^0 and ΔS^0 values were 27.9 kJ/mol and 90.7 J/mol respectively. The positive values of enthalpy indicate the endothermic nature of the reaction. The positive value of ΔS^0 shows the increasing randomness at the solid- liquid interface of Cr(VI) ions on the adsorbent.

6.6. Mass transfer model

Due to porous nature of the adsorbent used in this study, pore diffusion is also expected in addition to surface adsorption. The contact time variation experiments were used to study the rate-determining step in the adsorption process (Inbarej, B. S., 2002). Since the particles were agitated at a speed of 600 rpm, it can be safely assumed that the rate is not limited by mass transfer from the bulk liquid to the external surface of the particle. Therefore, the rate determining step might be either film or intra-particle diffusion. As both act in series, the slower one of the two would be the rate-determining step.

The k_{id} values were determined from the slope of the linear plot between q_t verses $t^{1/2}$ and the results for different experiments are shown in Table 6.6 as describe in chapter 3. From 'R^2' values, it can be concluded that the process is pore diffusion controlled.

The initial curved portion relates to the film diffusion (D_1) and the later linear portion represents the diffusion (D_2) within the adsorbent. Assuming spherical geometry of the adsorbent particles, the relationship between weight uptake and time using Ficks law is shown equation 3.18-3.19. Using these equations, 'D_1', 'D_2' values were calculated. Table 6.6 shows the 'D_1', and 'D_2' values along with the 'R^2' values. The low values of same order of magnitude indicate that both film and pore diffusion control led the adsorption mechanism.

6.7. Adsorption isotherm studies

The adsorption isotherm can be explained by two classical mechanisms such as Freundlich and Langmuir, as discussed in Chapter 3. The isotherm constant values of both the models were calculated. The results are shown in Table 6.7. From the values of coefficient of determinant (R^2) it can be concluded that the adsorption isotherm followed both Freundlich and Langmuir models. The 'Q^0' value is the maximum value of q_{eq} that is

important to identify which adsorbent showed the highest uptake capacity and as such, was useful in scaling-up. The values varied between 23 to 232 mg/g, which compared well with other bio-sorbents as shown in Table 6.8. Although it is not possible to compare the results with other adsorbents due to varying experimental conditions, it could be concluded that the present adsorbent is a potential adsorbent in treating Cr(VI) contaminated water.

6.8. Conclusions

Following conclusions can be drawn as discussed above:

- The rate of adsorption increased with increase of agitation speed upto 600 rpm and beyond that the increase was marginal.
- The rate of adsorption may be due to both surface diffusion and intra-particle diffusion.
- The adsorption efficiency increased with the decrease of pH, which may be due to protonation of adsorbent that facilitates adsorption of anions like Cr(VI).
- The higher adsorbent concentration increased the percentage of adsorption, whereas a reverse trend was observed in case of uptake. The increase of adsorbate concentration brought down the percentage of adsorption.
- The kinetics of adsorption followed pseudo second order model.
- The low activation energy suggested the adsorption process followed diffusion controlled mechanism.
- From the maximum uptake values, it can be concluded that the present adsorbent has the potentiality to treat Cr(VI) contaminated water.
- The rate-determining step is observed to be both film and intraparticle diffusion controlled.

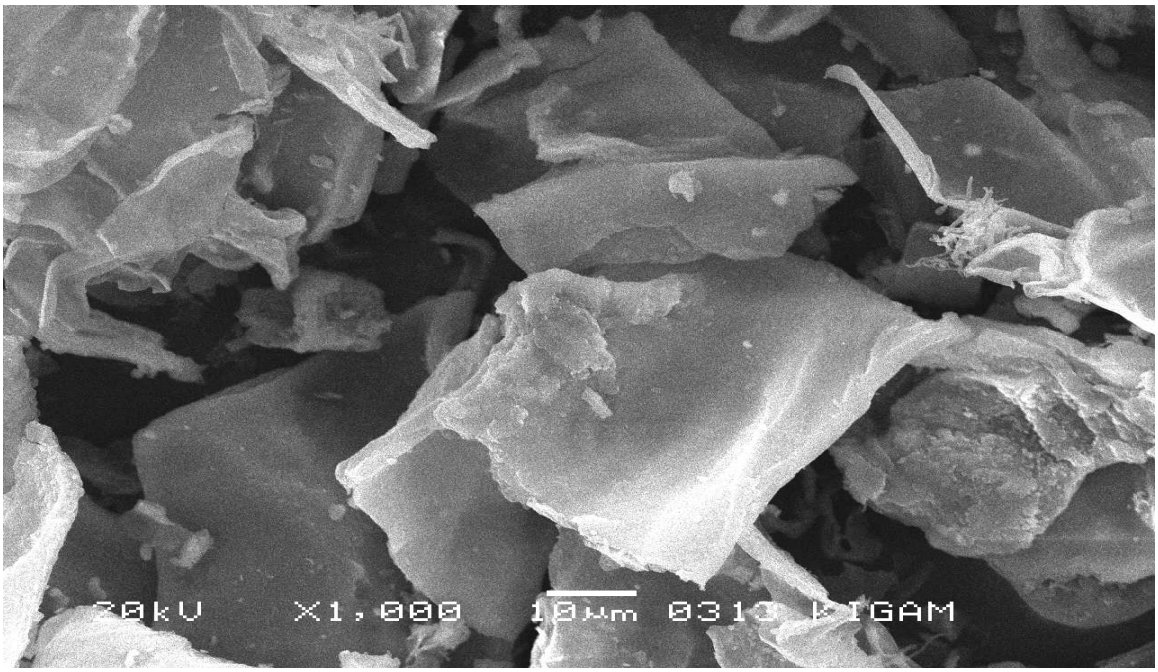

Fig.6.1. SEM image for weed as such

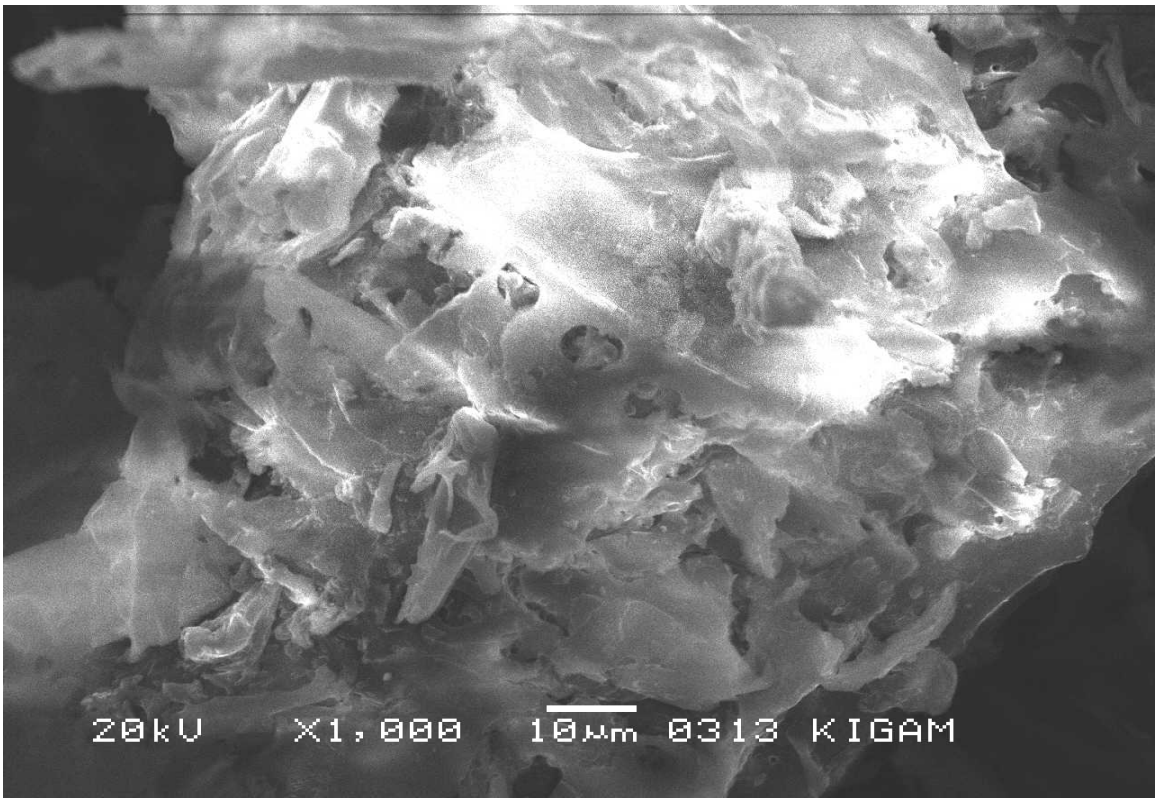

Fig.6.2. SEM image for weed after adsorption

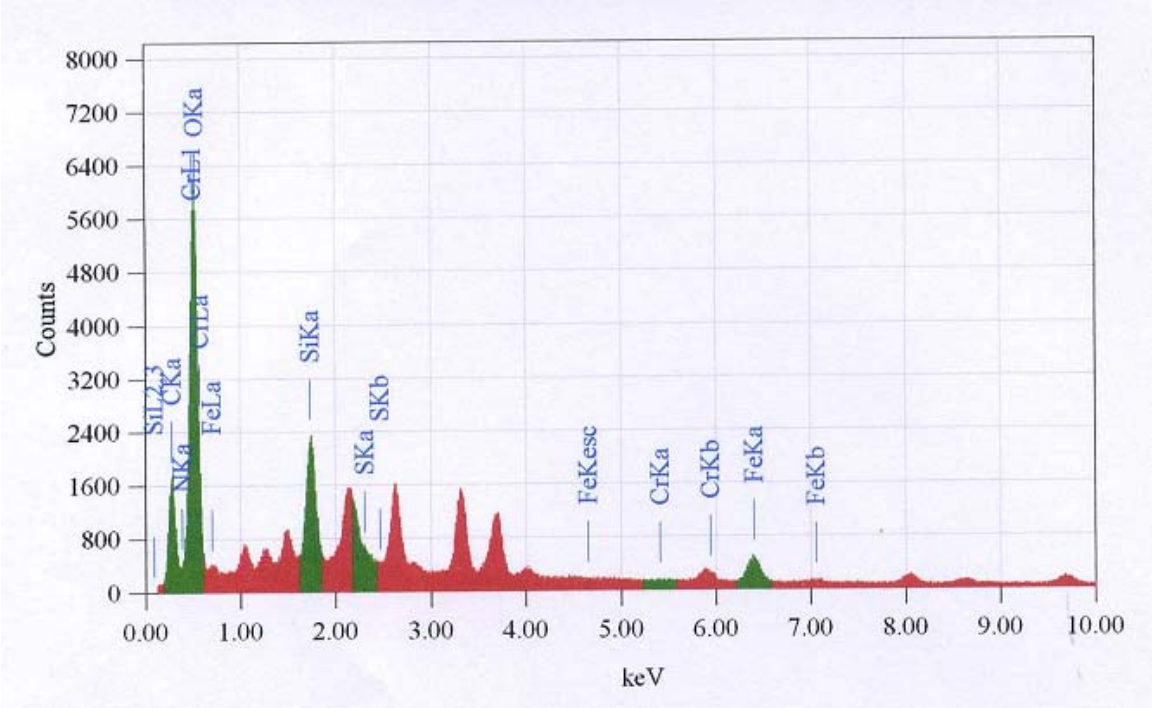

Fig.6.3. EDAX image for weed as such

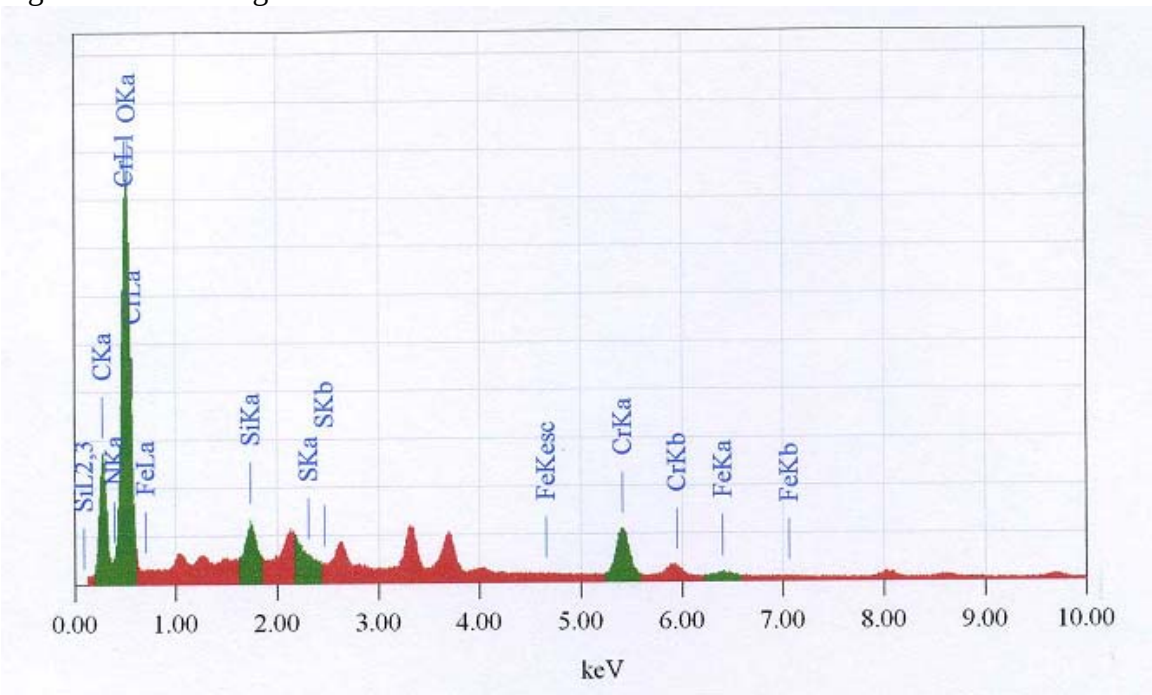

Fig.6.4. EDAX image for weed as such after adsorption

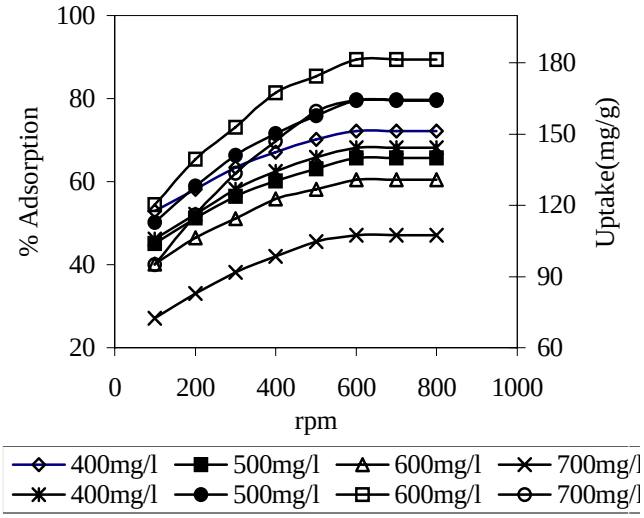

Fig.6.5: Effect of agitation on adsorption. [Conditions: pH 1.7, Adsorbate Concentration 500 mg/L, Adsorbent Concentration 2 g/L, Temp 30^0C, Time 12h, Particle size 53.55 micron]

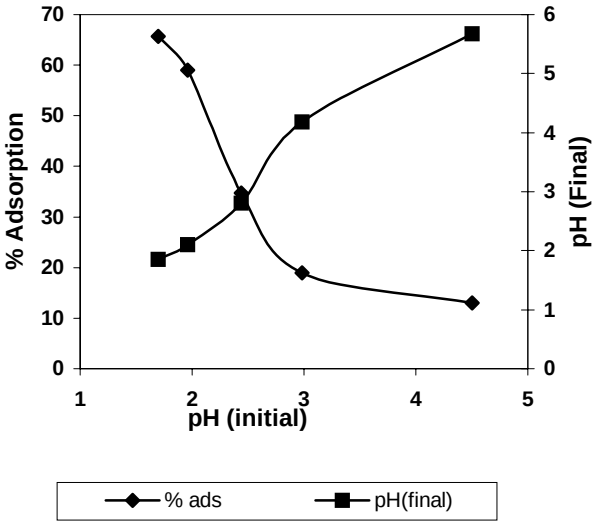

Fig.6.7: Effect of pH on adsorption [Conditions: Time 12h, Adsorbate Concentration 500 mg/L, Adsorbent Concentration 2 g/L, Temp 30^0C, Agitation speed 600 rpm, Particle size 53.55 microns]

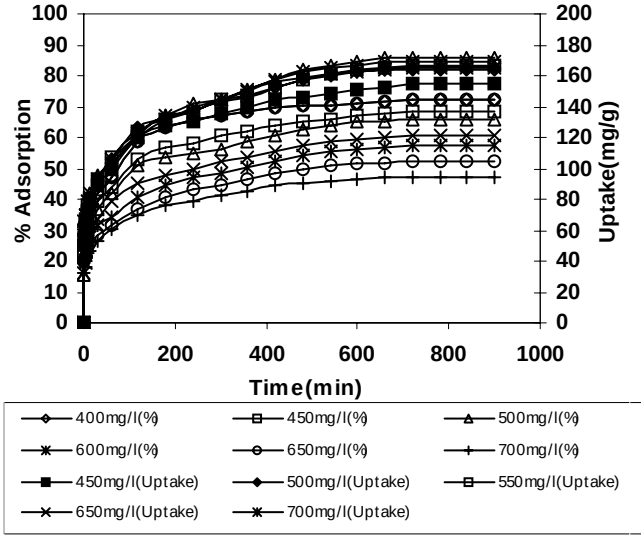

Fig.6.6: Effect of Contact time on adsorption- [Conditions: pH 1.7, Adsorbate Concentration 500 mg/L, Adsorbent Concentration 2 g/L, Temp 30^0C, Agitation speed 600 rpm, Particle size 53.55 microns]

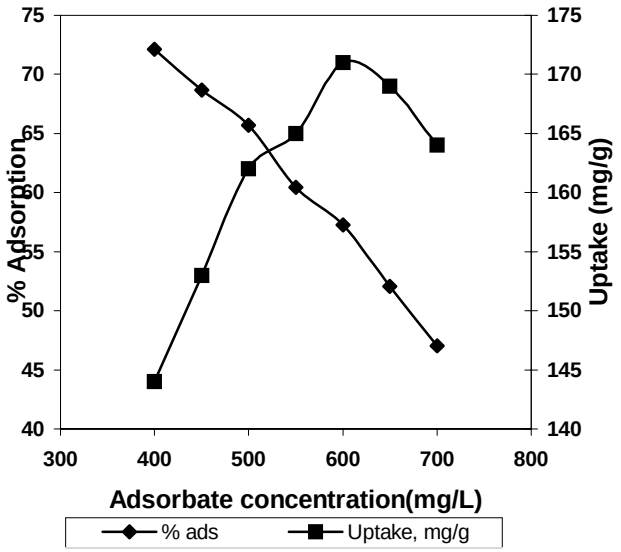

Fig.6.8: Effect of Adsorbate concentration on adsorption. [Conditions: Time 12h, pH 1.7, Adsorbent Concentration 2 g/L, Temp 30^0C, Agitation speed 600 rpm, Particle size 53.55 microns]

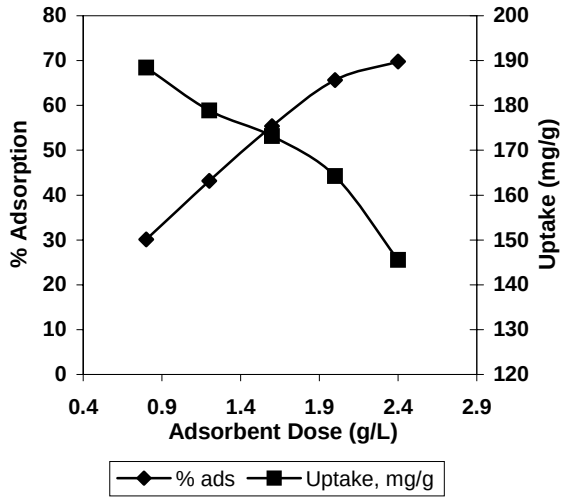

Fig.6.9: Effect of Adsorbent dose on adsorption [Conditions: Time 12h, pH 1.7, Adsorbate Concentration 500 mg/L, Temp 30^0C, Agitation speed 600 rpm, Particle size 53.55 microns]

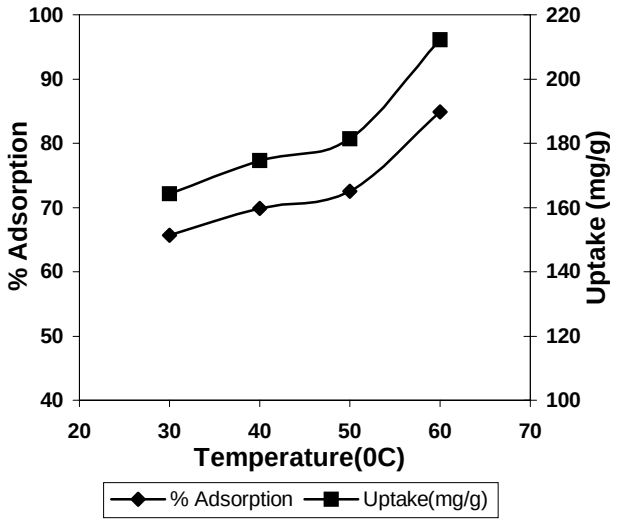

Fig.6.10: Effect of Temperature on adsorption-

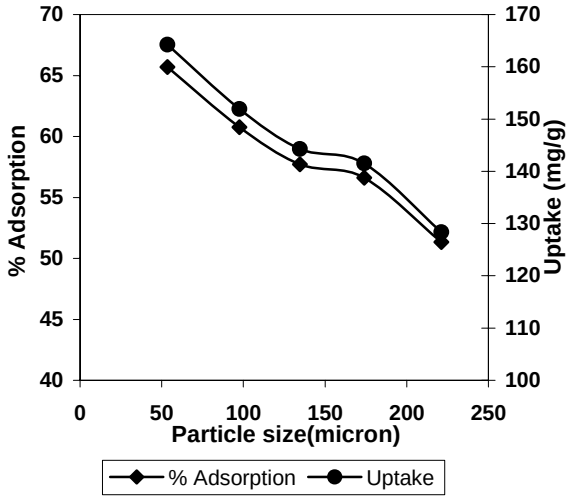

Fig.6.11: Effect of Particle size on desorption [Conditions: Time 12h, pH 1.7, Adsorbate Concentration 500 mg/L, Adsorbent concentration 2 g/L, Agitation speed 600 rpm, Temp30^0C]

[Conditions: Time 12h, pH 1.7, Adsorbate Concentration 500 mg/L, Adsorbent concentration 2 g/L, Agitation speed 600 rpm, Particle size 53.55 microns]

Table 6.1: Physical properties of the weed as such

Parameters	Value
Specific gravity	0.63
Bulk density (g/cc)	0.59
Porosity (%)	75
Surface area (m^2/g)	22.31
Average particle size	75micron
Moisture content (%)	60
Loss on ignition	96.88(w/w %)
Al_2O_3	1.78(w/w %)
SiO_2	1.15(w/w %)
FeO_2	0.26(w/w %)

Table 6.2: FT-IR peaks and group assignment

Peak (cm^{-1})	Group assigned
3350	OH group
2930	Aliphatic
1630	Unsaturated C=C
1560	Amide = bond
1420	C-O stretch
1020	C-O and Si-O stretch
880	Aromatic CH

Table 6.3: First order reversible kinetic rate constants with regression coefficients for different adsorption parameters

pH	K_c	k_r	k_1	k_2	R^2
4.5	0.0747	0.0049	0.0003	0.0046	0.83
3	0.1167	0.0033	0.0004	0.003	0.92
2.44	0.2675	0.0056	0.0012	0.0044	0.96
1.96	0.7184	0.0046	0.0019	0.0027	0.96
1.7	0.9571	0.0049	0.0024	0.0025	0.93
Ads Conc(mg/L)					
400	1.3855	0.007	0.0041	0.0029	0.98
450	1.0233	0.0052	0.0026	0.0026	0.93
500	0.9571	0.0049	0.0024	0.0025	0.95
550	0.7651	0.0049	0.0021	0.0028	0.98
600	0.6693	0.0045	0.0018	0.0027	0.99
650	0.5436	0.0047	0.0017	0.0031	0.98
700	0.4436	0.0052	0.0016	0.0036	
Ads dose (mg/L)					
2.4	0.9636	0.0057	0.0028	0.0029	0.98
2	0.9571	0.0049	0.0024	0.0025	0.93
1.6	0.7768	0.0044	0.0019	0.0025	0.95
1.2	0.6339	0.0044	0.0017	0.0027	0.96
0.8	0.5396	0.0076	0.0027	0.0049	0.98
Temp (^{0}C)					
30	0.9571	0.0049	0.0024	0.0025	0.93
40	1.1594	0.0043	0.0023	0.002	0.97
50	1.3207	0.0044	0.0025	0.0019	0.96
60	2.8103	0.0053	0.0039	0.0014	0.99
Particle Size (micron)					
54	0.957124	0.0049	0.002396	0.002504	0.9294
98	0.77464	0.0069	0.003012	0.003888	0.9884
134	0.682487	0.0092	0.003732	0.005468	0.974
174	0.652375	0.0094	0.003711	0.005689	0.901
221	0.52773	0.0095	0.003282	0.006218	0.9352

Table 6.4: Pseudo first order kinetic rate constants with regression coefficients for different adsorption parameters

pH	k_2	R^2
4.5	0.0046	0.83
3	0.003	0.92
2.44	0.0044	0.96
1.96	0.0027	0.96
1.7	0.0025	0.93
Ads Conc(mg/L)		
400	0.0029	0.98
450	0.0026	0.93
500	0.0025	0.95
550	0.0028	0.98
600	0.0027	0.99
650	0.0031	0.98
700	0.0036	
Ads dose (mg/L)		
2.4	0.0029	0.98
2	0.0025	0.93
1.6	0.0025	0.95
1.2	0.0027	0.94
0.8	0.0049	0.98
Temp (^{0}C)		
30	0.0025	0.93
40	0.002	0.97
50	0.0019	0.96
60	0.0014	0.99
Particle Size (micron)		
54	0.0025	0.93
98	0.0039	0.99
134	0.0055	0.97
174	0.0057	0.90
221	0.0062	0.94

Table 6.5: Pseudo second order kinetic rate constants with regression coefficients for different adsorption parameters

pH	h	k	R^2
4.5	0.2108	0.0045	1
3	0.316	0.0014	0.99
2.44	0.1436	0.0009	0.99
1.96	0.1087	0.0004	0.99
1.7	0.0801	0.0005	1
Ads Conc(mg/L)			
400	0.0845	0.0005	1
450	0.0884	0.0005	1
500	0.0801	0.0005	1
550	0.0851	0.0004	1
600	0.086	0.0004	1
650	0.0889	0.0004	0.99
700	0.0872	0.0004	0.9943
Ads dose (mg/L)			
2.4	0.1355	0.0004	1
2	0.1394	0.0003	0.99
1.6	0.1453	0.0002	0.99
1.2	0.1537	0.0002	0.99
0.8	0.1337	0.0002	0.99
Temp (^{0}C)			
30	0.0801	0.0005	1
40	0.0689	0.0005	1
50	0.0592	0.0005	1
60	0.0722	0.0003	0.99
Particle Size (micron)			
54	0.0801	0.0005	1
98	0.1012	0.0004	0.99
134	0.1113	0.0004	0.99
174	0.1237	0.0004	0.99
221	0.0874	0.0007	1

Table 6.6: Intra particle diffusion parameters with the regression coefficients for different adsorption parameters

pH	k_{id}	R^2	$D_{1*}10^{-12}$	R^2	D_2*10^{-12}	R^2
4.9	0.34	0.98	1.463	0.94	0.262	0.99
2.98	0.94	0.98	0.478	0.9	0.218	0.95
2.44	1.28	0.93	0.356	0.84	0.393	0.94
1.96	2.68	0.97	0.46	0.88	0.298	0.99
1.7	2.65	0.93	0.604	0.95	0.276	0.95
Conc (mg/L)						
400	2.48	0.92	0.184	0.9	0.32	0.97
450	2.13	0.8	0.126	0.98	0.473	0.98
500	2.69	0.93	0.463	0.91	0.284	0.95
550	2.8	0.95	0.394	0.97	0.291	0.98
600	3.1	0.96	0.071	0.94	0.284	0.98
650	3.04	0.95	0.09	0.95	0.313	1
700	2.78	0.93	0.196	0.98	0.334	0.99
Adsorbent Dose (g/L)						
2.4	2.27	0.9	0.151	0.94	11	0.99
2	2.72	0.94	0.463	0.91	33.69	0.97
1.6	3.07	0.95	0.168	0.99	12.2	0.97
1.2	3.34	0.97	0.292	1	21.2	0.98
0.8	3.43	0.85	0.78	0.85	56.71	0.98
Temp (^{0}C)						
30	2.69	0.93	0.463	0.91	0.284	0.95
40	2.88	0.96	0.079	0.94	0.262	0.98
50	2.79	0.97	0.163	0.98	0.254	0.98
60	3.64	0.93	0.137	0.96	0.356	1
Particle Size (micron)						
54	2.69	0.93	0.463	0.91	0.284	0.95
98	2.46	0.85	0.551	0.93	1.596	0.98
134	2.32	0.89	0.894	0.87	4.496	0.96
174	2.3	0.88	1.96	0.93	7.365	0.97
221	1.41	0.86	6.049	0.97	9.8	0.9

Table 6.7. Adsorption isotherm parameters with regression coefficients for different adsorption parameters

	Langmuir Constant			Freundlich Constant		
Parameters	Q_0	b	R^2	b_f	K_f	R^2
pH	23.98	-0.01	0.86	-0.62	843917.5	0.92
Conc.	175.4	0.058	0.99	-1.43	6054	0.98
Adsorbent dose	232.6	0.013	0.99	3.7	39.25	0.89
Temperature	232.6	0.013	0.99	3.7	39.25	0.98
Particle size	84.75	-0.01	0.99	-0.699	43.91	.989

Table 6.8. Comparison of adsorption capacity of weed with other adsorbents

Biosorbent	q_{max}(mg/L)	pH	T(^{0}C)	C_0(mg/L)	Reference
Aeromonas cavae	124.46	2.5	20	5-350	(Loukidou, M. X., 2004)
Chlorella vulgaris	24	2	25	25-250	(Veglio, F., 1997)
Zooglera ramigera	3	2	25	25-400	(Veglio, F., 1997)
Halimeda opuntia	40	4.1	26	25-400	(Veglio, F., 1997)
Rhizopaus arrhizus	62	2	25	25-400	(Prakasan, S., 1999)
Rhizopus arrhizus	8.8	2	25		(Veglio, F., 1997)
Rhizopaus nigrificans	123.45	2	25	50-500	(Abraham, T. E., 2002)
Sargassum	40	2			(Kratochvil, D., 1998)
Spirogira	14.7	2	18	25-Jan	(Kratochvil, D., 1998)
Pinus sylvestris	201.81	1	25	50-300	(Ucun, H., 2002)
Salvinia cucullata	232	1.7	30	500	Current studies

CHAPTER-7

ADSORPTION OF Cr (VI) ON ACID TREATED WEED

Adsorption of Cr(VI) on acid treated weed

7.1. Adsorbent preparation

The weed used in the previous section contained some water-soluble compounds, which was likely to deter the quality of treated water. Therefore, acid treatment of the weed before use was done for the treatment of Cr(VI) contaminated water. This was not only improved its physical and chemical characteristics but also removed the soluble fraction. The weed was dried at 60 ^{0}C for 4 h and then ground and sieved to different size fractions. 200 g of the smallest size fraction (-75micron) was mixed with 500 mL of 1N acetic acid and kept overnight. The treated weed was then washed several times by distilled water to remove excess acid followed by drying at 60 ^{0}C for 4h. The treated material was used to remove Cr(VI) from contaminated water. The physico-chemical characters of the adsorbent used are shown in Table 7.1. SEM analyses were made to find out the change in morphology after adsorption. The SEM images for the acid treated weed before and after adsorption are shown in Figs.7.1 and 7.2 respectively. It shows smooth and irregular surface before and after adsorption respectively. Again to confirm the adsorption of Cr(VI) on the adsorbent surface, EDAX analyses were carried out. The elemental analysis showed (Figs. 7.3 and 7.4) higher Cr concentration on the adsorbent after adsorption.

7.2. Adsorption experiments

In the present study, batch adsorption experiments were carried out in a 500 mL beaker using 250 mL of Cr (VI) solution and stirred with the help of a Remi make mechnical stirrer. At regular intervals 5 mL of the samples were drawn and filtered. All other experimental procedure were same as described previously.

7.3. Results and discussion

7.3.1. Effect of stirring speed

The percentage of adsorption and uptake increased from 43 to 57.9 and 107.5 to 144.7 mg/g respectively when the stirring speed was increased from 200 to 600 rpm (Fig.7.5). The increase in stirring speed might have reduced the film resistance to the adsorption process, which caused increase in net adsorption. Beyond 600 rpm, there was no further increase in adsorption, which might be due to complete removal of the film diffusion barrier.

7.3.2. Effect of contact time

In order to find out the equilibrium contact time, experiments were carried out for 15 h. From the experimental data it was observed that percentage adsorption increased with increase in contact time up to 12 h and after that it attained a stationary phase. From Fig.7.6 it is observed that initially the adsorption rate was fast followed by a slower rate. Further, the plots between time vs. percentage adsorption were smooth and continuous suggesting the possible monolayer adsorption of Cr (VI) on the surface of adsorbent. As equilibrium was achieved in 12 h, rest of the experiments were carried out for 12 h time only.

7.3.3. Effect of pH

Adsorption experiments were performed at different pH values (1.7, 2.0, 2.5, 3.5, 4.5). From Fig.7.7 it is observed that the percentage of adsorption and uptake increased from 6.2 to 57.9 and 15.5 to 144.7 mg/g respectively when the initial pH of the solution decreased from 4.5 to 1.7. The increase in percentage adsorption as well as uptake at lower pH could be well explained by protonation properties of the adsorbent. At low pH values, i.e., higher hydrogen ion concentration, the negative charge at the surface of internal pore were neutralized and some more new adsorption sites were developed which provided a positive charge for anionic Cr(VI) complex to get adsorbed on the surface. Again it is observed that the final pH of the solution was always greater than the initial

pH of the solution, which confirmed the neutralization of H^+ ions with the negative charge at the surface and envelopment of more H^+ ions in formation of positively charged surface. As a result, the concentration of H^+ ions decreased in the solution and hence the pH of the solution increased. Many authors also reported similar results [Yu, L. J., 2003]. From the adsorption uptake at both higher and lower pH (4.5 and 1.7) it is concluded that the adsorbent can be used for the treatment of Cr(VI) contaminated mining water at higher pH and Cr(VI) contaminated industrial water at lower pH.

7.3.4. FT-IR analysis

Apart from electrostatic force of atraction, the adsorption might be due to formation of complex in the ligands available in the adsorbents. The adsorbent as such showed peaks at 3450, 3330, 2920, 1670, 1363 and 1035 cm^{-1} which correspond to bonded OH group, NH stretching, aliphatic C-H group, C=O stretching, C-O stretching and C-C stretching respectively. The Cr(VI) loaded adsorbent showed either shift or reduction in adsorption peaks suggesting the vital role played by the functional groups. Therefore FT-IR studies showed the vital role played due to chelation. Chelation is favoured at lower pH and so the adsorption efficiency was more. The results are shown in Table 7.2.

7.3.5. Effect of initial adsorbate concentration

As discussed in the previous section, initially adsorption experiments were carried out at low adsorbate concentrations i.e. from 5 to 50 mg/L. It was observed that within very short time the Cr(VI) concentration of the solution reached to non-detectable limit. So to find out the optimum adsorption capacity and to interpret the adsorption data kinetically, adsorption experiments were carried out at higher adsorbate concentrations. The effect of initial Cr(VI) concentration on percentage adsorption and uptake was studied by varying the initial Cr(VI) concentration from 400 mg/L to 700 mg/L. It was observed that the percentage of adsorption increased from 46.8 to 60.8 and the uptake decreased from 163.7 to 121.6 mg/g of adsorbent when the concentration was decreased

from 700 to 400 mg/L (Fig.7.8). The percentage adsorption increased uniformly with the decrease of adsorbate concentration indicating that the adsorbent material did not reach saturation. The increase in uptake of Cr(VI) might be due to the competition between the adsorbate ions for limited adsorbent surface.

7.3.6. Effect of adsorbent dose

Batch experiments were carried out by varying the adsorbent dose from 0.8 to 2.4 g/l. The percentage of adsorption increased from 31.5 to 66% and the uptake decreases from 196.5 to 137 mg/g when the adsorbent dose was increased from 0.8 to 2.4 g/l [Fig.7.9]. The increase in percentage adsorption with the increase in adsorbent dose might be due to the increased number of free surface available, which caused increased number of adsorbate molecules to adsorb. The decrease in uptake might be due to the larger surface area at higher dose which remained free for adsorption at equilibrium.

7.3.7. Effect of temperature

Experiments were performed at different temperatures varying from 30 to 70 ^{0}C. The percentage of adsorption and uptake of Cr(VI) increased from 49.4 to 70 and 123.5 to 175 mg/g respectively when the temperature increased from 30 to 70 ^{0}C (Fig.7.10). The increase in percentage adsorption and uptake confirmed the endothermic nature of the process. Apart from endothermic nature, the adsorption process might be controlled by diffusion mechanism, as the adsorbent was porous in nature. The increase in temperatures also favored adsorbate transport within the pore of the adsorbent. The increase in adsorption with temperature could also be attributed to the increase in the number of adsorption sites generated due to breaking of some initial bonds near the edge of the active surface sites of the adsorbent (Sing, K. K., 2005).

The activation energy (E) for Cr(VI) adsorption was calculated by using Arrhenius equation (equation.3.23). By plotting lnk vs. 1000/T (Fig.7.11), the activation energy was calculated from the slope. The activation energy was found to be 18.252kj/mol. The low activation energy indicates that physical forces governing the

adsorption. The standard Gibb's energy (ΔG^0) was evaluated by using equation 3.20. The equilibrium constant (K_c) was evaluated at each temperature using the following equation:

$$K_c = \frac{q_e}{C_e}$$

The thermodynamic parameters such as standard enthalpy (ΔH^0) and standard entropy (ΔS^0) were determined using the van't Hoff's equation (equation.3.21). The positive value of ΔH^0 (47.76Kj/mol) indicated the endothermic nature of the process. The negative value of ΔG^0 (-16.588Kj/gmol) reflected the feasibility of the process and the values became more negative with increase in temperature. Standard entropy ΔS^0 (6.21j/mol) determined the disorderness of the adsorption at the solid liquid interface.

7.4. Adsorption kinetic modeling

In many cases, the kinetics of adsorption by any biological material was tested for pseudo first order expression (Cemioglu. B. A., 2005). However, it was also been shown that pseudo second order and Ritchie second order equation (Loukhido, M. X., 2004, Cheung, C. W., 2001), sometimes provided a better description of the adsorption kinetics. So in the present studies, pseudo first order, pseudo second order and Ritchie second order equations were used for modeling the kinetics of Cr (VI) sorption

7.4.1. Pseudo first order kinetics

The plot for first order rate equation (equation.3.7) was made at different adsorption parameters the rate constant along with the statistical parameters such as coefficient of determination and the absolute percentage deviations between the experimental values and predicted values from the pseudo first order kinetic model are given in Table 7.3. From the table it is observed that there is hardly any change in the value of rate constant at various adsorption parameters. The R^2 values varied between 0.9

to 0.99. But the absolute percentage deviation between the experimental uptake value and predicted value varied between 19 to 34, which are very high.

7.4.2. Ritchie second order kinetics

Similarly, Ritchie second order equation (Equation.3.16) was also fitted to the experimental data. The estimated values of the kinetic model parameters are reported along with other statistical parameters such as correlation coefficient R^2 and the average absolute percentage deviation (% Dev) between $q_{e(cal)}$ and $q_{e(exp)}$ in Table 7.4. From the table, it was observed that rate constant values did not follow any particular ascending or descending trend. The R^2 values varied from 0.56 to .99 for different adsorption parameters. But the absolute percentage deviation varied from 22 to 35. So from the R^2 and absolute percentage deviation values, it is concluded that the Ritchie second order model is not suitable for the adsorption process.

7.4.3. Pseudo second order kinetics

Finally, the pseudo second order kinetic model (equation.3.15) was tried to the experimental data to find out the goodness of fit. The values of k_2 were calculated from the plots between t/q_t vs. t/q_e. The values of rate constants along with the statistical parameters are listed in Table 7.5. From the table it is observed that, with increase in pH from 1.7 to 4.5, the value of rate constant decreased from 0.00125 to 0.00016. For all other parameters, kinetic rate constant did not follow any particular trend. The R^2 values in this case varied from 0.99 to 1 and the absolute percentage deviation varied from 4 to 2. From the R^2 and absolute percentage deviation values it is concluded that the adsorption process followed pseudo second order kinetic model.

7.5. Adsorption isotherm studies

Analysis of equilibrium data is important for developing an equation that can be used for design purpose. An attempt was made to find out the adsorption isotherm, which fitted best to the experimental data. Three adsorption isotherms model were considered:

- Langmuir (Hamid, N. K., 2001)
- Frendluich (Tiwari, N., 2005)
- Temkin isotherm (Karthikeyen, T., 2005)

Langmuir constants (Q_0, b), Frendluich constants (h_f, b_f) and Temkin constants (A, B) were calculated from the plot between 'C_e/q_e' vs. 'C_e', lnq_e vs. lnC_e and 'q_e' vs. 'C_e' respectively. In Tables 7.6-7.8 the estimated values of the model parameters are reported along with other statistical parameters such as correlation coefficient 'R^2', and the average absolute percentage deviation between '$q_{e(cal)}$' and '$q_{e(exp)}$'. From Tables 7.5-7.7 it is concluded that the experimental data fitted well to both Langmuir and Frendluich adsorption isotherm model. Almost all 'b_f' values were in the range of 0.1 to 1 indicating the adsorption to be favorable (Raji, C., 1998).

7.6. Mass transfer model

The adsorption process for porous solid can be separated in to three stages such as:

- Mass transfer (boundary layer/film diffusion),
- Sorption of ions into sites and
- Intra-particle diffusion.

In many cases, there is a possibility that intra-particle diffusion is the rate-limiting step and is given by equation.3.17 (Karthikeyen, T., 2005). The plot between 'q' vs. '$t^{1/2}$' gives the values of 'k_{id}' for different adsorption parameter. Again, the plot between time vs. percentage adsorption under different adsorption parameters were not linear over the entire time range indicating that more than one process affected the adsorption. So the adsorption process could be divided into two, the initial portion relating to film diffusion

(D_1) and the later portion relating to the diffusion within the adsorbent. The equation for 'D_1' and 'D_2' are given in equations.3.18 and 3.19 respectively. 'D_1' was calculated from the slope of the plot between 'q_t/q_e' vs. '$t^{1/2}$' for the initial curved portion. 'D_2' can be calculated from the slope of the curve between $\ln(1-q_t/q_e)$ vs. 't'. The values of 'D_1', 'D_2' and 'k_{id}' along with 'R^2' for different adsorption parameters are shown in Table 7.9.

7.7. Determination of number of stages

The number of stages required to decrease the concentration to a required level is found out from batch experiments (Aksu, Z., 1991). Fig. 7.12 shows a plot between C_e vs. q_e for various adsorbent concentrations by keeping the initial pH at 1.7. The operating line was drawn which passed through the point (C_o 500 mg/L, q_0 0.0 mg/g) and had slope V_0/X_0 as $-1/2$ where, V_0 and X_0 expressed in dm^3 and g respectively. From Fig.7.12 it is concluded that the Cr (VI) concentration can be reduced from 500 to <1 mg/L in three stages.

7.8. Conclusions

The acid treated weed, *Salvinia cuccullata,* used in this experiment was found to be a good adsorbent for the removal of Cr(VI). The percentage removal of Cr(VI) increased with the increase in time, temperature, adsorbate concentration, stirring speed and decreased with increase in pH and adsorbent dose. The adsorption kinetics followed pseudo second order rate equation. The average absolute percentage deviations (% Dev) between the experimental and calculated equilibrium uptake varied between 3 to 0.4 percent for all the three adsorption isotherms considered in this study. The adsorption process followed monolayer model. So experimental values were well fitted to all the three adsorption isotherms. Among film diffusion and intra-particle diffusion, film diffusion was found to be the rate controlling mechanism because of its lower diffusion coefficients. The percentage adsorption increased with increase in temperature, which indicated that the adsorption process was endothermic in nature.

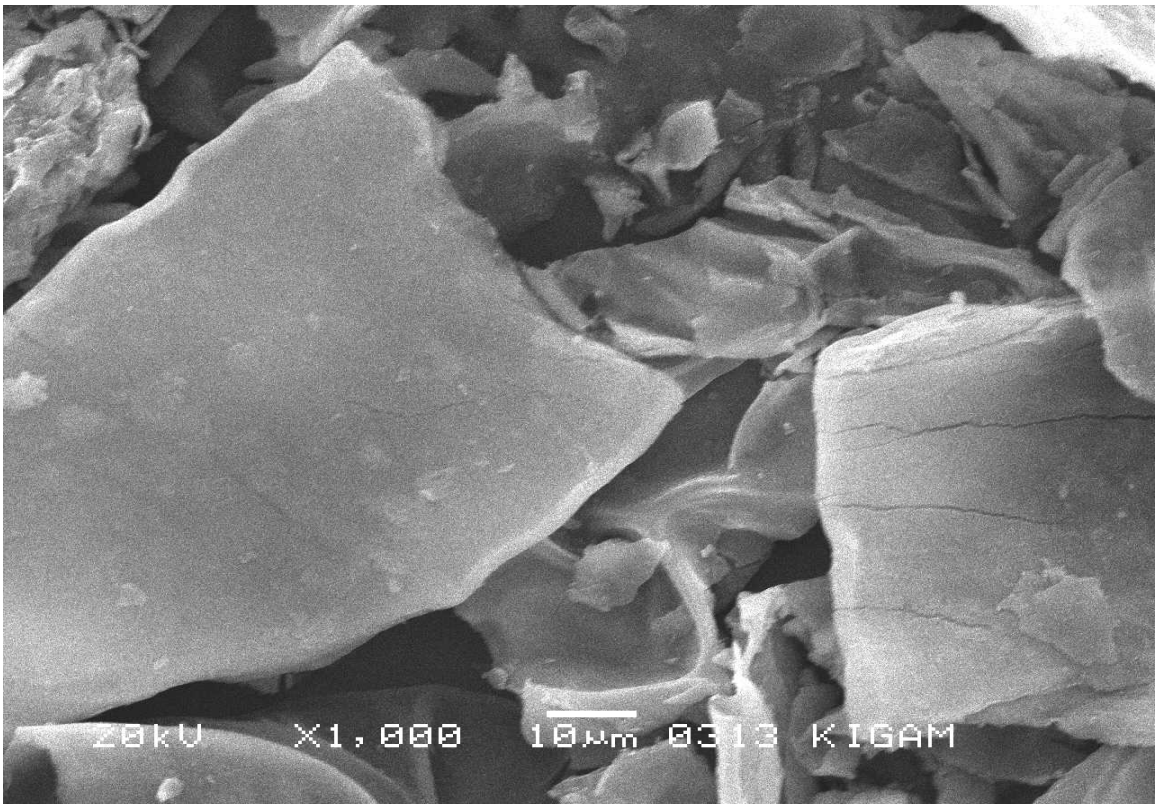

Fig.7.1. SEM image for acid treated weed

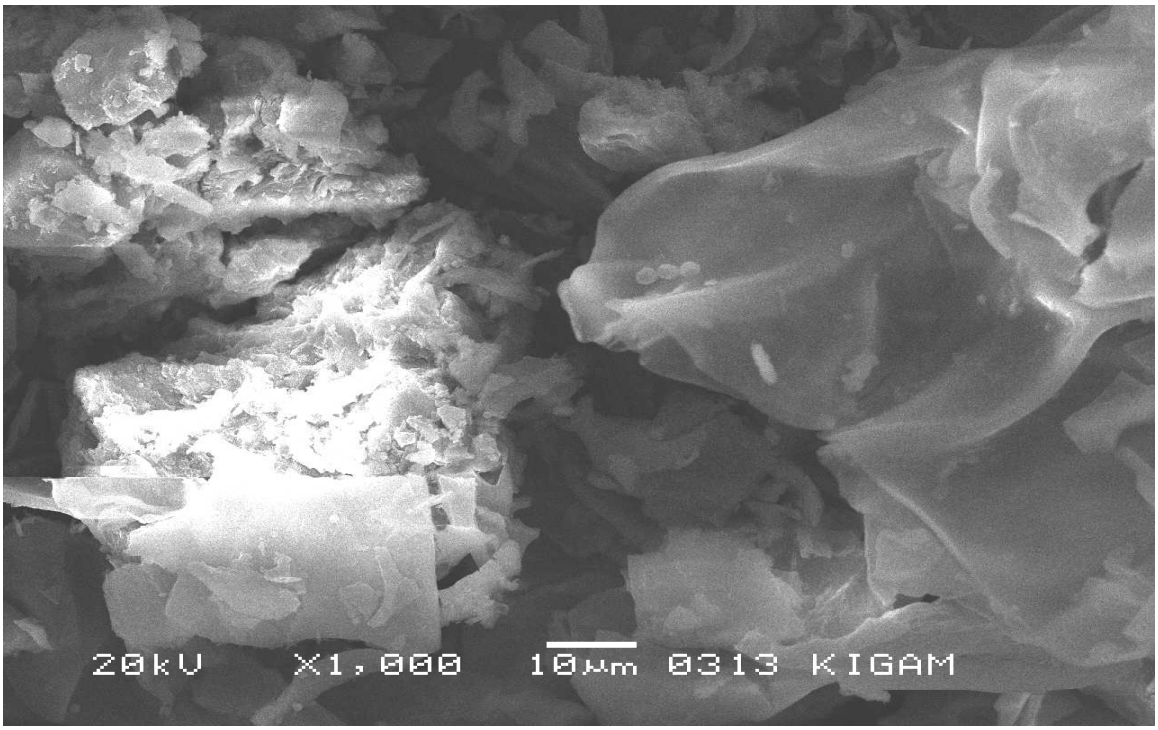

Fig.7.2. SEM image for acid treated weed after adsorption

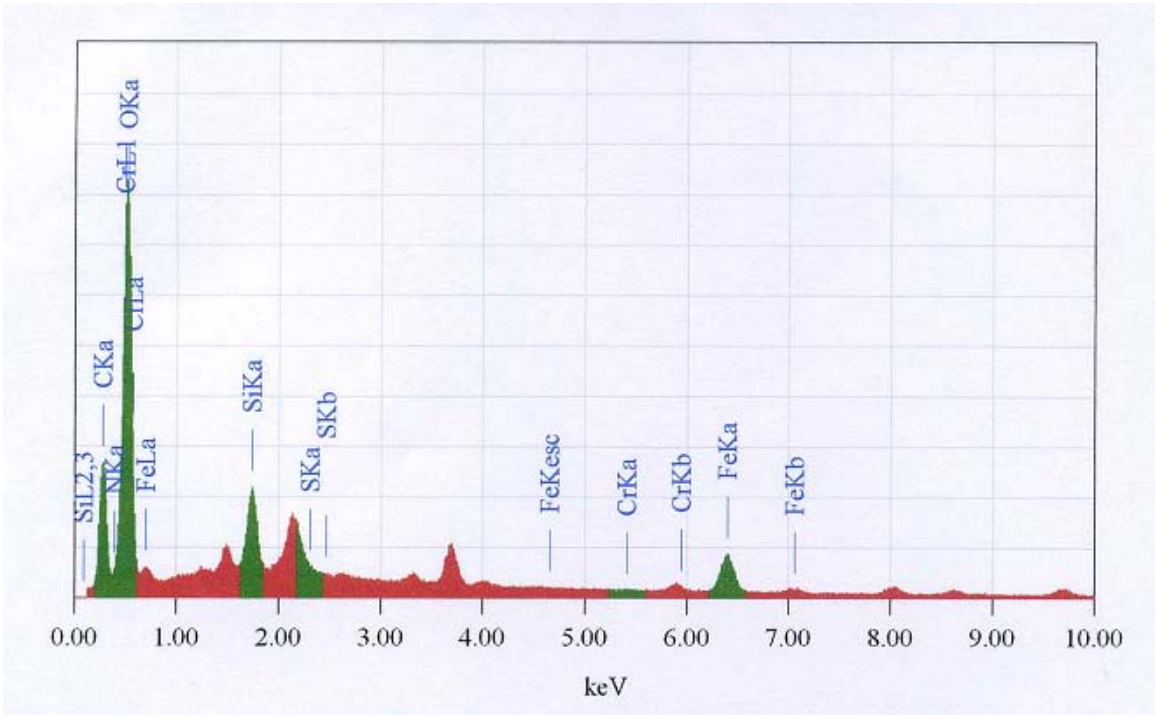

Fig.7.3. EDAX image for acid treated weed

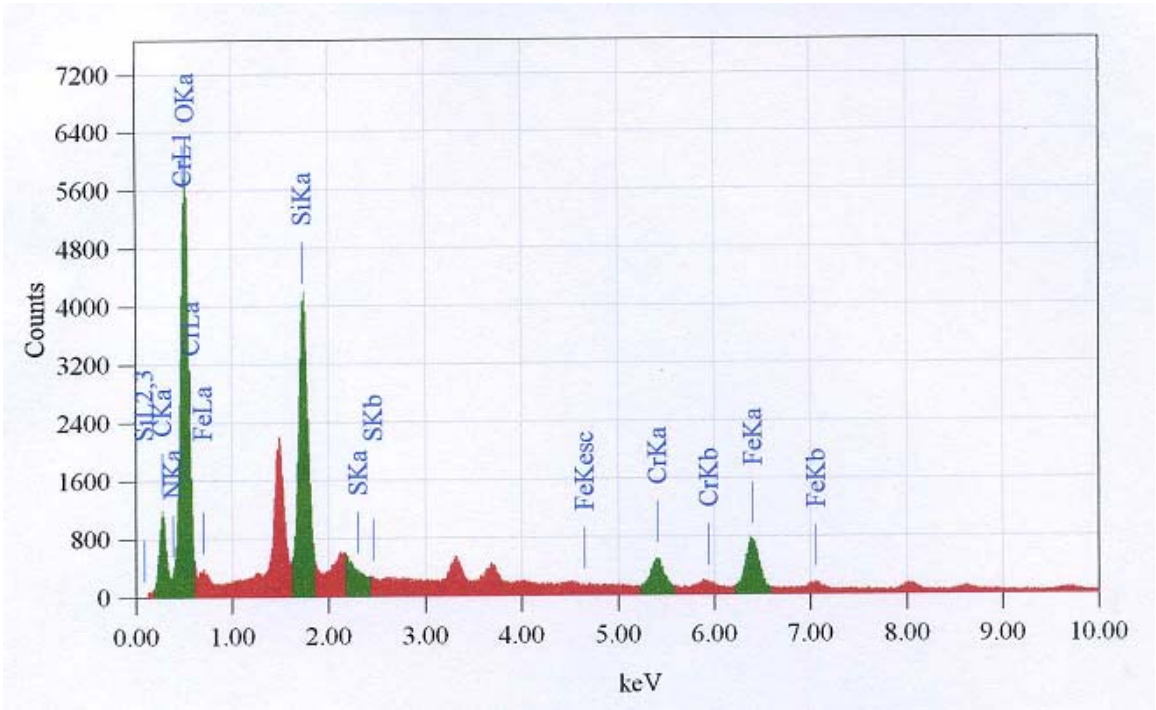

Fig.7.4. EDAX image for acid treated after adsorption

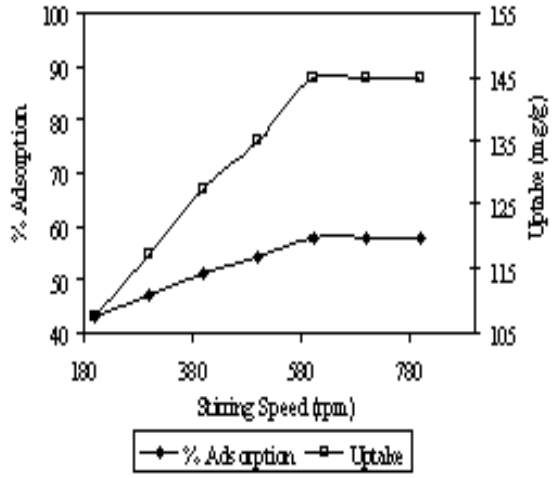

Fig.7.5. Effect of stirring speed on adsorption (Conditions: time 720min, adsorbate concentration 500 mg/L, adsorbent dose 2g/L, pH 1.7, temperature 30^0C.)

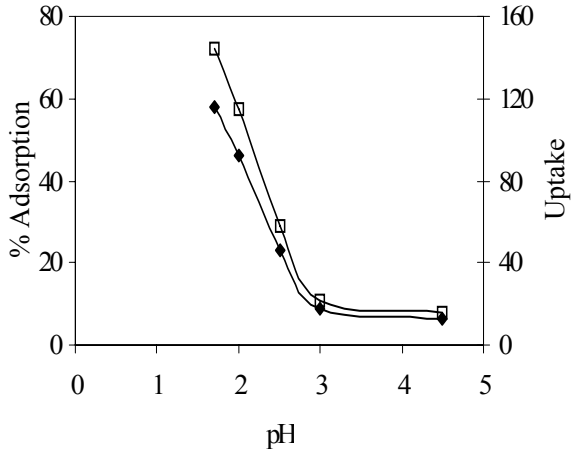

Fig.7.7. Effect of pH on adsorption. (Conditions: time 720min, adsorbate concentration 500 mg/L, adsorbent dose 2g/L, stirring speed 600rpm, temperature 30^0C.)

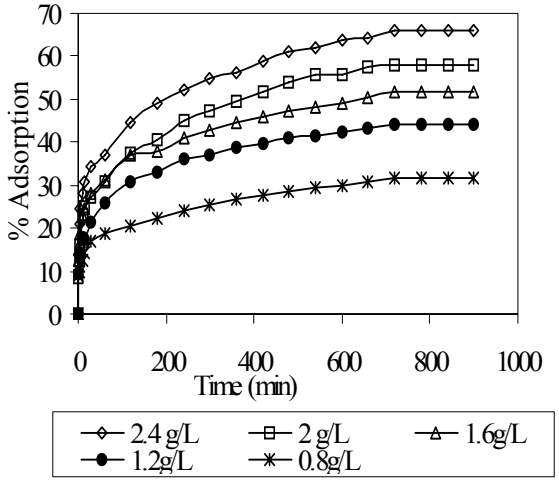

Fig.7.6. Effect of contact of time on adsorption. (Conditions: pH 1.7, adsorbate concentration 500 mg/L, adsorbent dose 2g/L, stirring speed 600rpm, temperature 30^0C)

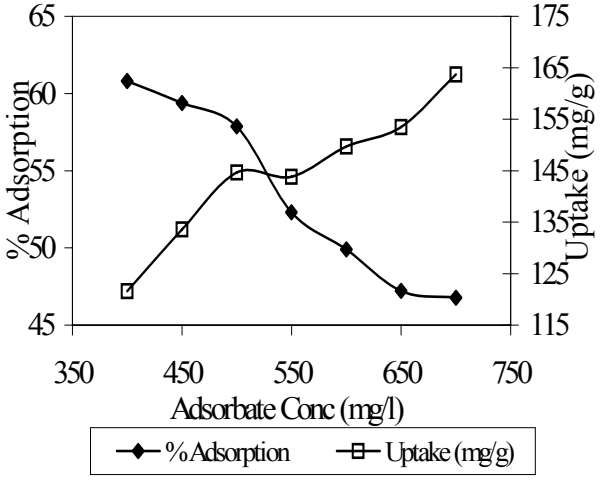

Fig.7.8. Effect of adsorbate concentration on adsorption. (Conditions: time 720min, pH 1.7, adsorbent dose 2g/L, stirring speed 600rpm, temperature 30^0C)

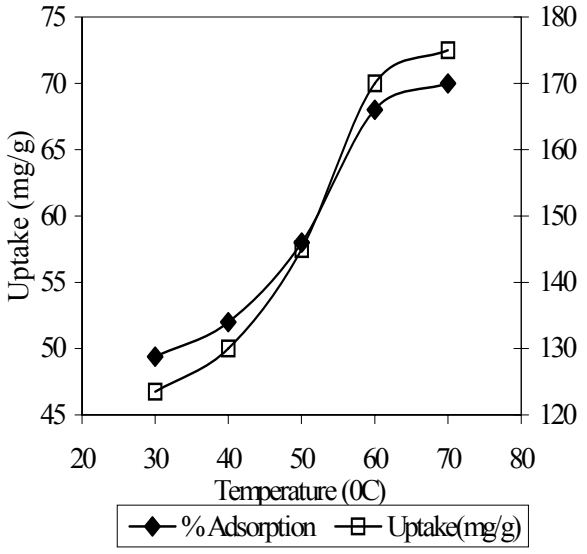

Fig.7.9. Effect of adsorbent dose on adsorption. (Conditions: time 720min, adsorbate concentration 500 mg/L, pH 1.7, stirring speed 600rpm, temperature 30^0C)

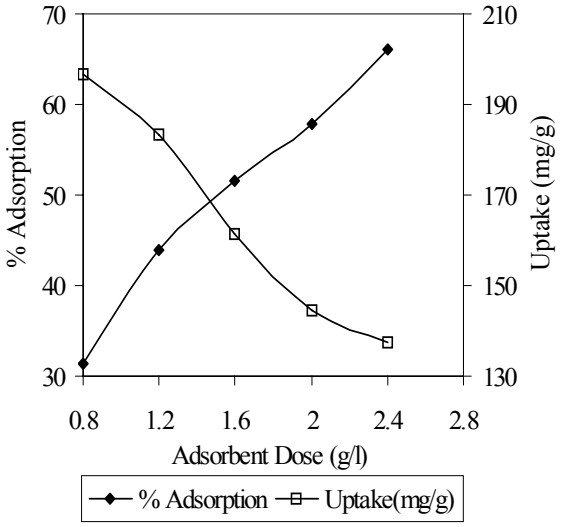

Fig.7.10. Effect of temperature on adsorption (Conditions: time 720min, adsorbate concentration 500 mg/L, adsorbent dose 2g/L, stirring speed 600rpm, pH 1.7.)

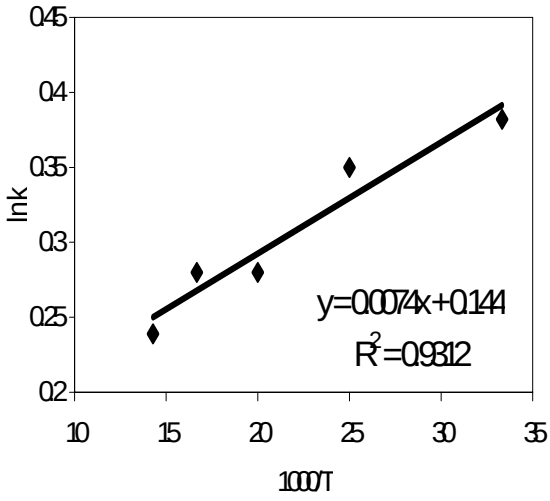

Fig.7.11. Arrhenius plot for evaluation of activation energy

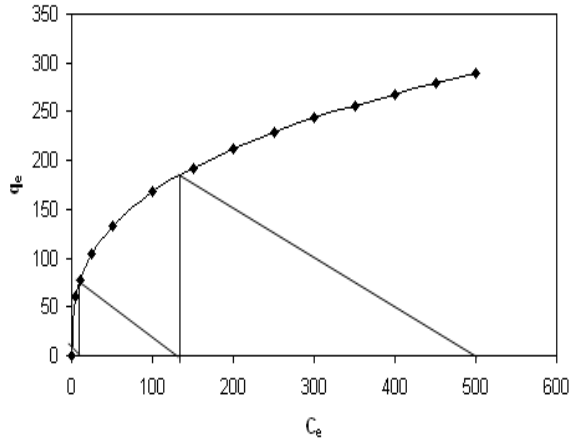

Fig.7.12.Determination of number of stages using adsorption isotherm

Table 7.1: Physical properties of acid treated weed

Parameters	Value
Specific gravity	0.65
Bulk density (g/cc)	0.61
Porosity (%)	71
Surface area	23.82
Average particle size	73 micron
Moisture content (%)	55
Loss of ignition	96.2(w/w %)
Al_2O_3	1.98(w/w %)
SiO_2	1.75(w/w %)
FeO_2	0.26(w/w %)

Table 7.2: FT-IR peaks and group assignment

Peak at wavelength	Group assigned
3450	OH grouph
3330	NH streching
2920	Aliphatic C-H group
1670	C=O streching
1363	C-O streching
1035	C-C streching

Table 7.3: Pseudo first order kinetic parameters with calculated adsorption capacity, regression coefficients and absolute percentage deviations for different adsorption parameters

pH	k_1'	R^2	q_{ecalc}	q_{eExp}	Abso. % Dev
1.7	0.003	0.94	143.4	144.7	2.12
2	0.002	0.98	113.6	114.8	
2.5	0.003	0.92	57.0	57.8	
3	0.002	0.97	21.0	21.64	
4.5	0.002	0.99	14.8	15.41	
Adsorbent dose (mg/L)					
2.4	0.002	0.99	135.9	137.6	1.02
2	0.003	0.94	143.4	144.7	
1.6	0.002	0.97	159.4	161.2	
1.2	0.002	0.97	181.6	183.2	
0.8	0.002	0.97	194.5	196.5	
Adsorbate conc. (mg/L)					
400	0.002	0.9	120.3	121.6	0.91
450	0.002	0.94	132.2	133.6	
500	0.003	0.94	143.4	144.7	
550	0.002	0.95	142.5	143.8	
600	0.002	0.96	148.3	149.7	
650	0.002	0.98	151.8	153.5	
700	0.003	1	162.9	163.7	
Stirring rate (rpm)					
200	0.002	0.98	106.0	107.5	1.22
300	0.002	0.94	115.9	117.5	
400	0.002	0.95	125.7	127.5	
500	0.002	0.95	133.6	135	
600	0.003	0.94	143.4	144.7	
Temp^{0}C					
30	0.002	0.97	121.6	123.5	1.14
40	0.002	0.94	128.6	130	
50	0.002	0.99	143.2	145	
60	0.002	0.97	168.5	170	
70	0.002	0.98	173.4	175	

Table 7.4: Ritchie second order kinetic parameters with calculated adsorption capacity, regression coefficients and absolute percentage deviations for different adsorption parameters

pH	k_m	R^2	q_{ecalc}	q_{eExp}	% Dev
1.7	0.223	0.88	104.6	144.7	23.47
2	0.288	0.9	90.5	114.8	
2.5	0.107	1	52.0	57.8	
3	0.147	0.96	16.2	21.64	
4.5	0.16	0.89	10.3	15.41	
Adsorbent dose (mg/L)					
2.4	0.342	0.84	103.7	137.6	26.19
2	0.223	0.88	104.6	144.7	
1.6	0.4	0.78	121.5	161.2	
1.2	0.354	0.77	134.6	183.2	
0.8	0.5	0.63	142.5	196.5	
Adsorbate concentration (mg/L)					
400	0.404	0.66	83.0	121.6	36.65
450	0.306	0.77	92.2	133.6	
500	0.223	0.88	104.6	144.7	
550	2.798	0.72	36.1	143.8	
600	0.448	0.56	99.7	149.7	
650	0.367	0.76	110.7	153.5	
700	0.38	0.75	126.1	163.7	
Stirring rate (rpm)					
200	0.208	0.87	72.0	107.5	30.76
300	0.2	0.88	78.2	117.5	
400	0.185	0.9	87.1	127.5	
500	0.19	0.91	97.3	135	
600	0.223	0.88	104.6	144.7	
Temp^{0}C					
30	0.382	0.7	86.6	123.5	26.55
40	0.401	0.72	94.9	130	
50	0.221	0.93	111.7	145	
60	0.352	0.72	123.0	170	
70	0.239	0.88	130.8	175	

Table 7.5: Pseudo second order kinetic parameters with calculated adsorption capacity, regression coefficients and absolute percentage deviations for different adsorption parameters

pH	k_m	R_2	q_{ecalc}	q_{eExp}	% Dev
1.7	0.00016	0.99	141.0	144.7	2.30
2	0.00029	1	113.0	114.8	
2.5	0.00062	1	56.7	57.8	
3	0.00081	0.99	21.1	21.64	
4.5	0.00125	0.99	15.0	15.41	
Adsorbent dose (mg/L)					
2.4	0.00019	0.99	133.9	137.6	2.70
2	0.00016	0.99	141.0	144.7	
1.6	0.00018	0.99	156.4	161.2	
1.2	0.00015	1	179.9	183.2	
0.8	0.00013	0.99	189.7	196.5	
Adsorbate Conc. (mg/L)					
400	0.00016	0.99	118.7	121.6	2.00
450	0.00015	0.99	130.3	133.6	
500	0.00016	0.99	141.0	144.7	
550	0.00016	0.99	140.9	143.8	
600	0.00014	0.99	146.9	149.7	
650	0.00014	0.99	149.5	153.5	
700	0.00024	1	163.8	163.7	
Stirring rate (rpm)					
200	0.00016	0.99	104.2	107.5	2.74
300	0.00014	0.99	114.0	117.5	
400	0.00013	0.99	123.4	127.5	
500	0.00015	0.99	132.4	135	
600	0.00016	0.99	141.0	144.7	
$Temp^0C$					
30	0.00017	0.99	120.6	123.5	1.74
40	0.00019	0.99	128.1	130	
50	0.00017	1	141.7	145	
60	0.00016	1	167.1	170	
70	0.00016	1	173.5	175	

Table 7.6: Langmuir adsorption isotherm parameters with calculated adsorption capacity, regression coefficients and absolute percentage deviations for different adsorption parameters

pH	q_{ecalc}	q_{eExp}	% Dev	Q_0	b	R^2
1.7	105.4	145	2.05	10.03	0.004	0.79
2	68.45	115				
2.5	25.08	57.8				
3	20.27	21.6				
4.5	19.73	15.4				
Adsorbent dose (mg/L)						
2.4	131.6	138	2.769	370.4	0.003	0.93
2	150.4	145				
1.6	162.9	161				
1.2	176.4	183				
0.8	195	196				
Adsorbate concentration (mg/L)						
400	124.8	122	2.439	200	0.011	0.99
450	131.9	134				
500	138.1	145				
550	147	144				
600	152.2	150				
650	156.8	153				
700	159.5	164				
Stirring rate (rpm)						
200	108.9	108	1.965	62.11	0.008	0.99
300	115.4	118				
400	124.1	128				
500	132.8	135				
600	148.3	145				
Temp (^{0}C)						
30	126.4	124	2.114	87.72	0.013	0.99
40	129.5	130				
50	139	145				
60	170	170				
70	181.4	175				

Table 7.7: Freundlich adsorption isotherm parameters with calculated adsorption capacity, regression coefficients and absolute percentage deviations for different adsorption parameters

pH	q_{ecalc}	q_{eExp}	% Dev	b_f	k_f	R^2
1.7	184.7	145	2.57	-2.68	3E+08	0.9
2	94.59	115				
2.5	36.77	57.8				
3	23.16	21.6				
4.5	21.55	15.4				
Adsorbent dose (mg/L)						
2.4	134.1	138	2.44	0.552	7.868	1
2	151.1	145				
1.6	163.1	161				
1.2	176.8	183				
0.8	197.7	196				
Adsorbate concentration (mg/L)						
400	126.1	122	2.44	0.281	30.49	0.9
450	131.7	134				
500	137.1	145				
550	145.8	144				
600	151.4	150				
650	157.2	153				
700	160.9	164				
Stirring rate (rpm)						
200	108.8	108	0.9	-0.98	27750	1
300	116.8	118				
400	126.2	128				
500	134.2	135				
600	146.3	145				
Temp (^{0}C)						
30	125.5	124	1.05	-0.66	4757	1
40	129.9	130				
50	141.8	145				
60	169.5	170				
70	176.9	175				

Table 7.8: Temkin adsorption isotherm parameters with calculated adsorption capacity, regression coefficients and absolute percentage deviations for different adsorption parameters

pH	q_{ecalc}	q_{eExp}	% Dev	b	A	R^2
1.7	150	145				
2	109.3	115				
2.5	51.97	57.8	1.11	-15.31	0.0019	0.99
3	23.89	21.6				
4.5	19.51	15.4				
Adsorbent dose (mg/L)						
2.4	132.4	138				
2	152	145				
1.6	164.6	161	2.787	27.403	0.0252	0.95
1.2	177.9	183				
0.8	196.3	196				
Adsorbate concentration (mg/L)						
400	125.8	122				
450	131.9	134				
500	137.6	145				
550	146.3	144	2.435	62.694	0.1507	0.91
600	151.7	150				
650	157	153				
700	160.3	164				
Stirring rate (rpm)						
200	108.2	108				
300	117.1	118				
400	126.8	128	0.462	-20.28	0.0015	1
500	134.6	135				
600	145.4	145				
Temp (^{0}C)						
30	124.8	124				
40	130	130				
50	143	145	0.637	-25.48	0.0011	1
60	169.7	170				
70	176	175				

Table 7.9: Intra particle diffusion parameters with calculated adsorption capacity, regression coefficients and absolute percentage deviations for different adsorption parameters

pH	k_{id}	R^2	$D_{1*}10^{-12}$	R^2	D_2*10^{-12}	R^2
1.7	3.552	0.981	0.492	0.923	17.486	0.912
2	2.078	0.987	0.537	0.873	13.473	0.987
2.5	0.813	0.966	0.965	0.964	15.479	0.849
3	0.631	0.980	0.335	0.791	16.626	0.962
4.5	0.387	0.980	0.378	0.986	13.473	0.974
Adsorbent dose (mg/L)						
2.4	2.994	0.979	0.284	0.906	12.613	0.984
2	3.552	0.981	0.365	0.908	17.486	0.911
1.6	3.161	0.986	0.274	0.954	12.039	0.953
1.2	3.755	0.975	0.200	0.929	14.046	0.938
0.8	4.275	0.996	0.209	0.992	13.186	0.944
Adsorbate concentration (mg/L)						
400	3.081	0.993	0.105	0.929	17.772	0.854
450	3.277	0.987	0.236	0.982	17.486	0.909
500	3.552	0.981	0.365	0.908	17.486	0.911
550	3.495	0.979	0.213	0.975	16.913	0.915
600	3.863	0.970	0.068	0.978	16.913	0.923
650	3.733	0.993	0.172	0.829	14.333	0.962
700	3.126	0.883	0.238	0.958	21.499	0.996
Stirring rate (rpm)						
200	3.113	0.984	0.266	0.923	14.619	0.979
300	3.432	0.993	0.294	0.965	15.193	0.901
400	3.530	0.997	0.412	0.977	14.333	0.925
500	3.445	0.989	0.425	0.939	16.626	0.924
600	3.552	0.981	0.365	0.908	17.486	0.911
Temp ^{0}C						
30	2.932	0.977	0.119	0.908	16.626	0.898
40	3.055	0.974	0.115	0.673	19.492	0.917
50	3.336	0.961	0.254	0.800	17.486	0.891
60	3.713	0.968	0.188	0.971	20.066	0.937
70	3.494	0.978	0.296	0.952	18.059	0.950

CHAPTER-8

ADSORPTION OF Cr(VI) ON CARBONIZED WEED

Adsorption of Cr(VI) on carbonized weed

8.1. Adsorbent preparation

As discussed earlier the weed contains water-soluble organic compounds, which impart color to the effluent after treatment. Acid treatment of the weed as described in the previous section can reduce the possibility of color leaching from the weed to the effluent. But it was observed that acid treatment of weed caused decrease in the uptake capacity of the adsorbent. Therefore, in the present study, heat activation method was used to improve the adsorption capacity of the adsorbent. An attempt was made to prepare activated carbon and to study its feasibility as an adsorbent for removal of Cr(VI) from aqueous solution. The weed *Salvinia cucullata* was washed with tap water followed by distilled water and sun-dried followed by drying at 60 ^{0}C for 1 h in an oven to remove the adhering moisture. The dried material was crushed to powder. The powdered material was transferred in a silica bowl to a muffle furnace and activation was carried out at 500 ^{0}C under nitrogen flow for 1 h. Subsequently, the carbonized mass was cooled to ambient temperature under nitrogen atmosphere to prevent complete combustion or oxidation. The carbonized mass thus produced was ground and sieved to different size fractions.

8.2. Adsorption experiment

Preparation of the adsorbate solution of different concentrations, quality of chemicals used, adjustment of pH, analytical procedure for the measurement of residual concentration of Cr(VI) etc are similar to those explained in the previous sections. The chemical and physical properties of the carbonized weed are shown in the Table 8.1. XRD analysis showed the peaks related to the major components corresponding to carbon. Again, to confirm the morphological change on the surface of the adsorbent due to adsorption of Cr(VI), SEM studies were performed. The SEM images for carbonized weed before and after adsorption are shown in Figs.8.1 and 8.2 respectively. To confirm the adsorption of Cr(VI) on the surface of the adsorbent, elemental analysis by EDAX (Fig.8.3 and 8.4) was performed. The higher weight percent of Cr in the adsorbent after

adsorption confirmed the adsorption process. The experimental procedure followed for the batch experiments in the present study was similar to that reported in the previous chapter.

8.3. Results and discussion

8.3.1. Effect of agitation speed

Adsorption studies were carried out by varying the agitation speed from 100 to 800 rpm to find out the speed at which the liquid boundary layer played an insignificant role. The results are shown in Fig.8.5. The adsorption efficiency increased with increase in agitation speed upto 600 rpm and thereafter, it attained a steady state. The extent of adsorption increased from 57.5 to 73.6% when the stirring speed was increased from 200 to 600 rpm, whereas the uptake increased from 144 to 184 mg/g when the stirring speed was increased from 200 to 600 rpm. This increase in adsorption efficiency with speed indicated that the thin liquid film surrounding the adsorbent played an insignificant role in the range of agitation applied allowing the adsorbate to reach the adsorbent surface.

8.3.2. Effect of contact time

Adsorption experiments were carried out for over 900 min to find the optimum contact time. The results are shown in Fig.8.6. It was observed that the kinetics was very fast initially which lasted for about 30 min followed by a slower rate. The faster kinetics accounted for about 60% of the total adsorption. The adsorption reaction attained equilibrium within 12 h and beyond that, there was hardly any change in concentration. Therefore, all further studies were carried out for 12 h contact time only. The dual adsorption kinetics may be due to the different mechanisms governing the process. Adsorption of the species normally takes place only when the adsorbate is transported from bulk to the adsorbent surface. The initial faster rate might be due to surface adsorption phenomenon and in the initial stage, the surface was free and consequently the reaction proceeded at a faster rate. Once the available free surface was clogged, then the

adsorbate molecules penetrated through the pores and got adsorbed inside the pore, known as intra-particle diffusion. The intra-particle diffusion accounted for the slower kinetics after faster adsorption. Similar dual mechanisms were also reported by others (Karthikeyen T., 2005).

8.3.3. Effect of pH

The initial pH was varied between 1.7 and 4.5. The results are shown in Fig.8.7. It was observed that adsorption efficiency decreased with increase in pH. It was further observed that the equilibrium pH in all the cases was more than the initial pH, which indicated ligand exchange mechanism governing the process. Adsorption might be occurring due to electrostatic force of attraction as well as formation of complex with the chelating agent present in the adsorbent. Evidence of complex formation was obtained from FT-IR (1600 Perkin Elmer make). Preparation of sample disks for the FT-IR study was already discussed in the previous section. Results showed that the adsorbent contained two or more functional groups. The bands at 1100 and 1700 cm^{-1} in the pure adsorbent corresponded to C-O and C=O stretching frequencies representing carbonyl and carboxyl groups. Several peaks were also observed around 3500 cm^{-1} for the anion groups present (Loukidou M. X., 2004). The Cr(VI) loaded materials showed either shift or reduction in adsorption peak suggesting the vital role played by the functional groups. The XRD analysis of the adsorbent showed the d-values to be 3.16, 2.84, 2.01 and 1.45 corresponding to carbon. The peak intensity decreased after adsorption indicating the reaction between carbon matrix with the anion.

8.3.4. Effect of initial Cr(VI) concentration

The initial Cr(VI) concentration was varied from 400 to 700 mg/L to evaluate its effect on adsorption efficiency. It was observed that with the increase in initial concentration of Cr(VI), the percentage of adsorption decreased as was generally expected in the equilibrium process. Adsorption increased from 58.6% to 78.12% when the initial concentration was decreased from 700 to 400 mg/L as shown in Fig.8.8. The

metal ion uptake capacity showed a reverse trend, i.e., it increased with increase in initial Cr(VI) concentration. The metal uptake capacity increased from 156.24 to 205.11 mg/g, when the initial Cr(VI) concentration was increased from 400 to 700 mg/L. The uptake capacity increased with the increase in initial Cr(VI) concentration as higher metal ion concentration enhanced the driving force to overcome mass transfer resistance between the aqueous and solid phases of the adsorbent resulting in higher probability of collision between adsorbate molecule and adsorbent surface.

8.3.5. Effect of adsorbent dose

The adsorbent concentration was varied from 0.8 to 2.4 g/L to find the effect of the same on the Cr(VI) adsorption efficiency of the carbonized weed. The uptake decreased from 247.35 to 167.93 mg/g when the adsorbent concentration was increased from 0.8 to 2.4 g/L. The percentage of adsorption increased from 39.58 to 80.61 when the adsorbent concentration was increased from 0.8 to 2.4 mg/L. The results are shown in Fig.8.9.

8.3.6. Effect of temperature

During this experiment, the temperature was varied from 30 to 60 ^{0}C and the results are shown in Fig.8.10. The percentage of adsorption and uptake increased from 54.7 to 76.5 and 136.75 to 191.25 mg/g respectively when the temperature was raised from 30 to 60 ^{0}C. The increase in efficiency with rise in temperature indicated that the reaction followed endothermic pathway. This might be due to various factors such as enhancement of inter-reaction between adsorbent and adsorbate, creation of new adsorption sites and increased rate of intra-particle diffusion (Namasivayam C., 1995) at higher temperatures.

8.3.7. Effect of particle size of adsorbent

The particle size of the adsorbent was varied from 53.55 to 312.76 μm to evaluate the effect of particle size on adsorption. The results are shown in Fig.8.11. The percentage of adsorption decreased from 73.6 to 39.5 when the particle size increased from 53.55 μm to 312.76 μm while the uptake decreased from 184 to 98.75 mg/g under the same conditions. The decrease in percentage adsorption as well as uptake with increase in particle size may be attributed to the decrease in specific surface area of the adsorbent. From the above studies, it is concluded that three parameters such as pH, contact time and adsorbate concentration determined the kinetics of adsorption.

8.4. Adsorption kinetic modeling

In order to determine a suitable kinetics model, the adsorption rate was fitted into four kinetic equations such as-

- Pseudo first order
- First order reversible
- Ritchie second order
- Pseudo second order

The rate constants for each kinetic equation at different adsorption parameters were calculated as discussed in the earlier section. The statistical parameters like regression coefficient and absolute deviation between the experimental and predicted values from the kinetic model were calculated to find out the goodness of the fit. Tables 8.2 to 8.5 show the specific reaction rate constant along with R^2 values. In case of the first order reversible kinetic model, the R^2 values varied from 0.89 to 0.96. R^2 values varied from 0.89 to 0.97 in case of pseudo first order kinetic model. Similarly the R^2 values varied from 0.32 to .76 for Ritchie second order equation. But in case of pseudo second order kinetic model, the R^2 values varied from 0.99 to 1.0. From both R^2 and absolute percentage deviation values it is concluded that the adsorption process followed pseudo second order kinetic model.

The adsorption kinetics depended on adsorption parameters like pH, particle size, adsorbent and adsorbate concentrations. Therefore the rate equation is written as:

$$\text{Rate} = -dC/dt = k\,(pH)^{n_1}\,(\text{particle size})^{n_2}\,(\text{adsorbate})^{n_3}\,(\text{adsorbent})^{n_4} \quad (8.1)$$

where C= Cr(VI) concentration

By converting the equation into logarithmic form, we get:

$$\log(\text{rate}) = \log k + n_1 \log(pH) + n_2 \log(\text{particle size}) + n_3 \log(\text{adsorbate concentration}) + n_4 \log(\text{adsorbent concentration}) \quad (8.2)$$

To determine the order of reaction, experimental data obtained was arranged to fit into the equation 8.2. For this purpose, only one parameter was varied keeping all other parameters constant. Since specific rate is proportional to the rate of the reaction, to evaluate the rate order, the respective specific rate was plotted against the percentage adsorption. Using the n and logk values from the Arrhenius equation, the rate equation could be written as:

$$\log(\text{rate}) = -7.1732 - 1.5677/T - 2.92\log(pH) - 0.2266\log(\text{particle size}) + 0.9278\log(\text{adsorbate concentration}) - 0.3895(\text{adsorbent concentration}) \quad (8.3)$$

8.5. Evaluation of thermodynamic parameters

The activation energy (E) for Cr(VI) adsorption was calculated by using Arrhenius equation. By plotting lnk vs. 1000/T, the activation energy was calculated from the slope. The activation energy was found to be 13.033 kJ/mol. The low activation energy indicated that physical forces governed the adsorption process. The standard free energy change (ΔG^0) was calculated by using equation 3.20. The other thermodynamic parameters such as change in standard enthalpy (ΔH^0) and standard entropy (ΔS^0) were

determined using the vant Hoff's equation (equation 3.21). ΔS^0 and ΔH^0 were obtained from the slope and intercept of the vant Hoff's plot of lnk vs. 1/T. The calculated ΔH^0 and ΔS^0 values were 1.57 kJ/mol and 59.64 J/mol respectively. The positive values of enthalpy indicated the endothermic nature of the reaction. The positive value of ΔS^0 showed the increasing randomness at the solid- liquid interface of Cr(VI) ions on the adsorbent.

8.6. Mass transfer model

Due to porous nature of the adsorbent used in this study, pore diffusion was also expected in addition to surface adsorption. The contact time variation experiment was used to study the rate-determining step in the adsorption process (Inbaraj B. S., 2006). Since the particles were agitated at a speed of 600 rpm, it could be safely assumed that mass transfer from the bulk to the external surface of the particle did not limit the rate. Therefore, the rate determining step might be either surface or intra-particle diffusion. As they happened simultaneously, the slower one of the two would be the rate-determining step. The intra-particle diffusion rate varied with the square root of time (Karthikeyen T., 2005) as shown equation 3.17

The 'k_{id}' values were determined from the slope of the linear plot between 'q_t' vs. '$t^{1/2}$' and the result for different experiments are shown in Table 8.9. From 'R^2' values, it was concluded that the process is pore diffusion controlled.

The initial curved portion of the plot related to the surface diffusion (D_1) and the linear portion represented the intra-particle diffusion (D_2) within the adsorbent. Assuming spherical geometry of the adsorbent particles, the relationship between weight uptake and time, using Fick's law was shown in equation 3.18 to 3.19.

'D_1' was calculated from the slope of the plot between 'q_t/ q_e' vs. '$t^{1/2}$' for the initial curved portion. For calculation of 'D_1' equation 3.18 was used, 'D_2' was calculated

from the slope of the curve between $\ln(1-q_t/q_e)$ vs. 't'. The values of 'D_1' and 'D_2' for different adsorption parameters are shown in Table 8.9.

8.7. Adsorption isotherm studies

Experimental data were fitted to different isotherm models such as Freundlich, Langmuir and Temkin adsorption isotherms as discussed in the earlier section. The results are shown in Tables 8.6-8.8. The average absolute percentage deviation between the experimental and predicted optimum adsorption capacity from the isotherm model are also included in Tables 8.6-8.8, which were calculated by using equation 3.24. It is concluded from percentage Dev. and R^2 values that the isotherm model could be explained by Temkin model. The b_f values were found to be between 0.1 to 1, which proved the ease of reaction.

The number of stages or batch reaction required for the removal of Cr(VI) was calculated from the equilibrium curve (Aksu Z., 1991) obtained from the plot between predicted 'C_e' and 'q_e' values at 35 ^{0}C and pH-1.7. The operating line was drawn which passed through the point representing C_o 500 mg/L, q_0 0.0 mg/g and had slope V_0/X_0 as – 1/2, where, V_0 and X_0 were expressed in dm^3 and gm respectively. Fig.8.12 shows the adsorption isotherm. From Fig.8.12 it is concluded that Cr(VI) concentration could be reduced from 500 to <1 mg/L in three stages.

8.8. Conclusions:

The activated carbonized weed was found to be a good adsorbent for Cr(VI). Results showed that the initial part of the adsorption process was confined only to surface adsorption and the slower kinetics might be due to intra-particle diffusion. The pseudo second order kinetics fitted well to the observed data. Further it was also observed that the adsorption isotherm followed Temkin model. Theoretical number of stages were determined from the adsorption isotherm curve to reduce the Cr(VI) concentration to the

predetermined level. The FTIR showed the anionic bonding with the chelate forming part of the adsorbent.

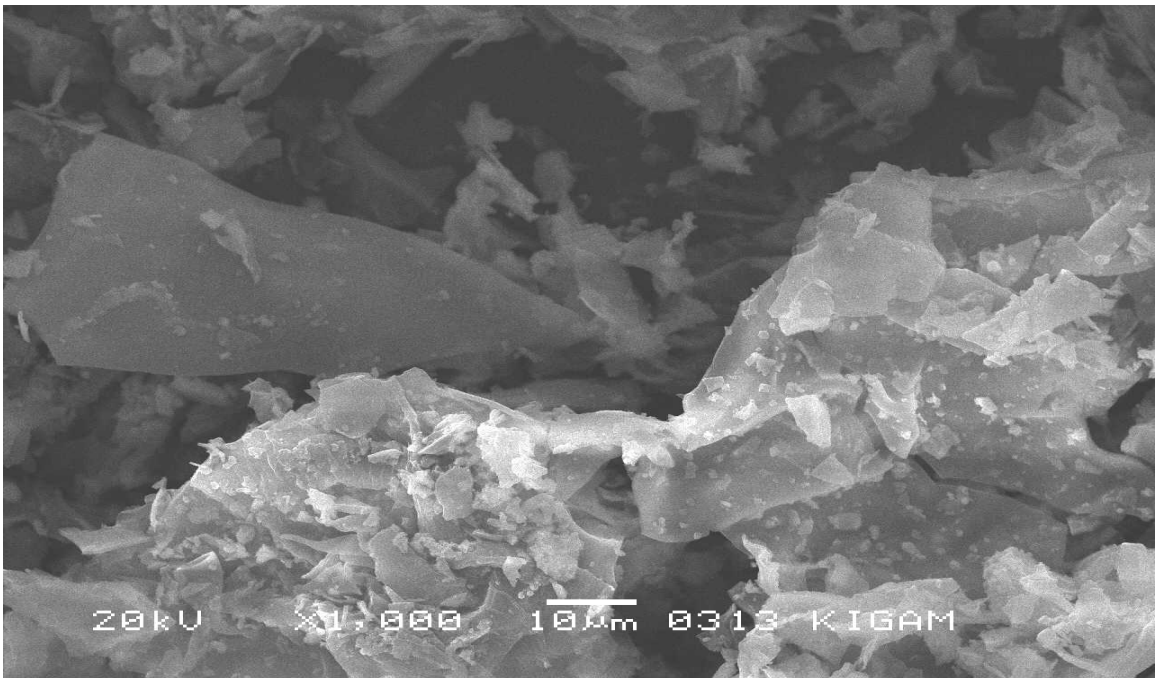

Fig.8.1. SEM image for carbonized weed

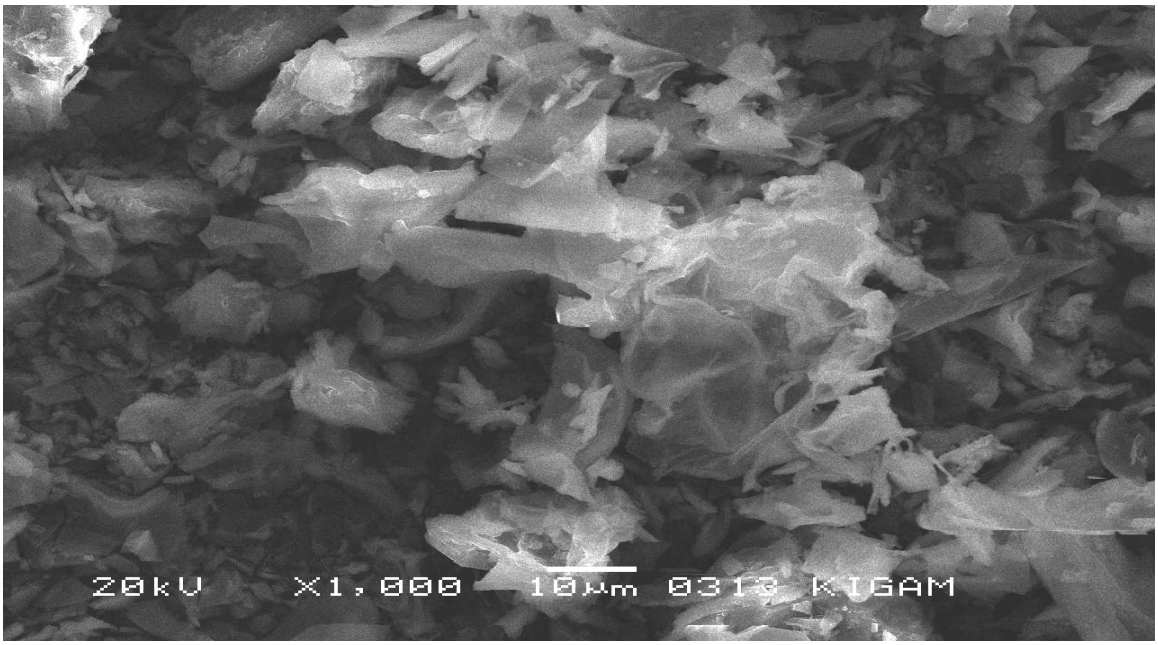

Fig.8.2. SEM image for carbonized weed after adsorption

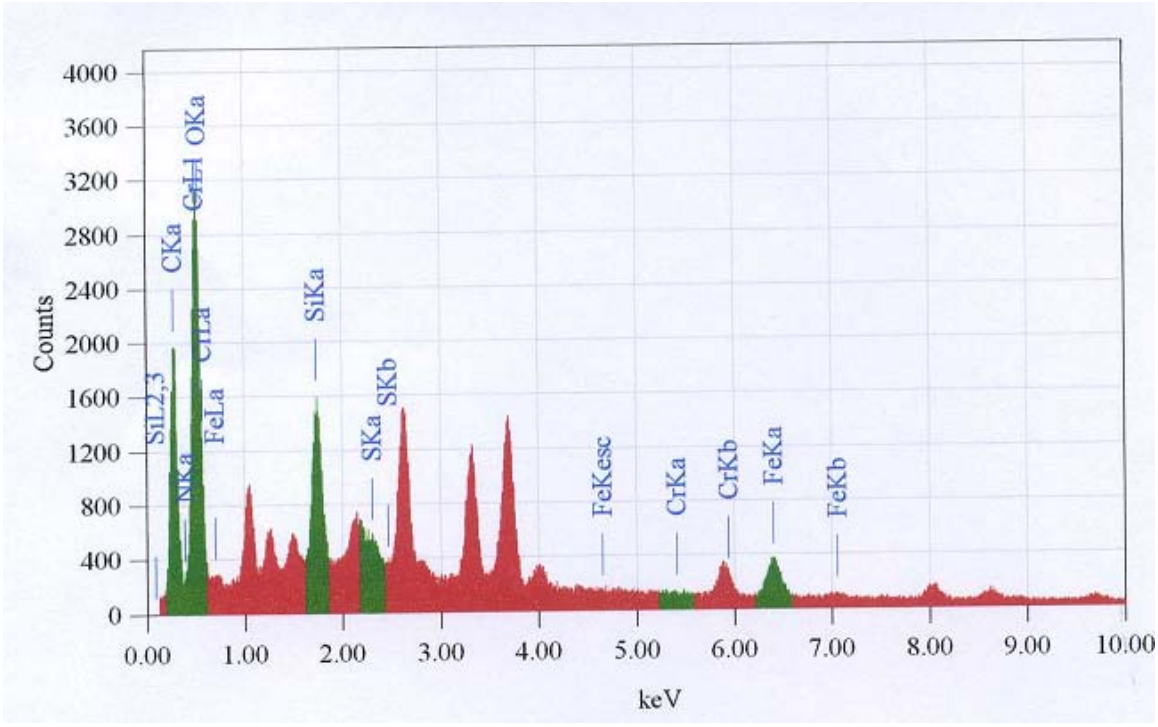

Fig.8.3. EDAX image for carbonized weed

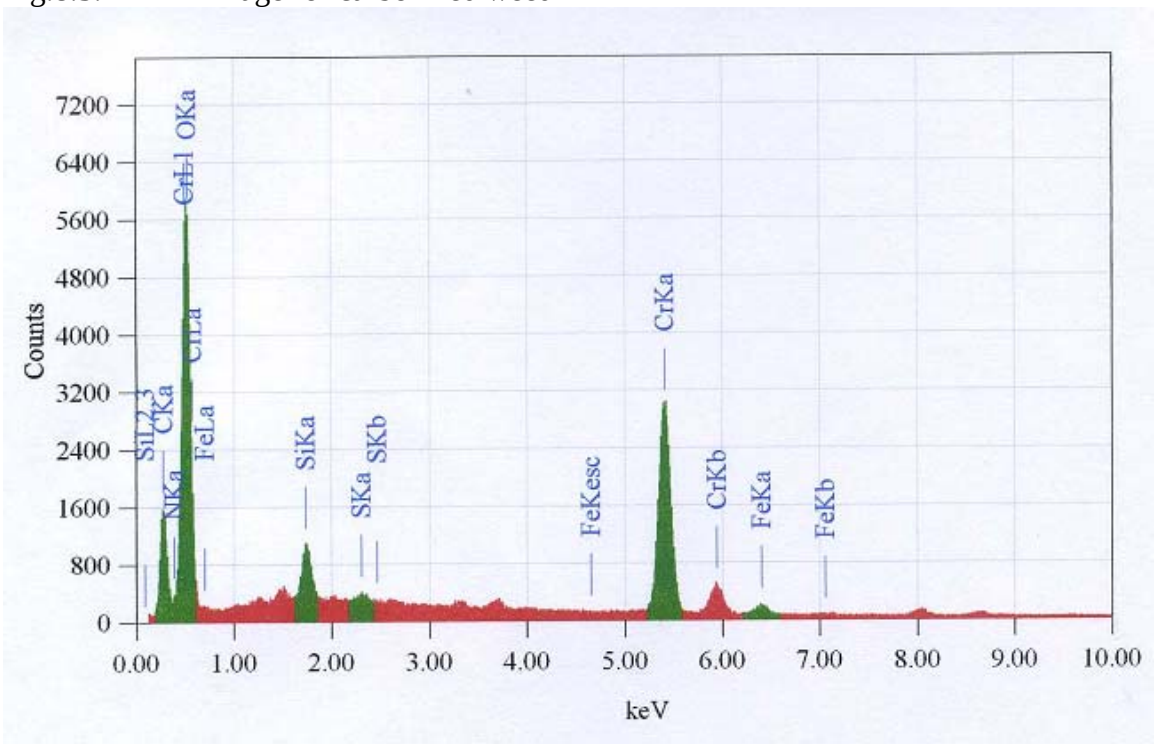

Fig.8.4. EDAX image for carbonized weed after adsorption

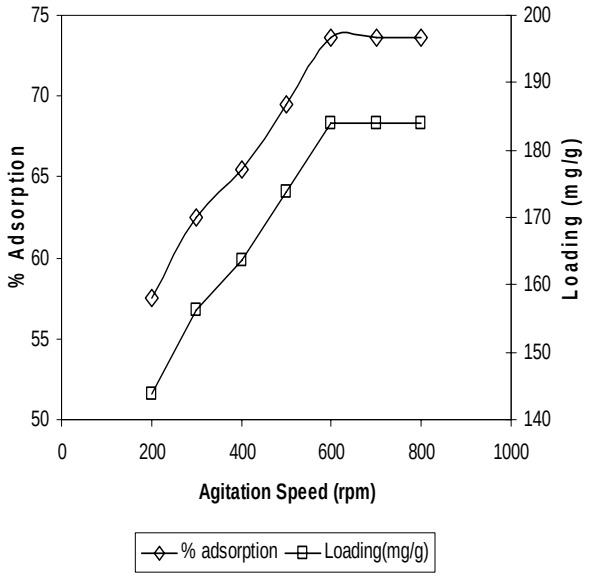

Fig.8.5. Effect of agitation speed on adsorption [Conditions: pH 1.7, temp. 30 ^{0}C, adsorbate conc. 500 mg/L, adsorbent dose 2 g/L, contact time 12 h, particle size 53.55 µ]

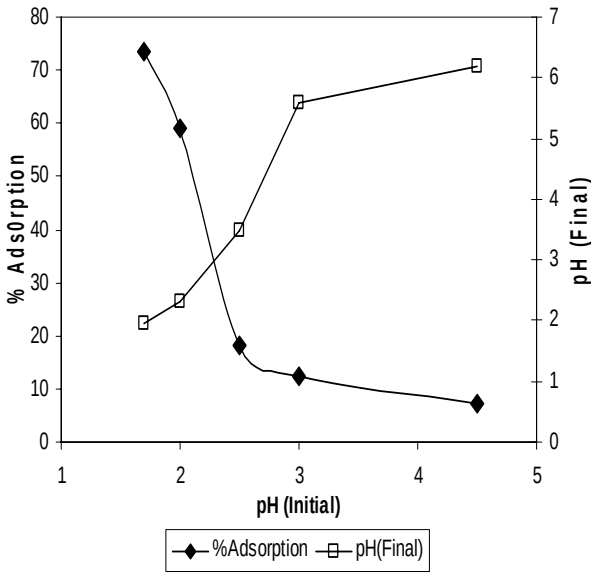

Fig.8.7. Effect of pH on adsorption [Conditions: temp. 30 ^{0}C, adsorbate conc. 500 mg/L, adsorbent dose 2 g/L, contact time 12 h, stirring rate 600 rpm, particle size 53.55 µ]

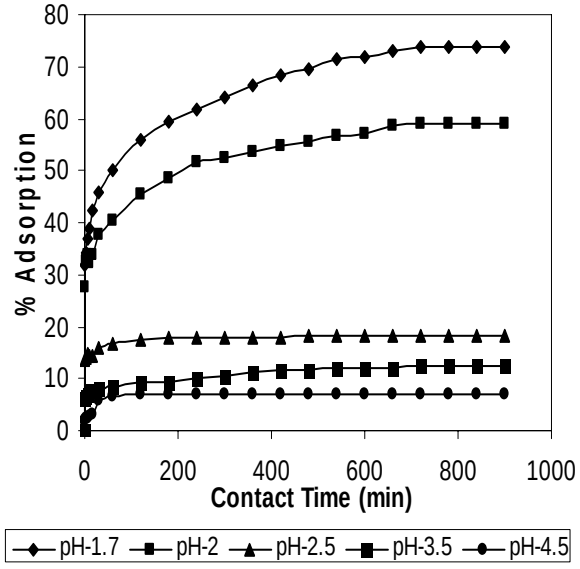

Fig.8.6. Effect of contact time on adsorption [Conditions: temp. 30 ^{0}C, adsorbate conc. 500 mg/L, adsorbent dose 2 g/L, stirring rate 600 rpm, particle size 53.55 µ]

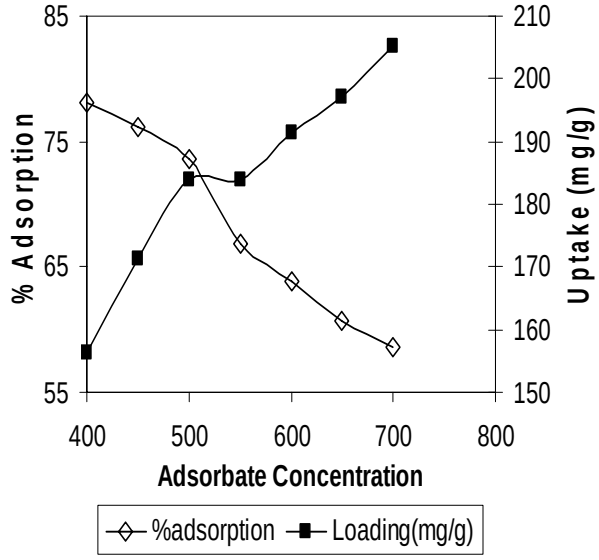

Fig. 8.8. Effect of initial adsorbate concentration on adsorption [Conditions: pH 1.7, temp. 30 ^{0}C, adsorbent dose 2 g/L, contact time 12 h, stirring rate 600 rpm, particle size: 53.55 µ]

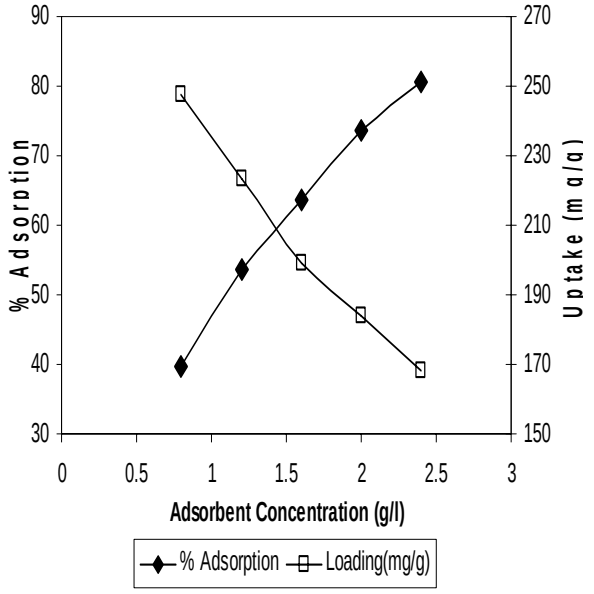

Fig.8. 9. Effect of adsorbent dose on adsorption [Conditions: pH:1.7, temp.:30 ^{0}C, adsorbate conc.: 500 mg/L, contact time: 12 h, stirring rate 600 rpm, particle size: 53.55µ]

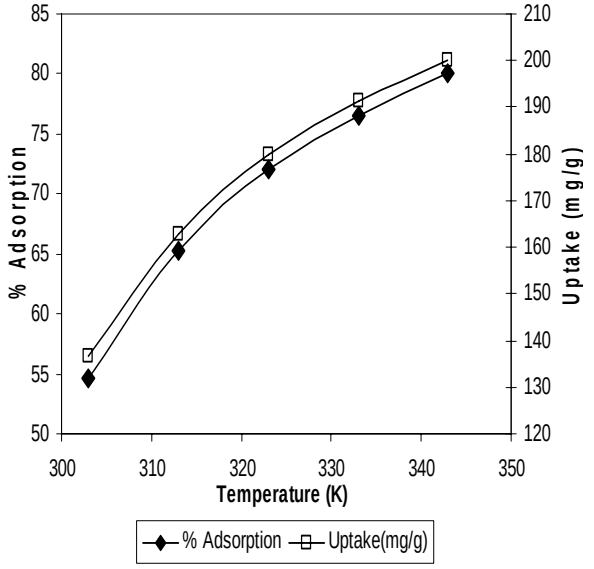

Fig. 8.10. Effect of temperature on adsorption [Conditions: pH: 1.7, adsorbate conc.: 500 mg/L, adsorbent dose: 2 g/L, contact time: 12 h, stirring rate 600 rpm, particle size: 53.55 µ]

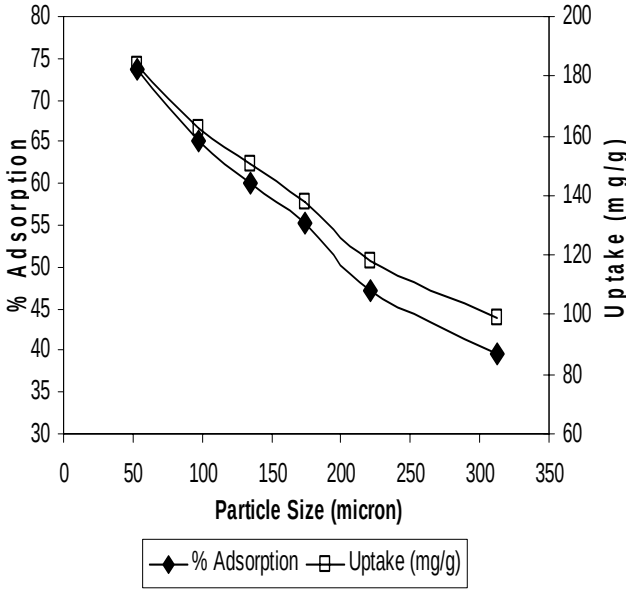

Fig. 8. 11. Effect of particle size on adsorption [Conditions: pH: 1.7, temp.:30 ^{0}C, adsorbate conc.: 500 mg/L, adsorbent dose: 2 g/L, contact time: 12 h, stirring speed: 600 rpm]

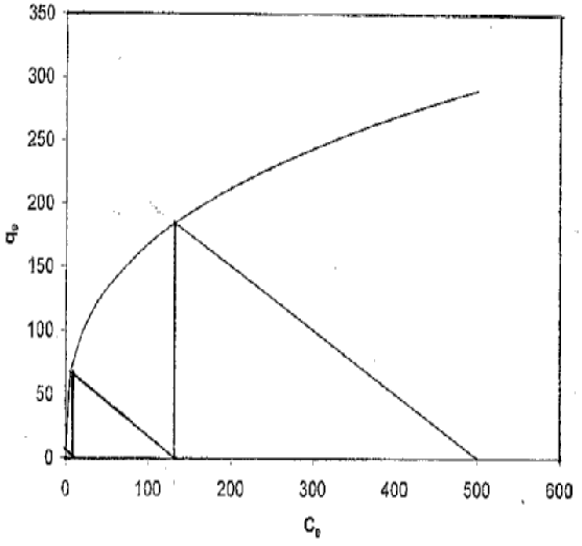

Fig.8. 12. Determination of number of stages using adsorption isotherm

Table 8.1: Physico-chemical characteristics of the weed after carbonization at different temperatures

Parameter	Carbonization Temperature			
	400 ^{0}C	500 ^{0}C	600 ^{0}C	700 ^{0}C
Volatile matter (%)	34.1	28.4	17	15.6
Ash (%)	45.4	44.3	58.3	58.4
Fixed Carbon (%)	20.5	27.3	24.7	22.7
Surface area, m^2/g	25.8	30.96	32.75	34.25
Particle size, cm	73	73	73	73
Porosity (%)	68	72	73.3	75.5
Density, g/cc	0.48	0.44	0.42	0.40
XRD peak	Carbon	Carbon	Carbon	Carbon

Table 8.2: First order reversible kinetic parameters with calculated adsorption capacity, regression coefficients and absolute percentage deviations for different adsorption parameter

pH	K_c	k_r	k_1	k_2	R^2	q_{ecalc}	q_{eExp}	% Dev
1.7	1.3934	0.0054	0.0031	0.0023	0.96	187.8	184.0	1.60
2	0.7245	0.0049	0.0021	0.0028	0.93	152.4	147.9	
2.5	0.1110	0.0087	0.0009	0.0078	0.92	45.5	45.4	
3	0.0704	0.0053	0.0003	0.0050	0.96	31.6	30.9	
4.5	0.0386	0.0076	0.0003	0.0073	0.89	18.0	17.9	
Ads Conc(ppm)								
400	1.7852	0.0047	0.0030	0.0017	0.95	161.7	156.2	3.33
450	1.5932	0.0048	0.0029	0.0019	0.95	176.8	171.3	
500	1.3934	0.0054	0.0031	0.0023	0.96	187.8	184.0	
550	1.0096	0.005	0.0025	0.0025	0.95	189.1	183.9	
600	0.8817	0.0049	0.0023	0.0026	0.93	197.2	191.4	
650	0.7704	0.0047	0.0020	0.0027	0.93	204.0	197.1	
700	0.7078	0.0042	0.0017	0.0025	0.94	215.6	205.1	
Ads dose (mg/L)								
0.8	0.8187	0.005	0.0023	0.0027	0.94	254.3	247.3	3.06
1.2	0.9652	0.0045	0.0022	0.0023	0.95	232.7	223.6	
1.6	1.0974	0.0045	0.0024	0.0021	0.95	207.2	199.1	
2.0	1.3934	0.0054	0.0031	0.0023	0.96	187.8	184.0	
2.4	1.7317	0.0053	0.0034	0.0019	0.95	171.7	167.9	
Temp (^{0}C)								
30	0.6038	0.0047	0.0018	0.0029	0.94	141.6	136.8	2.24
40	0.9368	0.0055	0.0027	0.0028	0.94	166.2	163.0	
50	1.2857	0.0059	0.0033	0.0026	0.97	182.6	180.0	
60	1.6277	0.0057	0.0035	0.0022	0.95	194.5	191.3	
70	2.0000	0.0051	0.0034	0.0017	0.96	205.2	200.0	
Particle Size (micron)								
54	1.3934	0.0054	0.0031	0.0023	0.96	187.8	184.0	1.30
98	0.9321	0.006	0.0029	0.0031	0.97	164.9	162.7	
135	0.7528	0.0065	0.0028	0.0037	0.96	151.6	150.2	
174	0.6156	0.0065	0.0025	0.0040	0.97	139.2	138.0	
221	0.4466	0.0062	0.0019	0.0043	0.97	119.3	118.0	
313	0.3264	0.0049	0.0012	0.0037	0.95	101.7	98.8	
Stirring rate (rpm)								
600	1.3934	0.0054	0.0031	0.0023	0.97	187.8	184.0	1.89
500	1.1393	0.0056	0.0030	0.0026	0.95	176.9	173.8	
400	0.9493	0.0056	0.0027	0.0029	0.96	166.7	163.8	
300	0.8333	0.0056	0.0025	0.0031	0.96	159.1	156.3	
200	0.6765	0.0055	0.0022	0.0033	0.96	146.5	143.8	

Table 8.3: Pseudo first order reversible kinetic parameters with calculated adsorption capacity, regression coefficients and absolute percentage deviations for different adsorption parameters

Parameters	k_1'	R^2	$q_{e, Calc}$	q_{eExp}	% Dev
pH					
1.7	0.0053	0.96	182.56	183.98	1.07
2	0.0048	0.93	146.51	147.92	
2.5	0.0088	0.92	45.26	45.42	
3	0.0053	0.96	30.22	30.86	
4.5	0.0076	0.89	17.71	17.94	
Ads Conc. (ppm)					
400	0.0048	0.95	154.68	156.24	0.83
450	0.0048	0.95	169.66	171.26	
500	0.0053	0.96	182.56	183.98	
550	0.0051	0.95	183.39	183.92	
600	0.0048	0.93	189.64	191.44	
650	0.0048	0.93	195.28	197.08	
700	0.0041	0.94	202.85	205.11	
Ads dose (mg/L)					
0.8	0.0051	0.94	245.61	247.35	0.84
1.2	0.0044	0.95	221.50	223.61	
1.6	0.0046	0.95	197.21	199.11	
2.0	0.0053	0.96	182.56	183.98	
2.4	0.0053	0.95	166.56	167.93	
Temp (^{0}C)					
30	0.0048	0.94	135.25	136.75	0.79
40	0.0055	0.94	161.69	163.00	
50	0.0060	0.97	178.89	180.00	
60	0.0058	0.95	189.94	191.25	
70	0.0051	0.96	198.50	200.00	
Particle Size (micron)					
54	0.0053	0.96	182.56	183.98	0.84
98	0.0060	0.97	161.51	162.72	
135	0.0064	0.96	149.25	150.22	
174	0.0064	0.97	137.00	137.96	
221	0.0062	0.97	116.97	117.95	
313	0.0048	0.95	97.41	98.75	
Stirring rate (rpm)					
600	0.0053	0.96	182.56	183.98	0.83
500	0.0055	0.95	172.41	173.75	
400	0.0055	0.96	162.41	163.75	
300	0.0055	0.96	154.91	156.25	
200	0.0055	0.96	142.42	143.75	

Table 8.4: Ritchie second order reversible kinetic parameters with calculated adsorption capacity, regression coefficients and absolute percentage deviations for different adsorption parameters

Parameters	k_m	R^2	$q_{e, Calc}$	$q_{e, Exp}$	% Dev
pH					
1.7	0.0832	0.62	183.98	187.05	1.16
2	0.0717	0.53	147.92	150.78	
2.5	1.2916	0.63	45.42	45.47	
3	0.0852	0.66	30.86	31.36	
4.5	0.2658	0.72	17.94	18.03	
Ads Conc(mg/L)					
400	0.0555	0.55	156.24	160.15	2.51
450	0.0558	0.60	171.26	175.52	
500	0.0832	0.62	183.98	187.05	
550	0.052	0.62	183.92	188.83	
600	0.0615	0.47	191.44	195.76	
650	0.0562	0.49	197.08	201.95	
700	0.0346	0.63	205.11	213.34	
Ads dose (g/L)					
0.8	0.0771	0.51	247.35	251.81	2.18
1.2	0.045	0.64	223.61	230.51	
1.6	0.0451	0.65	199.11	205.24	
2.0	0.0832	0.62	183.98	187.05	
2.4	0.0897	0.49	167.93	170.53	
Temp (^{0}C)					
30	0.1541	0.33	135.50	136.72	1.43
40	0.0982	0.53	163.00	165.31	
50	0.0843	0.76	180.00	182.97	
60	0.1088	0.49	191.25	193.69	
70	0.0693	0.68	200.00	204.01	
Particle Size (micron)					
54	0.0832	0.62	183.98	187.05	1.37
98	0.0997	0.57	162.72	164.98	
135	0.1682	0.50	150.22	151.46	
174	0.1527	0.50	137.96	139.21	
221	0.1234	0.51	117.95	119.28	
313	0.057	0.52	98.75	101.16	
Stirring rate (rpm)					
600	0.0846	0.62	183.98	187.00	1.5
500	0.1021	0.50	173.75	176.11	
400	0.0962	0.50	163.75	166.11	
300	0.0918	0.50	156.25	158.61	
200	0.0845	0.50	143.75	146.11	

Table 8.5: Pseudo second order reversible kinetic parameters with calculated adsorption capacity, regression coefficients and absolute percentage deviations for different adsorption parameters

Parameters	k_m	R_2	$q_{e, Calc}$	q_{eExp}	% Dev
pH					
1.7	0.0003	1.00	181.82	183.98	0.66
2	0.0004	1.00	144.93	147.92	
2.5	0.0076	1.00	45.45	45.42	
3	0.0017	0.99	30.49	30.86	
4.5	0.0052	1.00	18.12	17.94	
Ads Conc(mg/L)					
400	0.0003	0.99	151.52	156.24	2.59
450	0.0003	1.00	166.67	171.26	
500	0.0003	1.00	181.82	183.98	
550	0.0001	0.98	181.82	183.92	
600	0.0002	0.99	185.19	191.44	
650	0.0002	0.99	192.31	197.08	
700	0.0002	0.99	196.08	205.11	
Ads dose (g/L)					
0.8	0.0002	0.99	243.90	247.35	1.90
1.2	0.0002	0.99	217.39	223.61	
1.6	0.0002	0.99	192.31	199.11	
2.0	0.0003	1.00	181.82	183.98	
2.4	0.0003	1.00	166.67	167.93	
Temp (^{0}C)					
30	0.0002	0.99	138.89	136.75	1.88
40	0.0002	1.00	166.67	163.00	
50	0.0003	1.00	181.82	180.00	
60	0.0002	1.00	196.08	191.25	
70	0.0002	1.00	204.08	200.00	
Particle Size (micron)					
54	0.0003	1.00	181.82	183.98	0.30
98	0.0002	0.99	163.93	162.72	
135	0.0003	1.00	151.52	150.22	
174	0.0003	0.99	138.89	137.96	
221	0.0003	0.99	117.65	117.95	
313	0.0004	0.99	96.15	98.75	
Stirring rate (rpm)					
600	0.0003	1.00	181.82	183.98	1.12
500	0.0003	0.99	172.41	173.75	
400	0.0003	0.99	161.29	163.75	
300	0.0002	0.99	153.85	156.25	
200	0.0002	0.99	142.86	143.75	

Table 8.6: Langmuir adsorption isotherm constants with calculated adsorption capacity, regression coefficients and absolute percentage deviations for different adsorption parameters

Parameters	Q_0	b	R^2	$(q_e)_{Exp}$	$(q_e)_{cal}$	% Dev
PH						
1.7	16.75	0.0063	0.75	184	85.75	23.42
2				147.9	73.81	
2.5				45.42	27.27	
3				30.86	26.18	
4.5				17.94	25.38	
Adsorbate Concentration						
400	227.3	0.0264	1	156.2	158.6	1.887
450				171.3	168	
500				184	176.6	
550				183.9	188.1	
600				191.4	193.5	
650				197.1	197.9	
700				205.1	201	
Adsorbent Concentration						
0.8	322.6	0.0102	0.99	247.3	243.4	2.611
1.2				223.6	226.4	
1.6				199.1	209.2	
2				184	184.9	
2.4				167.9	160.1	
Particle size						
54	73.53	0.0107	0.96	184	253.4	11.92
98				162.7	158.8	
135				150.2	138.7	
174				138	126.4	
221				118	114	
313				98.75	106.5	
Stirring speed						
600	106.4	0.0171	0.99	184	191.2	0.59
500				173.8	172.7	
400				163.8	161.1	
300				156.3	154.7	
200				143.8	146.9	
Temp (^{0}C)						
30	108.7	0.0198	0.99	136.8	139.9	4.8
40				163	153.1	
50				180	170	
60				191.3	190.6	
70				200	219.6	

Table 8.7: Freundlich adsorption isotherm constants with calculated adsorption capacity, regression coefficients and absolute percentage deviations for different adsorption parameters

Parameters	b_f	k_f	R^2	$(q_e)_{Exp}$	$(q_e)_{cal}$	% Dev
pH						
1.7	-1.71	959339	0.90	183.98	205.07	25.8
2				147.92	96.46	
2.5				45.42	28.96	
3				30.86	25.71	
4.5				17.94	23.29	
Adsorbate Concentration						
400	0.193	68.422	0.91	156.24	161.97	1.97
450				171.26	168.52	
500				183.98	175.33	
550				183.92	186.55	
600				191.44	192.97	
650				197.08	199.16	
700				205.11	204.01	
Adsorbent Concentration						
0.8	0.34	35.009	0.99	247.35	243.89	1.22
1.2				223.61	222.84	
1.6				199.11	205.08	
2				183.98	184.08	
2.4				167.93	165.74	
Particle size						
54	-0.74	7161.7	0.95	183.98	194.86	4.20
98				162.72	158.57	
135				150.22	143.66	
174				137.96	131.88	
221				117.95	116.82	
313				98.75	105.68	
Stirring speed						
600	-0.51	2295	0.99	183.98	185.99	0.92
500				173.75	172.69	
400				163.75	162.08	
300				156.25	155.28	
200				143.75	145.59	
Temp (^{0}C)						
30	-0.46	1723.7	0.97	136.75	140.66	2.16
40				163.00	158.89	
50				180.00	175.68	
60				191.25	190.50	
70				200.00	205.23	

Table 8.8: Temkin adsorption isotherm constants with calculated adsorption capacity, regression coefficients and absolute percentage deviations for different adsorption parameters

Parameters						
pH	A	b	R^2	$(q_e)_{Exp}$	$(q_e)_{cal}$	A
1.7	0.0018	-18.63	0.99	183.98	193.01	0.0018
2				147.92	134.64	
2.5				45.42	41.55	
3				30.86	32.34	
4.5				17.94	24.67	
Adsorbate Concentration						
400	1.1966	71.763	0.93	156.24	161.66	1.97
450				171.26	168.81	
500				183.98	175.95	
550				183.92	187.14	
600				191.44	193.24	
650				197.08	198.94	
700				205.11	203.27	
Adsorbent Concentration						
0.8	0.1089	35.942	0.97	247.35	242.42	1.86
1.2				223.61	224.00	
1.6				199.11	207.03	
2				183.98	184.98	
2.4				167.93	163.56	
Particle size						
54	0.0012	-24.33	0.98	183.98	188.79	2.41
98				162.72	160.16	
135				150.22	146.44	
174				137.96	134.55	
221				117.95	117.71	
313				98.75	103.79	
Stirring speed						
600	0.0008	-29.61	1.00	183.98	185.15	0.61
500				173.75	173.02	
400				163.75	162.64	
300				156.25	155.61	
200				143.75	145.07	
Temp (^{0}C)						
30	0.0007	-32.28	0.99	136.75	139.91	1.49
40				163.00	160.28	
50				180.00	177.08	
60				191.25	190.62	
70				200.00	203.09	

Table 8.9: Intra particle diffusion parameters with calculated adsorption capacity, regression coefficients and absolute percentage deviations for different adsorption parameters

Parameter	k_{id}	R^2	$D_{1*}10^{-12}$	R^2	D_2*10^{-12}	R^2
pH						
1.7	3.0447	0.99	0.1167	0.98	0.3926	0.95
2	2.1376	0.91	0.0544	0.76	0.3271	0.89
2.5	0.1407	0.65	0.0449	0.85	0.4871	0.94
3	0.5313	0.97	0.0689	0.90	0.4071	0.97
4.5	0.0768	0.89	0.7158	0.83	0.3489	0.97
Adsorbate Concentration						
400	2.8013	0.99	0.1036	0.99	0.3344	0.92
450	2.9152	0.99	0.0861	0.99	0.3344	0.93
500	3.0447	0.99	0.1167	0.98	0.3927	0.95
550	4.91	0.99	0.3668	0.87	0.3998	0.94
600	3.7981	0.97	0.0912	0.91	0.3489	0.87
650	3.6162	0.99	0.1594	0.94	0.3344	0.86
700	3.5691	0.97	0.0504	0.90	0.2835	0.89
Adsorbent Concentration						
0.8	3.9915	1.00	0.1046	0.92	0.3635	0.90
1.2	4.1303	0.99	0.0265	0.76	0.3199	0.93
1.6	3.922	1.00	0.0673	0.99	0.3344	0.93
2	3.0447	0.99	0.1167	0.98	0.3926	0.95
2.4	2.7831	0.97	0.0593	0.99	0.378	0.92
Particle size						
54	3.0447	0.99	0.0018	0.98	68.8952	0.95
98	3.3456	0.97	0.0075	0.99	230.046	0.95
135	2.5855	0.95	0.0167	0.99	428.249	0.93
174	2.6898	0.96	0.0296	0.81	734.332	0.96
221	2.27	0.98	0.0423	0.99	1164.55	0.94
313	1.8916	0.97	0.0471	0.96	2243.94	0.90
Stirring speed						
600	3.0447	0.99	0.1167	0.98	0.3926	0.95
500	3.1162	0.99	0.1289	0.98	0.4144	0.93
400	3.1162	0.99	0.1452	0.98	0.4144	0.93
300	3.1162	0.99	0.1594	0.98	0.4144	0.93
200	3.1162	0.99	0.1884	0.98	0.4144	0.93
Temp						
30	2.7842	0.99	0.0319	0.92	0.3635	0.92
40	2.7354	0.99	0.0585	0.99	0.4071	0.90
50	2.6027	0.98	0.245	0.98	0.6979	0.97
60	3.018	1.00	0.2554	1.00	0.4071	0.90
70	2.7021	0.99	0.0917	0.89	0.3344	0.96

CHAPTER-9

EXPERIMENTAL DESIGN AND EVALUATION OF OPTIMIZED PARAMETERS

Experimental design and evaluation of optimized parameters

9.1. Objective of the study

Adsorption studies were carried using various adsorbents. Among the adsorbents, acid treated weed and carbonized weed were observed to be most efficient considering the kinetics and uptake capacity. Therefore, it was thought worthwhile to carry out the optimization studies using the said adsorbents. The effect of various adsorption parameters were studied such as agitation speed, contact time, pH, temperature, concentration of adsorbate and adsorbent dose. Since the main objective of this study was to develop a process to treat wastewater containing Cr(VI), the pH, Temperature and adsorbate concentration were varied widely. Apart from these parameters, it was observed that contact time played a crucial role in determining the kinetics. The kinetics followed dual rate, i.e., the initial faster rate followed by a slower one. The initial rate lasted for the first 30 mins and accounted for more than 70% of the total adsorption. The remaining 30% adsorption took place in more than 6 h. Therefore, optimum time was to be found out during the initial faster kinetics phase, so as to reduce the processing time as well as to arrive at the size of the equipment. It was observed that adsorption efficiency increased with decrease of pH. Therefore, optimization studies were carried out at lower pH. The wastewater temperature also varied depending on the process streams, therefore in this study optimization studies were carried out just above the ambient temperature.

In respect of Cr(VI) adsorption using adsorbents, different factors influence the process independently. While it is comparatively easy to determine the effect of individual factors and establish the relationship mathematically, a statistical method of analysis, as described above, is required to establish the optimum process conditions when several factors are variable.

9.2. Factorial design for the adsorption of Cr(VI) on acid treated weed

A full factorial design of type 'n^k' (n=2 and k=4) was used to find out the optimum conditions for the adsorption process. Where n is the number of levels and 'k' is

the number of factors under verification. Thus the total number of trial experiments needed for an investigation is 2^4. The regression equation with four parameters and their interaction with each other is given by (Akhnazarova, S., 1982):

$$Y=b_0+b_1x_1+b_2x_2+b_3x_3+b_4x_4+b_{12}x_1x_2+b_{13}x_1x_3+b_{14}x_1x_4+b_{23}x_2x_3+b_{24}x_2x_4+b_{34}x_3x_4+b_{123}x_1x_2x_3+b_{124}x_1x_2x_4+b_{234}x_2x_3x_4+b_{134}x_1x_3x_4+b_{1234}x_1x_2x_3x_4 \quad (9.1)$$

where b_1, b_2, b_3 and b_4 are the regression interaction coefficients of the concerned variables and x_1, x_2, x_3 and x_4 are the variables affecting the process.

The experiments were designed and adsorption experiments were carried out using a design matrix. The variable parameters and their coded values are given in Table 9.4. The higher, lower and base parameters were designated as +, - and 0 respectively. Sixteen numbers of designed trial experiments were carried out together with three base level experiments to estimate the error and standard deviation. The regression interaction coefficients were calculated using following formula:

$$b_j= \{\sum X_{ij}Y_i\}/N \quad (9.2)$$

where j=1, 2, 3, 4,-----n

where ‘i’ and ‘j’ are the number of rows and columns respectively. The results obtained from the trial runs are shown in Table 9.5 after incorporation in equation 9.2

$$Y=37.128+ 3.178x_1-3.711x_2- 2.399x_3+ 2.803x_4- 0.534x_1x_2- 0.306x_1x_3- 0.123-0.575x_2x_3- 0.064x_2x_4+ 0.311x_3x_4+ 0.04x_1x_2x_3+ 0.204x_1x_2x_4- 0.308x_2x_3x_4-0.236\ x_1x_3x_4+3.178x_1x_2x_3x_4 \quad (9.3)$$

The significance of each coefficient was assessed using the student ‘t’ test at 5% significance level (Akhnazarova, S., 1982) and insignificant terms were neglected from equation 9.3. The regression equation was tested to see how it fitted with the observation

using Fisher's adequacy test (Akhnazarova, S., 1982) at the 95% significant level and it was observed that the following equation is adequate.

$$Y=37.128+3.178x_1-3.711x_2-2.399x_3+2.803x_4-0.534x_1x_2-0.575x_2x_3+3.178x_1x_2x_3x_4 \quad (9.4)$$

From equation 9.4 it can be concluded that all four parameters played an important role in the efficiency of adsorption. Among the combined effects, only time-pH, pH-temperature and pH-time-temperature-adsorbate concentration played important roles in determining the overall efficiency of the process. The adsorption efficiency calculated by equation 9.4 matches well with the experimental values.

Table 9.1: Factorial levels and variation intervals for adsorption of Cr(VI) on acid treated weed

x_1=Time in min, x_2=pH, x_3= adsorbate concentration (mg/L), x_4= Temperature in ^{0}C				
Factors	-1	0	1	Variation interval
x_1	60	120	180	60
x_2	1.6	1.7	1.8	0.1
x_3	450	500	550	50
x_4	30	35	40	5

Table 9.2: Design of trial run in coded form for the adsorption of Cr(VI) on acid treated weed

Trial No	x_1	x_2	x_3	x_4	x_1x_2	x_1x_3	x_1x_4	x_2x_3	x_2x_4	x_3x_4	$x_1x_2x_3$	$x_1x_2x_4$	$x_1x_3x_4$	$x_2x_3x_4$	$x_1x_2x_3x_4$	Y
1	+	+	+	+	+	+	+	+	+	+	+	+	+	+	+	35.75
2	+	+	+	-	+	+	-	+	-	-	+	-	-	-	-	29.89
3	+	+	-	+	+	-	+	-	+	-	-	+	-	-	-	42.5
4	+	-	+	+	-	+	+	-	-	+	-	-	+	-	-	45.45
5	-	+	+	+	-	-	-	+	+	+	-	-	-	+	-	30.62
6	+	+	-	-	+	-	-	-	-	+	-	-	+	+	+	36.1
7	+	-	-	+	-	-	+	+	-	-	+	-	-	+	+	49.22
8	+	-	+	-	-	+	-	-	+	-	-	+	-	+	+	39.31
9	-	+	+	-	-	-	+	+	-	-	-	+	+	-	+	25.51
10	-	+	-	+	-	+	-	-	+	-	+	-	+	-	+	35.75
11	-	-	+	+	+	-	-	-	-	+	+	+	-	-	+	39.55
12	+	-	-	-	-	-	-	+	+	+	+	+	+	-	-	44.22
13	-	+	-	-	-	+	+	-	-	+	+	+	-	+	-	31.21
14	-	-	+	-	+	-	+	-	+	-	+	-	+	+	-	31.75
15	-	-	-	+	+	+	-	+	-	-	-	+	+	+	-	40.6
16	-	-	-	-	+	+	+	+	+	+	-	-	-	-	+	36.61
17	0	0	0	0	0	0	0	0	0	0	0	0	0	0	0	37.65
18	0	0	0	0	0	0	0	0	0	0	0	0	0	0	0	36.81
19	0	0	0	0	0	0	0	0	0	0	0	0	0	0	0	37.5
20	0	0	0	0	0	0	0	0	0	0	0	0	0	0	0	38

9.3. Factorial design for adsorption of Cr(VI) on carbonized weed

In order to obtain the optimum conditions for adsorption of Cr(VI) on the carbonised weed, a full factorial design of the type n^k was used, where n is the number of levels and k is number of factors under verification. Here time, pH and temperature are chosen as three independent factors or variables (k=3 and n=2) and the percentage of adsorption as the dependent out-put response variable. A 2^3 full-factorial experimental design (Mayer, R. H., 2002) with number of 3 triplicates at the center point and thus a total of 11 experiments were employed in this study. For statistical calculation the base levels, which is the average of two level are calculated using the following relation

$$x_i = \frac{\left(X_i - X_0\right)}{\delta X} \qquad (9.5);$$

The behavior of the system was explained by the following equation

$$Y = b_0 + b_1x_1 + b_2x_2 + b_3x_3 + b_{12}x_1x_2 + b_{23}x_2x_3 + b_{31}x_3x_1 + b_{123}x_1x_2x_3 \qquad (9.6)$$

where b_0, $b_{1...}$ b_{123} are the regression interaction coefficients of the concerned variables and x_1 x_2 and x_3 are the dimensionless coded factor affecting the process; x_1=time, x_2=pH and x_3=temperature. The factorial levels and variation intervals of the coded factor are shown in Table 9.6.

The parameters varied were time (5-15min) pH (1.6-1.8) and temperature (30-40 ^{0}C). The variable parameters in two levels, their coded values and the conditions for the base level experiments are given in Table 9.7. The +, - and 0 designations are given to the higher, lower and base levels respectively. The coefficients were calculated using equation 9.2. Substututing the 'b' values, equation 9.6 becomes:

$$Y = 38.89 + 2.8x_1 - 4.593x_2 + 4.074x_3 + 0.0088x_1x_2 - 0.981x_2x_3 - 0.784x_3x_1 - 0.579x_1x_2x_3 \qquad (9.7)$$

The significance of each coefficient was assessed using the student 't' test (Devy, S., 2004) and the insignificant terms were neglected from equation (9.7). Fisher's adequacy test (Akhnazarova, S., 1982) at 99% confidence level was used to test the regression equation and it was observed that the following equation was adequate:

$$Y = 38.89 + 2.8x_1 - 4.593x_2 + 4.074x_3 - 0.981x_2x_3 \quad (9.8)$$

Table 9.3. Factorial levels and variation intervals for adsorption of Cr(VI) on carbonized weed

x_1=Time in min, x_2=pH, x_3=Temperature in ^{0}C				
Factors	-1	0	1	Variation interval
x_1	5	10	15	5
x_2	1.6	1.7	1.8	0.1
x_3	30	35	40	5

Table 9.4. Design of trial runs in coded form for adsorption of Cr(VI) on carbonized weed

Trial No	x_1	x_2	x_3	x_1x_2	x_2x_3	x_3x_1	$x_1x_2x_3$	Y
1	+	+	+	+	+	+	+	38.84
2	-	+	+	-	+	-	-	35.94
3	+	-	+	-	-	+	-	51.13
4	-	-	+	+	-	-	+	45.95
5	+	+	-	+	-	-	-	35.38
6	-	+	-	-	-	+	+	27.03
7	+	-	-	-	+	-	+	41.43
8	-	-	-	+	+	+	-	35.43
9	0	0	0	0	0	0	0	27.14
10	0	0	0	0	0	0	0	27.1
11	0	0	0	0	0	0	0	27.15

CHAPTER-10

REMOVAL OF Cr(VI) BY THERMALLY ACTIVATED WEED IN A FIXED-BED COLUMN

Removal of Cr(VI) by thermally activated weed in a fixed-bed column

In the previous chapters, we had focused on the Cr(VI) adsorption capacity of the thermally activated weed in batch experiments . From these studies it was concluded that the thermally activated weed was highly effective for the treatment of Cr(VI) contaminated aqueous solution and ligand exchange mechanism was responsible for its high adsorption capacity. It was also observed that this adsorbent was suitable for the treatment of both mine water as well as industrial effluents containing Cr(VI). For industrial water treatment, adsorption in fixed bed column is preferable (Kundu, S. 2005). Therefore, experimental data obtained from the laboratory scale fixed-bed column were used to design an adsorption column for industrial application.

As a continuation of our previous work, the present study was focused on evaluating the performance of thermally activated weed for the removal of Cr(VI) ion from the aqueous solutions in a fixed-bed column. The Cr(VI) uptake capacity of the activated weed was investigated as a function of different operating conditions such as flow rate, initial Cr(VI) concentration and bed height. The experimental data were utilized in four different kinetic models such as Bohart-Adams model, Thomas model, BDST model and Yoon Nelson model to find out the best fit. In addition, the regeneration behavior of an exhausted activated weed was also examined.

10.1. Experimental

10.1.1. Adsorbent preparation

The adsorbent used in this study was collected from a sweet water reservoir near Bhubaneswar, details of which along with its activation process are given in Chapters6-8.

10.1.2. Adsorption studies

Continuous adsorption studies were carried out in a perspex column. The internal diameter and the height of the column were 5 cm and 30 cm respectively. A 500-mesh sieve was placed on both the inlet and outlet of the column to avoid any loss of adsorbent material. The Cr(VI) solution was pumped through a metered pump (Watson Marlow make) at the bottom (inlet) of the column and the output was collected at regular intervals for analysis from the top of the column. The flow rate of the solution was checked regularly. The pressure drop was measured through a manometer connected to the column. The concentration of the output solution was measured spectrophotometricaly (Perkin Elmer make Lambda-35) (Chun, L., 2004). The pumping was continued till there was no further adsorption, i.e., the Cr(VI) concentration at the inlet and outlet remained unchanged. All the experiments were performed in duplicates and the average result was taken for calculation.

In this study, the breakthrough point and bed volume (BV) numbers were used to compare and evaluate the adsorption performance of the activated weed bed under various conditions. The breakthrough point is defined as the time interval at which the output concentration (C) from the column is about 1% of the input concentration (C_0). The bed volume number is obtained as a ratio as shown bellow:

BV= volume of the solution treated / volume of the adsorbent bed (10.1)

The amount of the heavy metal ion adsorbed per unit mass of activated weed ,q (mg/g)in the column was calculated using the relationship:

$$q = \frac{Q_t}{m} = \frac{\sum_{i=1}^{n} v(t_i - t_{i-1})[1-(C/C_0)_i]C_0}{m} \qquad (10.2)$$

where 'Q_t' (mg) is the total amount of Cr(VI) ion adsorbed in the activated weed column, 'i' is the number of sampling points, 'm' (g) is the mass of activated weed packed in the

column, ‘v’ (mL/min) is the flow rate of the input, ‘t_i’ is the i^{th} time point and $(C/C_0)_i$ is the ratio of i^{th} output concentration over the initial input concentration.

The adsorbent exhaustion rate is the mass of adsorbent used per volume of liquid treated at breakthrough point (Ko, D. C. K., 2000). The equation used for the adsorbent exhaustion rate is as follows:

Adsorbent exhaustion rate = mass of adsorbent in column/volume fluid treated (10.3)

10.1.3. Desorption and regeneration experiments

After saturation with Cr(VI) ions, the adsorbent materials in the column were regenerated using 0.1M NaOH solution at a flow rate of 50 mL/min. The concentration of Cr(VI) ion in the regenerated solution was determined at 10 min interval. To verify the performance stability of the activated weed column, three cycles of adsorption-regeneration process were performed. In each cycle, the regenerating agent was 0.1M NaOH and the regeneration conditions were similar to that described above. After regeneration, the activated weed was washed with de-ionised water for 1 h and reused in the next cycle of the adsorption experiments.

10.2. Results and discussion

10.2.1. Effect of flow rate

Based on the batch studies, the pH of the output solution was maintained at 1.7. To find out the effect of flow rate on the breakthrough curve, adsorption experiments were carried out by varying the flow rate between 30 to 60 mL/min. In this process, the initial adsorbate concentrations, initial pH of the solution and bed height were maintained at 500 mg/L, 1.7 and 10 cm respectively. The effect of flow rate on breakthrough performance at the above operating conditions is shown in Fig.10.1. From the figure it was observed that the adsorption efficiency was higher at lower flow rate. This can be explained by the fact that at low flow rate, the diffusion process which controls the sorption becomes slow, and hence, the adsorbent needs more time to bond the metal

efficiently. In other words, if the residence time of the solute in the column is not large enough for adsorption equilibrium to be reached at that flow rate, the Cr(VI) solution leaves the column before equilibrium occurs. These breakthrough curves show the efficiency of the process kinetics.

It was also observed that the adsorbent gets saturated easily at higher flow rates. The uptake of Cr(VI) decreased with increase in flow rate. The optimum uptake capacity for flow rate of 30, 40, 50, and 60 mL/min was found to be 134.6, 132.6, 127.4, and 124.5 mg/g respectively (Fig.10.2). As shown in Fig.10.1-10.2, the saturation occurred at 1370, 990, 760 and 620 min when the flow rates were 30, 40, 50 and 60 mL/min and the respective empty bed residence time were 6.54, 4.91, 3.93 and 3.27 min (Table 10.1). It was also observed that the treated bed volume increased with a higher Empty Bed Residence Time (EBRT). In other words, with higher EBRT, Cr(VI) ions had more time to contact with the adsorbent, which resulted in higher removal of Cr(VI) ions in the fixed bed column.

10.2.2. Effect of initial adsorbate concentration

Column experiments were carried out by varying the concentration of Cr(VI) between 100 to 500 mg/L to determine the effect of adsorbate concentration on the performance of the breakthrough curve. During these experiments, other parameters like pH, bed height and flow rate were kept constant at 1.7, 10 cm and 60 mL/min respectively. The sorption breakthrough curve obtained for adsorbate concentrations of 100, 200, 300, 400 and 500 mg/L are given in Fig.10.3. The breakthrough time decreased with increase in inlet Cr(VI) concentration as the binding sites became more quickly saturated. The equilibrium Cr(VI) uptake and the total Cr(VI) adsorbed were found to increase with increase in inlet Cr(VI) concentration. The percentage of Cr(VI) removal decreased with increase in adsorbate concentration. With increase in initial Cr(VI) concentration from 200 to 500 mg/L, the uptake and total Cr(VI) were found to increase from 79.8 to 124.5 mg/g (Fig.10.4, Table 10.1) and 3990 to 6225 mg respectively. But the percentage removal of Cr(VI) decreased from 55 to 31 when the inlet Cr(VI) concentration was increased from 100 to 500 mg/L. The increase in uptake capacity of

the adsorbent might be due to the fact that high inlet Cr(VI) concentration provides higher driving force for the transfer process to overcome the mass transfer resistance. As seen in Fig.10.3, for low inlet concentrations of Cr(VI), the breakthrough occurred late and surface of the adsorbent was saturated with Cr(VI) after a long time whereas for higher Cr(VI) concentration, the breakthrough occurred in a short period of time. The saturation time for the adsorbent decreased from 1210 to 620 min (Fig. 10.4, Table 10.1) when the inlet Cr(VI) concentration was increased from 100 to 500 mg/L. At lower inlet Cr(VI) concentrations, the breakthrough were flatter indicating a relatively wide mass transfer zone and film controlled process. On the contrary, the breakthrough curves were sharp at high inlet Cr(VI) concentration, implying a relatively smaller mass transfer zone and intra-particle diffusion controlled process. The same trend was also observed by other authors related to metal ion adsorption. (Goel, J., 2005).

10.2.3. Effect of bed height

In order to find out the effect of bed height on the breakthrough curve, the adsorbate solution having Cr(VI) concentration 100 mg/L, pH 1.7 and flow rate 60 mL/min was passed through the adsorption column by varying the bed height. Fig.10.5 presents the performance of breakthrough curves at bed heights of 2, 4, 6, 8 and 10 cm. It is evident from Fig.10.5 that the steepness of the breakthrough curve was a function of bed height. With increase in bed height, the throughput volume was increased which might be due to higher contact time. At a relatively lower contact time, the curve was steeper showing the faster exhaustion of the bed. The treated volume varied between 28.8 and 21.6 L when the bed height was increased from 2 to 10 cm respectively. Similarly Cr(VI) adsorption uptakes were found to be 159.2, 133.5, 128.8, 126 and 124.5 mg/g (Fig.10.6, Table 10.1) when the bed heights were 2, 4, 6, 8 and 10 cm respectively and the corresponding total Cr(VI) adsorbed were 1592, 2670, 3864, 5040 and 622.5 mg respectively (Table 10.1). The increase in metal uptake capacity with the increase of bed height in the fixed bed column might be due to increased surface area of the adsorbent which provided more binding sites for the adsorption. The breakthrough time also increased with increase in bed height. The breakthrough curve followed a characteristic

'S' shape profile which was associated with adsorbate of smaller molecular diameter and simpler structure.

10.2.4. Application of different breakthrough curve models

In many cases, kinetics of adsorption in the column were tested for Bohart-Adams model. However, it has also been shown that BDST, Thomas Yoon-Nalson and Clark models can sometimes provide a better description of the adsorption kinetics. So in the present study, attempt was made to find out the best model describing the adsorption kinetics in column.

10.2.4.1. Application of the Bohart-Adams model

Bohart-Adams model was applied to experimental data for the description of the initial part of the breakthrough curve. This approach focused on the estimation of characteristic parameters such as maximum adsorption capacity (N_0) and the mass transfer coefficient (k_{AB}). In the present study, the range of time was considered from the beginning to the end of the breakthrough curve. $\ln(C_t/C_0)$ was plotted against 't' at different flow rates, bed heights and initial Cr(VI) concentrations. The mass transfer coefficient (k_{AB}) and saturation concentration (N_0) values were calculated from the slope and intercept of the curve respectively. To find the best fit, the statistical parameters such as SSE, SAE, ARE and ARS between the experimental and calculated maximum adsorption capacity were calculated. Predicted and experimental breakthrough curves with respect to flow rate, bed height and initial Cr(VI) concentrations are shown in Fig.10.7-10.9. The predicted and experimental uptake capacity along with 'K_{AB}' and 'N_0' and other statistical parameters are shown in Table 10.2. From the table it is observed that mass transfer coefficient increased with increase in flow rate. This shows that the overall system kinetics was dominated by external mass transfer (Aksu, Z., 2004)

10.2.4.2. Application of the Bed Depth Service Time (BDST) model

Experimental data obtained from the column studies were used to plot BDST curve. 'K' and 'N_0' values were calculated from the slope and intercept of the plot between $\ln(C_0/C_t\text{-}1)$ versus 't' at different adsorption parameters such as flow rate, bed height and inlet adsorbate concentration. The estimated values of characteristic parameters like 'k' and 'N_0' along with the other statistical parameters are presented in Table 10.3. The breakthrough curve predicted from BDST model was compared with the experimental breakthrough curve.

10.2.4.3. Application of Thomas model

The experimental data were fitted to the Thomas model to determine the Thomas rate constant (k_{TH}) and maximum solid phase concentration (q_0). The 'k_{TH}' and 'q_0' value were calculated by plotting $\ln(C_0/C_t\text{-}1)$ against 't' using values from the column experiments. From the regression coefficient (R^2) and other statistical parameters, it is concluded that the experimental data fitted well to the Thomas model. The predicted uptake capacity and experimental uptake capacity along with 'k_{TH}', 'q_0', and other statistical parameters are given in Table 10.4. As flow rate increased, the value of 'k_{TH}' increased whereas, the value of 'q_0' showed a reverse trend. The bed capacity (q_0) increased and the coefficient (k_{TH}) decreased with increase in initial Cr(VI) concentration. Similarly 'q_0' values decreased and 'k_{TH}' values increased with increase in the bed height. Similar trend was also observed by Aksu et al (Aksu, Z., 2004). The well fit of the experimental data on to the Thomas model indicated that the external and internal diffusion were not the rate limiting steps.

10.2.4.4. Application of the Yoon-Nelson model

A simple theoretical model developed by Yoon-Nelson was applied to investigate the breakthrough behavior of Cr(VI) on the activate carbon. The values of 'K_{YN}' and 'τ' were estimated from the plot between $\ln(C_t/C_0\text{-}C_t)$ versus 't' at different flow rates, bed heights and initial Cr(VI) concentrations. The values of 'K_{YN}' were found to decrease

with increase in both flow rate and bed height, whereas the corresponding values of 'τ' decreased. With increase in initial Cr(VI) concentration, the 'K_{YN}' values decreased whereas the 'τ' values showed a reverse trend. The predicted uptake values from the model, experimental uptake values along with the values of 'K_{YN}', 'τ' and statistical parameters are listed in Table 10.5. From the table it can be seen that simulation of the whole breakthrough curve is effective with the Yoon-Nelson model at higher flow rates and at higher inlet concentrations. For lower flow rates and inlet concentrations, the correlation between the experimental and predicted values using this model deviates significantly. From the table it can be seen that the theoretical uptake capacity is very close to those predicted by the Yoon-Nelson model.

10.2.4.5. Comparison between the applied models

The column adsorption models applied in this study to fit the Cr(VI) adsorption data can be essentially classified according to their equations. In general, the linearity of the Hutchins BDST, Thomas and Yoon-Nelson models can be represented as

$$\ln\left(\frac{C_0}{C_t}-1\right)=k_1-k_2t \qquad (10.4)$$

where $k_1 = N_0KZ/u = k_{TH}q_{TH}M/Q = \tau k_{YN}$ and $k_2 = KC_0 = k_{TH}C_0 = k_{YN}$

From the equation 10.4 it is obvious that the characteristic parameters associated with these models vary but all the three models predict essentially similar uptake capacity and C_t/C_0 values for a particular experimental data set. Hence they would give similar R^2 values and other statistical parameters like SSE, SAE, ARE and ARS as illustrated in Table 10.6. But the prominent and unique characteristic features of the respective models like service time (Hutchins BDST model), adsorption capacity (Thomas model) and time for 50% breakthrough (Yoon-Nelson model) enable further comparison. Therefore in the present study, the unique characteristics of each model were calculated from the predicted models equation. Similarly, the unique characteristics of Bohart-Adams, i.e., adsorption capacity, were calculated from the predicted model. Different statistical

parameters such as SSE, SAE, ARE and ARS amongst the experimental and calculated values as well as the unique characteristics of the above four models were obtained and are given in Table 10.6. From the statistical parameters in this table, Thomas model is the most appropriate model amongst the three followed by Yoon-Nelsons and BDST model. Again, on comparing the statistical parameters of the Thomas model with that of Bohart-Adams model (Table 10.6), it is observed that the later correlated fairly better.

10.2.5. Desorption and regeneration studies

Adsorption mechanism of Cr(VI) on any adsorbent can be physical, chemical bonding, ion-exchange or a combination of all the three. If adsorption is by physical bonding, then the loosely bound Cr(VI) ions can be easily desorbed in aqueous solution. However, if the adsorption process is through chemical bonding, ion-exchange or a combination of both, then desorption can be affected by the use of stronger eluents like acidic or alkaline solutions. Thus the desorption and regeneration studies can give a clear idea about the mechanism of adsorption along with the stability of the adsorbent for further use. Therefore, attempts were made to desorb Cr(VI) from the loaded adsorbent. Initially the loaded adsorbent was washed with de-ionized water and it was found that the percentage desorption was very low (5%). Hence, experiments were conducted with acidic and alkaline solutions to desorb Cr(VI). From the experiments, it was observed that effective desorption of Cr(VI) ion with acid was not achieved even with 0.2 N HCl. However, the desorption of Cr(VI) with alkaline solution was very high. It was found that the Cr(VI) desorption was 50%, 70% and 80% with 0.1M NaOH at 6, 9 and 12 h contact time respectively. Five consecutive sets of adsorption-desorption studies were carried out and it was found that the adsorption capacity of the adsorbent decreased slightly in each cycle.

From the desorption studies, the following conclusions can be drawn. The negligible desorption of Cr(VI) with de-ionized water indicated the predominance of the chemical bonding and ion-exchange between the adsorbate and adsorbent. This implied that physical adsorption played insignificant role in Cr(VI) adsorption on the thermally activated weed. The desorption of Cr(VI) in the alkaline solution suggested that either chemisorption or ion exchange are the possible mechanisms of metal adsorption. The

higher percentage of desorption (80%) indicated the bond between the adsorbate and adsorbent molecules were weak. Hence the chemisorption had insignificant role on the Cr(VI) adsorption process. From the above discussion, it can be concluded that ion exchange mechanism played a significant role in the sorption process. Similar adsorption mechanism was also observed in our batch experiments.

10.2.6. Comparison with other adsorbents reported in literature

In order to assess the viability of a treatment process, the adsorption column capacity of the present adsorbent was compared with other similar adsorbents. The results are shown in Table 10.7. Kim and Zoltek (Kim, I. J., 1977) reported an optimum column capacity of Filtrasorb-400 (Calgon type) as 123 mg/g using an initial Cr(VI) concentration of 104 mg/L at pH of 2.7. Bowers and Huang (Bowers, A. R., 1981) in their paper reported that at a flow rate of 44 mL/min and pH 2.5, the maximum adsorption capacity of Filtrasorb-400 in the column was 70 mg/g. Activated carbon based on coconut shell as an adsorbent in a column gave maximum adsorption capacity of 20 mg/g at pH of 2.5 and initial Cr(VI) concentration of 50 mg/L (Alaerts, G. J., 1989). Table 10.7 also gives the adsorption column capacity of peat moss (Sarma, D. C., 1995) and leaf mould and activated carbon derived from it (Sarma, D. C., 1996). From Table 10.7 it can be concluded that in a fixed flow column, the adsorption capacity of the present adsorbent is well compared with the other similar adsorbents reported.

10.3. Conclusions

The thermally treated weed was found to be very effective adsorbent for the efficient removal of Cr(VI) from aqueous solutions. The maximum removal of Cr(VI) in a fixed bed adsorption column was found to be 159.2 mg/g at pH 1.7, at an initial adsorbate concentration of 500 mg/L, flow rate of 50 mL/min and bed height of 2 cm. The effect of different adsorption parameters like flow rate, adsorbate concentration and adsorbent dose on the removal of Cr(VI) was studied. The percentage removal of Cr(VI) was found to increase with increase in adsorbent dose but decrease with increase in both adsorbate concentration and flow rate. The reverse trend was observed for the Cr(VI) uptake capacity of the adsorbent. Adams-Bohart, BDST, Thomas and Yoon-Nelson

models were applied to the experimental data obtained from dynamic studies performed in the fixed bed column to predict the breakthrough curves and to determine the characteristic parameters of the column. Prominent and unique characteristic features of the respective models like service time (Hutchins BDST model), adsorption capacity (Thomas model) and time for 50% breakthrough (Yoon-Nelson model) were determined by using linear regression technique. The experimental and predicted unique characteristics of the models were compared by using different statistical methods like SSE, SAE, ARE and ARS. From the statistical analysis, it was found that the experimental data well fitted to the Bohart-Adams model. Desorption and regeneration studies were carried out to find both mechanism of adsorption as well as the stability of the adsorbent towards the adsorption of Cr(VI). From these studies it was found that the adsorbent was quite stable for repeated use upto five times. From the desorption studies it was also observed that ion exchange mechanism predominated the adsorption process. From the comparative studies it was observed that the adsorption capacity of the present adsorbent is well compared to other similar adsorbents reported in literature.

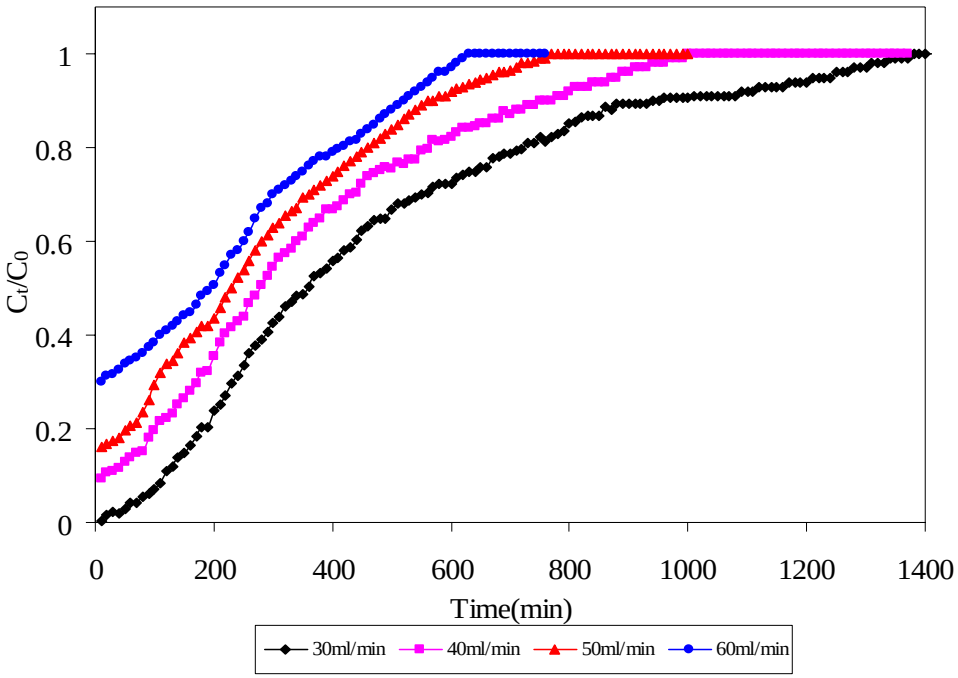

Fig.10.1. Effect of flow rate on the breakthrough curve. (Conditions: pH 1.7; adsorbate conc. 500 mg/L; bed height 10 cm)

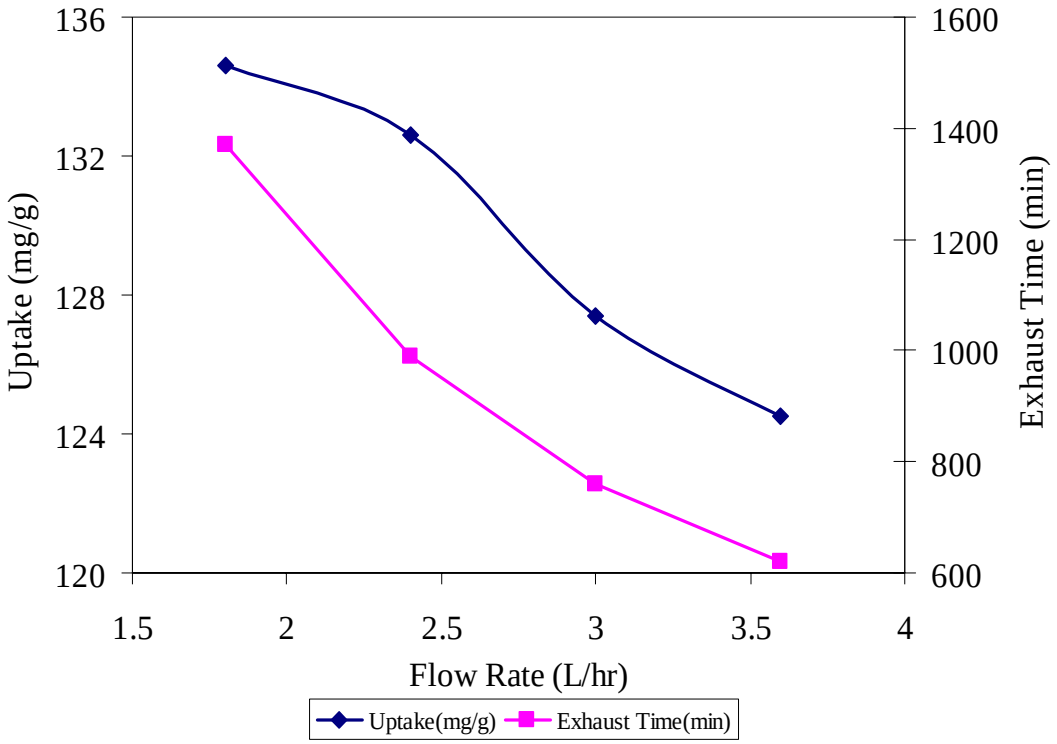

Fig.10.2. Effect of flow rate on uptake and exhaust time (Conditions: pH 1.7; adsorbate conc. 500 mg/L; bed height 10 cm)

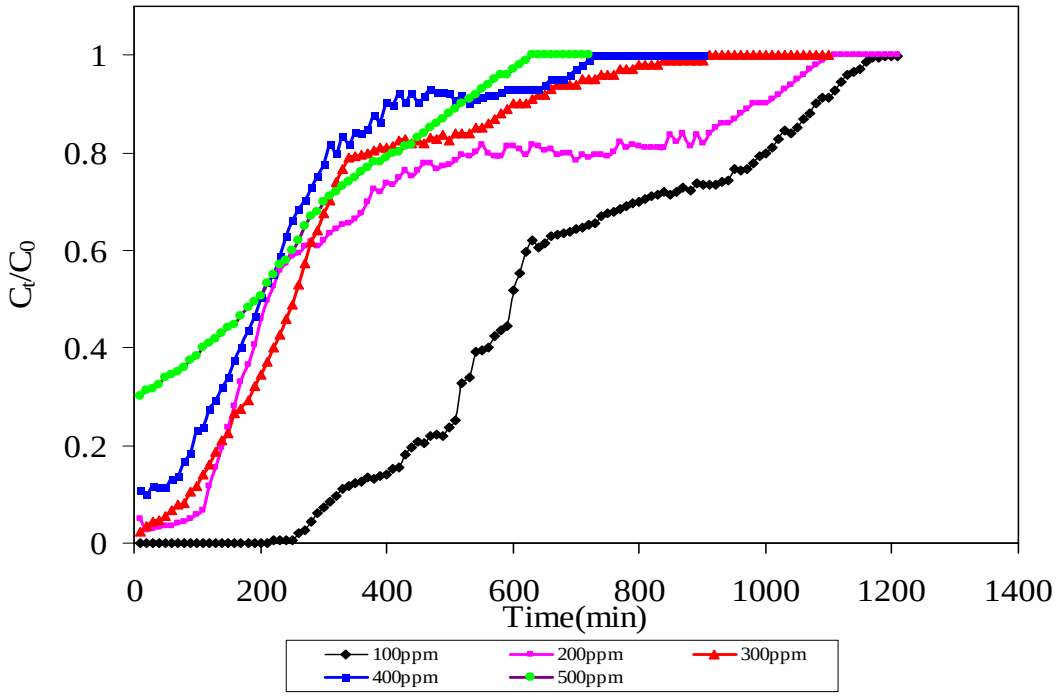

Fig.10.3. Effect of adsorbate concentration on the breakthrough curve (Conditions: pH 1.7; flow rate 3.6 L/h; bed height 10 cm)

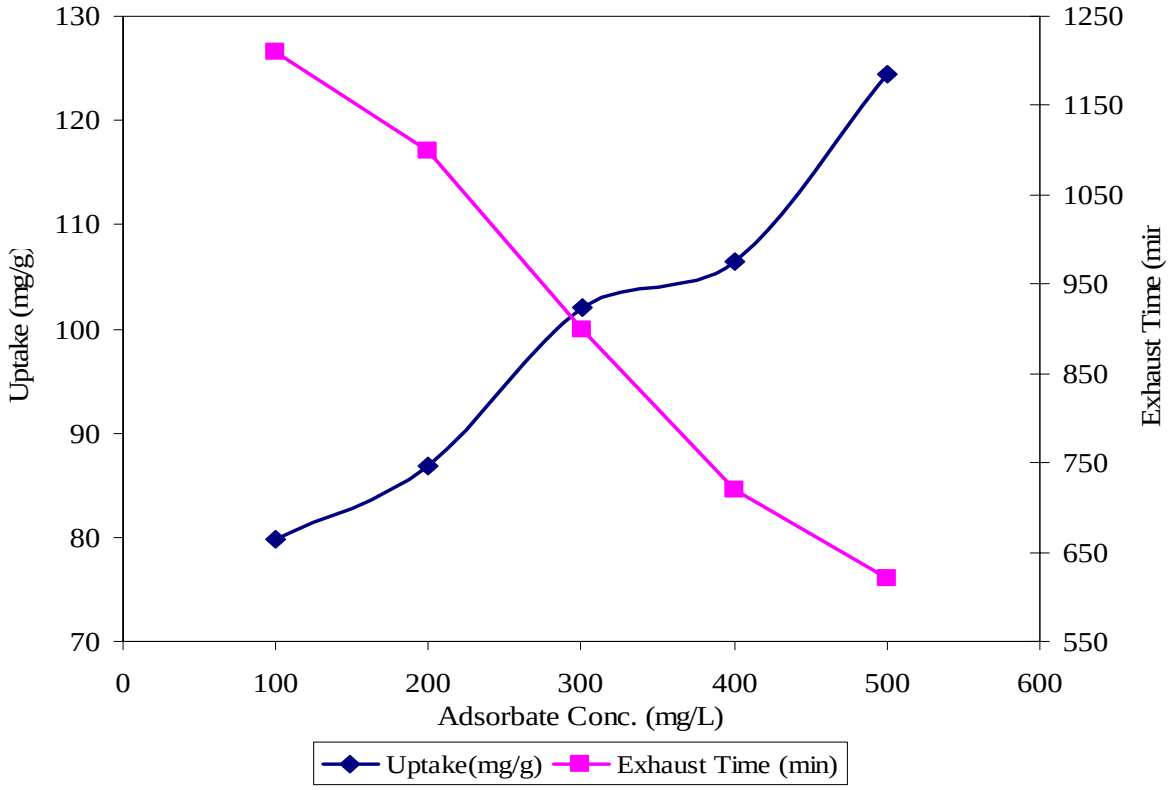

Fig.10.4. Effect of adsorbate concentration on uptake and exhaust time (Conditions: pH 1.7; flow rate 3.6 L/h; bed height 10 cm)

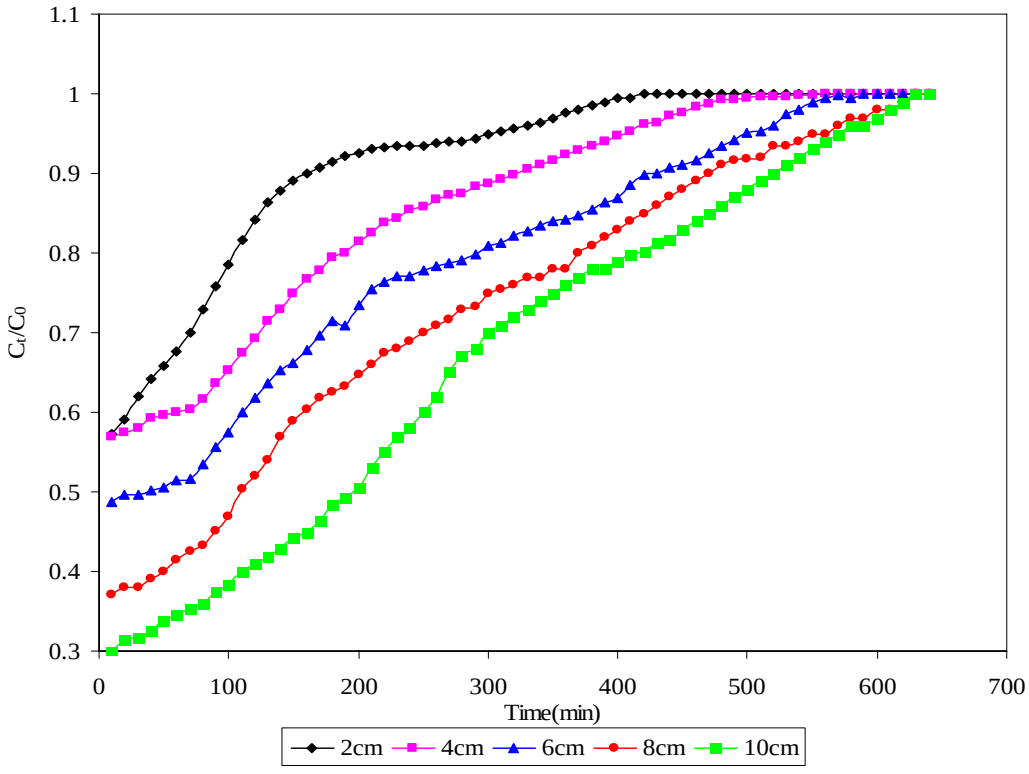

Fig.10.5. Effect of bed height on the breakthrough curve (Conditions: pH 1.7; flow rate 3.6 L/hr; adsorbate concentration 500 mg/L)

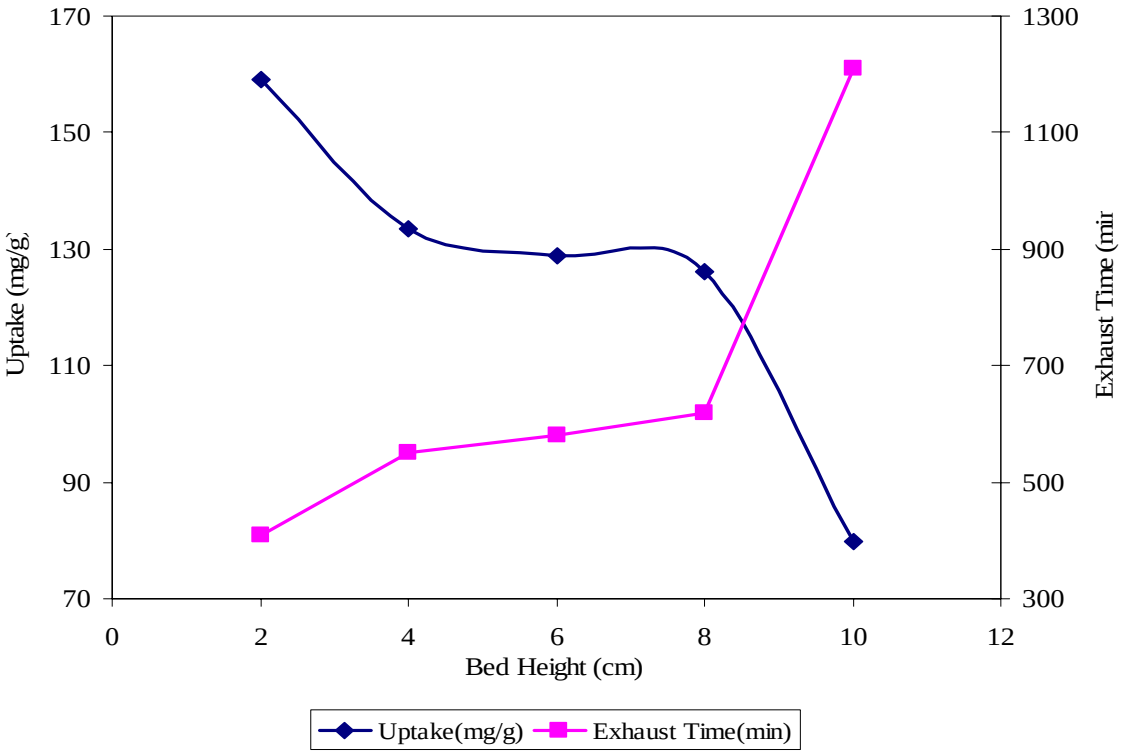

Fig.10.6. Effect of bed height on uptake and exhaust time (Conditions: pH 1.7; flow rate 3.6 L/h; adsorbate concentration 500 mg/L)

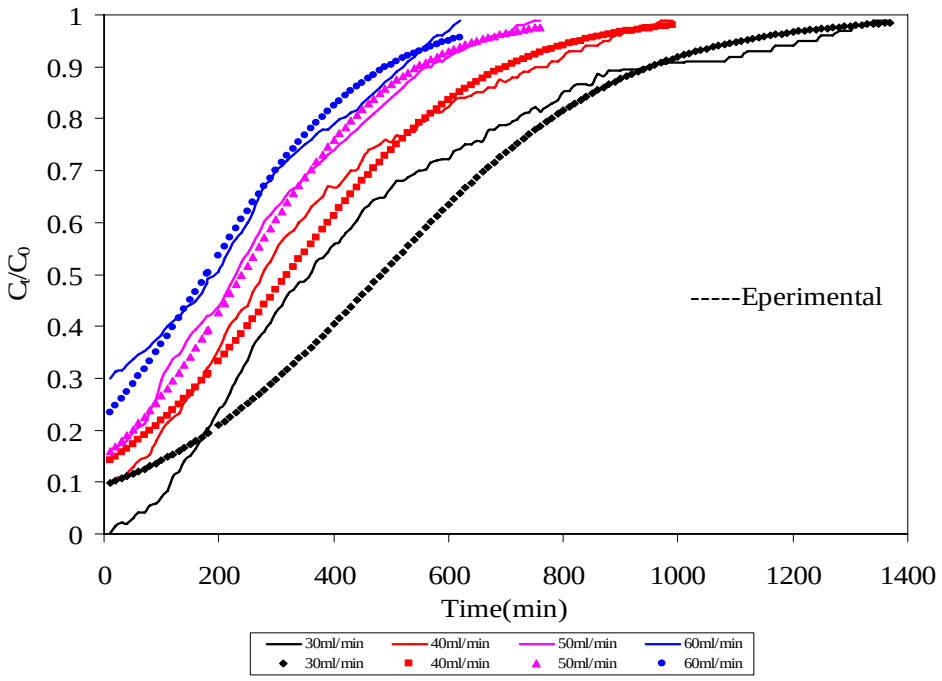

Fig.10.7. Experimental and theoretical breakthrough curve from Bohart-Adams model at different flow rate (Conditions: pH 1.7; bed height 10 cm; adsorbate concentration 500 mg/L)

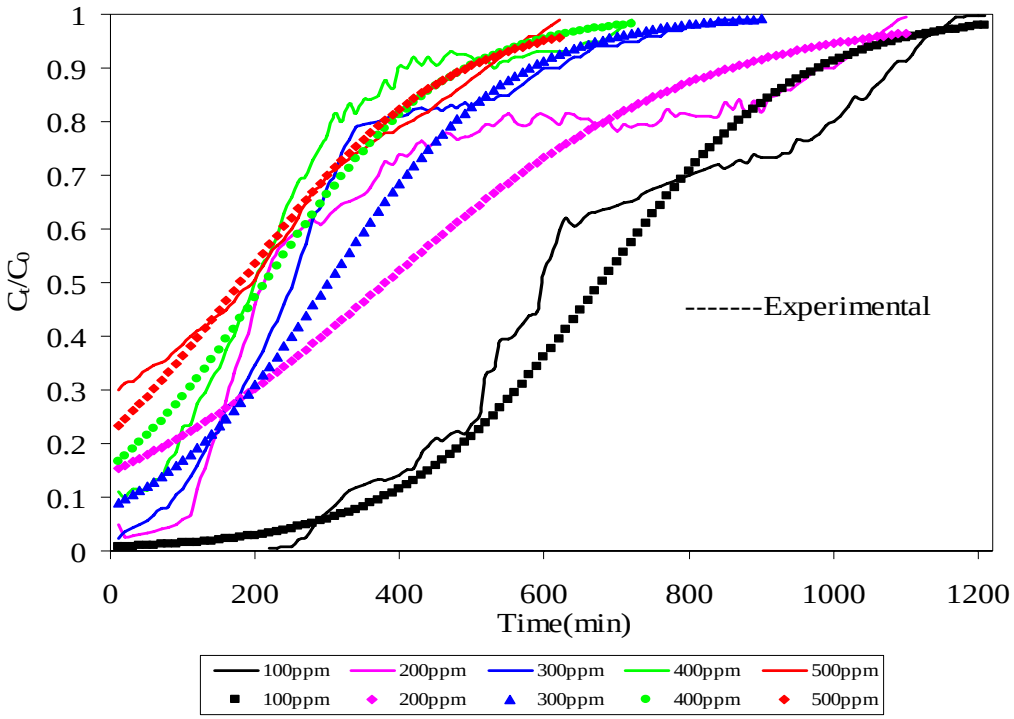

Fig.10.8. Experimental and theoretical breakthrough curve from Bohart-Adams model at different adsorbate concentration (Conditions: pH 1.7; bed height 10 cm; flow rate 3.6 L/h)

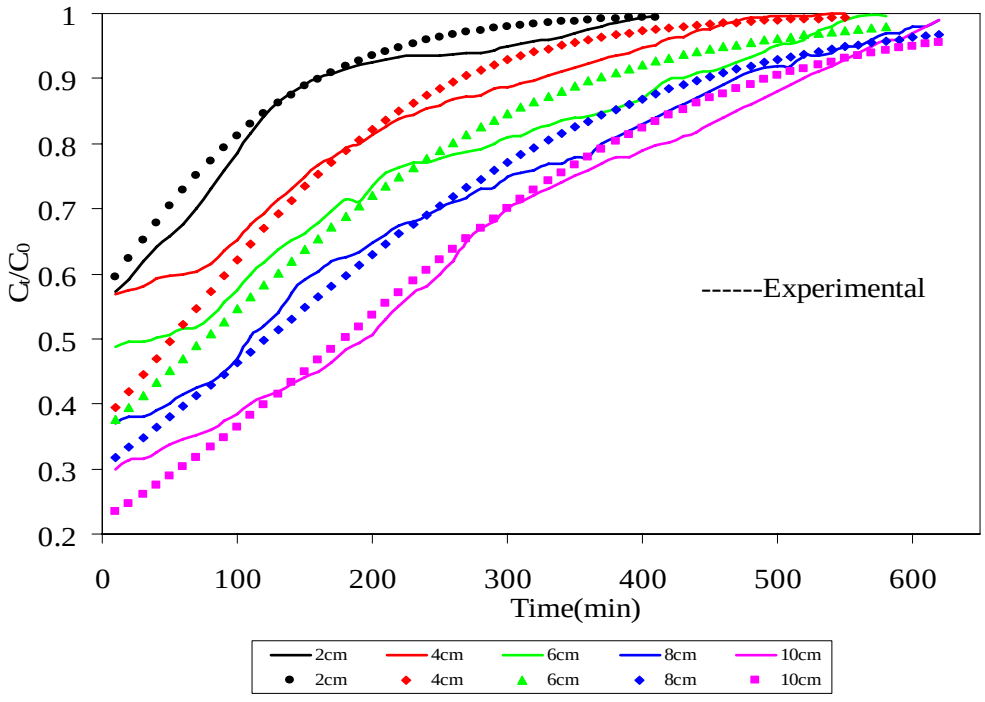

Fig.10.9. Experimental and theoretical breakthrough curve from Bohart-Adams model at different bed height (Conditions: pH 1.7; flow rate 3.6 L/h; adsorbate concentration 500 mg/L)

Table 10.1. Cr(VI) adsorption data on thermally treated weed in a fixed bed column nunder different process conditions

Flow rate (L/h)	Initial conc. (mg/L)	Bed depth (cm)	EBCT	Exhaust Time (min)	Vol. Treated (L)	Bed Vol.	Uptake (mg/g)
1.8	500	10	6.54	1370	41.1	209.4	134.6
2.4	500	10	4.91	990	39.6	201.7	132.6
3.0	500	10	3.93	760	38	193.6	127.4
3.6	500	10	3.27	620	37.2	189.5	124.5
3.6	400	10	3.27	720	43.2	220.1	106.4
3.6	300	10	3.27	900	54	275.1	102
3.6	200	10	3.27	1100	66	336.2	86.9
3.6	100	10	3.27	1210	72.6	369.8	79.8
3.6	500	8	2.62	620	37.2	236.9	126
3.6	500	6	1.96	580	34.8	295.4	128.8
3.6	500	4	1.31	550	33	420.2	133.5
3.6	500	2	0.65	410	24.6	626.6	159.2

Table 10.2. Boharat-Adams model parameters along with other statistical data

Flow rate (L/h)	$k_{AB}*10^{-6}$	N_0	R^2	q_{Exp}	q_{Cal}	SSE	SAE	ARE	ARS
1.8	3.8	78838.8	0.56	134.6	130.2	29.6	9.9	0.019	0.00056
2.4	3.8	80874.3	0.77	132.6	134.4				
3	4.4	78407.6	0.85	127.4	125.5				
3.6	4	83335	0.95	124.5	122.7				
Conc. (mg/L)									
100	34	31053.4	0.70	79.8	76.8	29.1	11.8	0.025	0.00087
200	10.5	52201.6	0.51	86.9	89.5				
300	9.33	62769.1	0.64	102.0	104.7				
400	7	67536.3	0.71	106.4	104.6				
500	4	83617.8	0.95	124.5	122.8				
Bed Height (cm)									
2	2.4	250000	0.77	159.2	150.4	187.2	28.4	0.041	0.0024
4	2.2	170446	0.90	133.5	127.2				
6	2.4	135478	0.92	128.8	134.6				
8	3	107223	0.91	126.0	131.8				
10	4	83617.8	0.95	124.5	122.8				

Table 10.3. BDST model parameters along with other statistical data

Flow rate (L/h)	k	N_0	R^2	q_{Exp}	q_{Cal}	SSE	SAE	ARE	ARS
1.8	0.0047	147.6	0.90	134.6	148.8	210.5	18.7	0.035	0.00388
2.4	0.0058	81.6	0.97	132.6	135.1				
3	0.0072	49.0	0.98	127.4	127.9				
3.6	0.007	27.3	0.95	124.5	122.9				
Conc. (mg/L)									
100	0.0073	207.5	0.88	79.8	80.6	186.9	24.4	0.051	0.00535
200	0.0046	116.3	0.75	86.9	96.8				
300	0.0079	92.1	0.95	102	110.5				
400	0.0079	65.6	0.92	106.4	110.1				
500	0.007	54.8	0.95	124.5	123.0				
Bed Height (cm)									
2	0.0102	40.0	0.94	159.2	134.4	651.3	32.9	0.044	0.00658
4	0.0103	39.4	0.89	133.5	139.2				
6	0.0076	38.7	0.85	128.8	128.7				
8	0.0068	46.6	0.96	126.0	125.2				
10	0.007	54.8	0.95	124.5	123.0				

Table10.4. Thomas model parameters along with the statistical data

Flow rate (L/h)	$k_{Th}*10^{-6}$	q_0	R^2	q_{Exp}	q_{Cal}	SSE	SAE	ARE	ARS
1.8	9.4	144823	0.90	134.6	148.8	210.5	18.7	0.035	0.00388
2.4	12	128138	0.97	132.6	135.1				
3	14	120319	0.98	127.4	127.9				
3.6	14	107306	0.95	124.5	122.9				
Conc. (mg/L)									
100	9.4	81438.9	0.88	79.8	80.6	186.9	24.4	0.051	0.00535
200	11.6	91309.6	0.75	86.9	96.8				
300	14.4	108488	0.95	102	110.5				
400	14	102914	0.92	106.4	110.1				
500		107494	0.95	124.5	123.0				
Bed Height (cm)									
2	0.0102	78558.8	0.94	159.2	134.4	651.3	32.9	0.044	0.00658
4	0.0103	77344.7	0.89	133.5	139.2				
6	0.0076	75986.8	0.85	128.8	128.7				
8	0.0068	91422.8	0.96	126.0	125.2				
10	0.007	107494	0.95	124.5	123.0				

Table10.5. The Yoon-Nelson model parameters along with other statistical data

Flow rate (L/h)	k_{YN}	T	R^2	q_{Exp}	q_{Cal}	SSE	SAE	ARE	ARS
1.8	0.0047	482.7	0.90	134.6	148.8	210.5	18.7	0.035	0.00388
2.4	0.0058	320.3	0.97	132.6	135.1				
3	0.0072	240.6	0.98	127.4	127.9				
3.6	0.007	178.8	0.95	124.5	122.9				
Conc. (mg/L)									
100	0.0073	678.7	0.88	79.8	80.6	186.9	24.4	0.051	0.00535
200	0.0046	380.5	0.75	86.9	96.8				
300	0.0079	301.4	0.95	102	110.5				
400	0.0079	214.4	0.92	106.4	110.1				
500	0.007	179.2	0.95	124.5	123.0				
Bed Height (cm)									
2	0.0102	26.2	0.94	159.2	134.4	651.3	32.9	0.044	0.00658
4	0.0103	51.6	0.89	133.5	139.2				
6	0.0076	76.0	0.85	128.8	128.7				
8	0.0068	121.9	0.96	126.0	125.2				
10	0.007	179.2	0.95	124.5	123.0				

Table 10.6. Comparison between the models

Boharat-Adams model						
Flow rate (L/h)	q_{Exp}	q_{Cal}	SSE	SAE	ARE	ARS
1.8	134.6	130.2	29.6	9.9	0.019	0.00056
2.4	132.6	134.4				
3	127.4	125.5				
3.6	124.5	122.7				
Conc. (mg/L)						
100	79.8	76.8	29.1	11.8	0.025	0.00087
200	86.9	89.5				
300	102	104.7				
400	106.4	104.6				
500	124.5	122.8				
Bed Height (cm)						
2	159.2	150.4	187.2	28.4	0.041	0.0024
4	133.5	127.2				
6	128.8	134.6				
8	126.0	131.8				
10	124.5	122.8				

BDST						
Flow rate (L/h)	$(t_{Ext.})_{Exp}$	$(t_{Ext.})_{Calc}$	SSE	SAE	ARE	ARS
1.8	1370	1030	180100.0	750.0	0.187	0.04969
2.4	990	790				
3	760	620				
3.6	620	550				
Conc. (mg/L)						
100	1210	1020	171600.0	880.0	0.192	0.0488
200	1100	860				
300	900	690				
400	720	550				
500	620	550				
Bed Height (cm)						
2	410	330	25200.0	340.0	0.639	0.09462
4	550	450				
6	580	540				
8	620	560				
10	620	560				
Thomas model						
Flow rate (L/h)	q_{Exp}	q_{Cal}	SSE	SAE	ARE	ARS
1.8	134.6	148.8	210.5	18.7	0.035	0.00388
2.4	132.6	135.1				
3	127.4	127.9				
3.6	124.5	122.9				
Conc. (mg/L)						
100	79.8	80.6	186.9	24.4	0.051	0.00535
200	86.9	96.8				
300	102	110.5				
400	106.4	110.1				
500	124.5	123.0				
Bed Height (cm)						
2	159.2	134.4	651.3	32.9	0.044	0.00658
4	133.5	139.2				
6	128.8	128.7				
8	126.03	125.2				
10	124.5	123.0				

Yoon-Nelson model						
Flow rate (L/h)	$(t_{50\%})_{Exp}$	$(t_{50\%})_{Calc}$	SSE	SAE	ARE	ARS
1.8	357	670	125095.0	537.0	0.437	0.38447
2.4	276	425				
3	230	300				
3.6	195	200				
Conc. (mg/L)						
100	600	810	195100.0	850.0	0.658	0.83392
200	210	530				
300	250	440				
400	200	310				
500	190	210				
Bed Height (cm)						
2	-	-	200.0	20.0	0.141	0.01076
4	-	-				
6	40	-				
8	110	100				
10	200	210				

Table 10.7. Comparison of results with other similar adsorbents reported

Sl. No.	Adsorbent	Uptake capacity (mg/g)	Reference
1	Activated carbon	123	[Kim, I. J., 1977]
2	Activated carbon	70	[Bowers, A. R., 1981]
3	Coconut shell carbon	20	[Alaerts, G. J., 1989]
4	Peat (pH 2; 80 mL/min)	65.9	[Sarma, D. C., 1995]
5	Peat (pH 2"5; 120 mL/min)	38.2	[Sarma, D. C., 1995]
6	Leaf mould	25.9	[Sarma, D. C., 1996]
7	Activated carbon from leaf mould	75.6	[Sarma, D. C., 1996]
8	Thermally activated weed	159.2	Current study

REFERENCES

CURICULUM VITAE

CURRICULUM- VITAE

NAME: SAROJ SUNDAR BARAL

Permanent address:
C/O- Bibudhendra Baral
At/Po – Batagaon
Via – Kamakhya Nagar
Dist- Dhenkanal (Orissa)
Pin-759018, INDIA
Ph. No. + 919861084217
E-mail : ss_baral2003@yahoo.co.in

Address of Correspondence:
Senior Researc Fellow
Dept. Of Enviroment and Sustainability
Institute of Minerals and Material Technology (formerly Regional Research Laboratory)
Bhubaneswar 751 013
Ph. No. +919861084217

PERSONAL DETAILS:

Date of Birth : 1st July 1975

Father's Name: Bibudhendra Baral

Marital Status : Single

Languages : Oriya, Hindi, English

Gender : Male

EDUCATIONAL QUALIFICATION:

Name of the Examination	School / College	Name of the Board / University	Year of passing	Class/ Division	% of marks/ CGPA
B. E (Chemical)	IGIT Sarang	Utkal University	2001	1st	69.4
M. Tech course work (20grade point)	NIT, Rourkela	NIT, Rourkela	2004-05	1st	8
Ph.D.	NIT, Rourkela	NIT, Rourkela	Continuing	-	Submitted in the month of Oct, 2007

PROFESSIONAL EXPERIENCE

Sl No	Position	Institute	From	To
1	JRF-GATE (CSIR)	RRL, Bhubaneswar	30.05.03	30.05.05
2	SRF-GATE (CSIR)	RRL, Bhubaneswar	30.05.05	Continuing